

**NUMERICAL TREATMENT OF SINGULARLY PERTURBED
DIFFERENTIAL EQUATIONS BY SOME HYBRID METHOD**

A Thesis

Submitted in partial fulfillment of the requirements for the
award of the degree of

DOCTOR OF PHILOSOPHY
in
Mathematics

By
Mandeep Kaur

41400197

Supervised By
Dr. Geeta Arora



Transforming Education Transforming India

LOVELY PROFESSIONAL UNIVERSITY
PUNJAB
2021

Declaration of Authorship

I, Mandeep Kaur, declare that this thesis titled, “Numerical treatment of singularly perturbed differential equations by some hybrid method” and the work presented in it is my own. I commit that:

- This work was done wholly or mainly while in candidature for a research degree at this University.
- It is declared that any part of this thesis has previously neither been submitted for a degree nor for any other qualification at this University or any other institution.
- The consulted published work of others is always clearly attributed.
- The source is always given, wherever I have quoted from the work. This thesis is entirely my own work, except some quotations.
- I have acknowledged all main sources of help.
- Where the thesis is based on work done by myself jointly with others, I have made clear exactly what was done by others and what I have contributed myself.

Signed:

A handwritten signature in blue ink that reads "Mandeep Kaur" with a horizontal line underneath.

Date: 24/06/2021

Certificate

The thesis titled “Numerical treatment of singularly perturbed differential equations by some hybrid method” submitted by Miss. Mandeep Kaur for the award of the degree of Doctor of Philosophy has been carried out under my supervision at the Department of Mathematics, Lovely Professional University, Punjab, India. The matter presented in this thesis is original and has not been submitted in any other University or Institute for award of any degree or diploma. The work is comprehensive, complete, and fit for evaluation.

Dr. Geeta Arora
Assistant Professor,
Department of Mathematics,
Lovely Professional University,
Punjab, India.

LOVELY PROFESSIONAL UNIVERSITY, PUNJAB

Lovely Faculty of Technology and Sciences

Department of Mathematics

Abstract

Doctor of Philosophy

By Mandeep Kaur

Differential equations are the mathematical models of the real-life problems which enable the researchers to do in depth investigation of the problem. For an instance, differential equations are used in economics to find the optimum investment strategies, in physics, it plays an important role to study the exponential decay of radioactive substances, in biosciences investigation regarding the rate of spew of diseases and factors liable to control the proliferation of certain infections is carried out with the help of mathematical modeling of the experiments. Thus, the numerical treatment of the differential equations is a flourishing concern for the researchers. A differential equation can be treated by an analytical method to find its exact solution or by a numerical method to provide an approximation to the solution. The analytical exploration of differential equations is often laborious, and it is tough to find the exact solution of the modelled differential equation. So, the advanced numerical methods are required for obtaining the precise solution of the differential equations. The well-known techniques for approximating the solution of the differential equations are finite difference method, finite element method, differential quadrature method and lie symmetry method. Collocation is another numerical technique for approximating the solution of the differential equation by satisfying it at collocation points, which are the few chosen points on the space domain of the problem. The collocation method is one of the rapidly progressing techniques because of its merits over

the other numerical techniques. The present thesis aims to demonstrate the significance of the numerical solution of singularly perturbed differential equations (SPDE) due to their broader scope of practices in each module of Science and Engineering, and the objectives of this research are:

- To explore the possibility of obtaining the numerical solution of SPDE by some hybrid methods.
- To study the effect of variation of perturbation and delay parameter on numerical solution of SPDE.
- To find the solution of SPDE of second and higher order.

The study of SPDE has become a full-grown mathematical subject with extended literature as numerical treatment of SPDE is a demanding practice because of the brisk variation of the solution at either side of the domain and due to the non-availability of the exact solutions of singularly perturbed delay differential equations. To fulfill the above indispensable gaps, we have focused on the numerical solution of these equations by various numerical techniques. In this work, these differential equations are approximated by various spline-based methods and various meshes have been selected to partition the boundary of the problem. The numerical results so obtained are scrutinized in all respects to capture the conduct of the solution of these equations with respect to the variation of delay and perturbed parameter. The maximum absolute error of the obtained solutions is also calculated by using double mesh principle. The convergence of the applied hybrid methods is incorporated to validate the stability of the schemes by using local truncation error.

This thesis includes five chapters. The first chapter is preliminary of introduction and short discussion on nature of singularly perturbed differential equations, with the brief specifications about the SPDE and the literature investigation. Additionally, some implementations of SPDE and some rudimentary stability conditions of the numerical schemes, collocation method and double mesh principle to calculate error are included in this chapter.

In chapter 2, modified cubic B-spline collocation method is implemented on singularly perturbed delay differential equation (SPDDE). The alteration in B-spline basis function has been considered because the resultant matrix system becomes diagonally dominant, which reduces the calculations on the boundary of the problem. So, modified cubic B-spline collocation scheme is applied to simulate SPDDE. In this chapter, two different SPDDE of second order for numerical solution.

Considered SPDDE is with small delay and the problem is as follows:

$$\varepsilon^2 y''(x) + a(x)y(x - \delta) + b(x)y(x) = f(x), 0 < x < 1$$

subject to the boundary condition:

$$y(x) = \phi(x) \text{ on } -\delta \leq x < 0 \text{ and } y(1) = \gamma.$$

Where $0 < \varepsilon \ll 1$ and $0 < \delta < 1$. The coefficients $a(x)$, $b(x)$, $c(x)$ and $f(x)$ are the continuous functions, $\phi(x)$ is sufficiently smooth functions and γ is a constant. The above class of SPDDE arises in the mathematical modeling of biological processes such as in Stein's model. This model describes the nerve cell system. In this model, the delay parameter appears due to the decay in the inputs of the nerve system. The variable y is assumed as first-exit time and the other term xy' in the equation represents the exponential delay in synaptic information. A portion of this chapter is published in AIP conference proceedings by American institute of physics.

Another second-order SPDDE

$$\varepsilon y''(x) + a(x)y'(x - \delta_1) + b(x)y(x - \delta_2) + c(x)y(x) = f(x), \quad 0 < x < l,$$

subject to the conditions

$$y(x) = \phi(x) \text{ on } -\delta \leq x < 0 \text{ where } \delta = \max(\delta_1, \delta_2) \text{ and } y(l)=\gamma,$$

where $0 < \varepsilon \ll 1$, and δ_1 and δ_2 are delay parameters. $a(x), b(x), c(x), f(x)$ are sufficiently smooth functions on $[0, l]$ and $\phi(x)$ is a smooth function on $[-\delta, 0)$ has been

treated numerically by using same scheme. For the different values of parameters there exists four different type of perturbed delay differential equations as follows:

- a. Considering $\delta_1=\delta_2=\delta$ and $l=1$, the problem becomes:

$$\varepsilon y''(x) + a(x)y'(x - \delta) + b(x)y(x - \delta) + c(x)y(x) = f(x), \quad 0 < x < 1,$$

subject to the conditions:

$$y(x) = \phi(x) \text{ on } -\delta \leq x < 0 \text{ and } y(1)=\gamma$$

- b. Considering $\delta_1=0, \delta_2=1, l=2$, and $c(x)=0$, problem becomes:

$$\varepsilon y''(x) + a(x)y'(x) + b(x)y(x - 1) = f(x), \quad 0 < x < 2,$$

subject to the conditions:

$$y(x) = \phi(x) \text{ on } -1 \leq x < 0 \text{ and } y(2)=\gamma$$

- c. Considering $\delta_2=\delta, a(x)=0$ and $l=1$, problem reduces to

$$\varepsilon y''(x) + b(x)y(x - \delta) + c(x)y(x) = f(x), \quad 0 < x < 1,$$

subject to the conditions:

$$y(x) = \phi(x) \text{ on } -\delta \leq x < 0 \text{ and } y(1) = \gamma$$

- d. Considering $\delta_1=\delta, b(x) = 0$ and $l=1$, problem reduces to

$$\varepsilon y''(x) + a(x)y'(x - \delta) + c(x)y(x) = f(x), \quad 0 < x < 1,$$

subject to the conditions:

$$y(x) = \phi(x) \text{ on } -\delta \leq x < 0 \text{ and } y(1) = \gamma$$

This work was presented in the international conference, "Recent Advances on Theoretical and Computational Partial Differential Equations" held at Panjab University, Chandigarh .

Chapter 3 comprises of a collocation technique with trigonometric spline as basis functions. The basis functions are piecewise in the space $\{1, \cos(x), \sin(x), \dots, \cos(kx), \sin(kx)\}$ and are periodic, and continuous differentiability functions. This method is applied on two SPDDE equations of order two and three.

Consider second order SPDDE of the following form:

$$Ly \equiv \varepsilon y''(x) + a(x)y(x - \delta) + b(x)y(x) = f(x), 0 < x < 1$$

under the constraints:

$$y(x) = \phi(x), x \in [-\delta, 0] \text{ and } y(1) = \gamma.$$

To obtain the approximate solution of this equation, trigonometric B-spline collocation technique is used. The domain is partitioned in a uniform mesh of equal length for each sub-interval. Work from this chapter is published in “International journal of Mathematical, Engineering and Management Sciences”.

Consider third order SPDDE of the following form:

$$-\varepsilon y'''(x) + a(x)y''(x) + b(x)y'(x) + c(x)y(x) + d(x)y'(x - 1) = f(x), \quad x \in \Omega^*$$

where $\Omega^* = \Omega^+ \cup \Omega^-$, $\Omega^- = (0,1)$, $\Omega^+ = (1,2)$ and $\Omega = (0,2)$.

with the boundary conditions:

$$y(x) = \phi(x), x \in [-1,0] \text{ and } y'(2) = \gamma$$

This equation has been treated numerically by quintic trigonometric B-spline collocation technique. This work is published in “International Journal of Mathematical, Engineering and Management Sciences”.

In chapter 4, exponential B-splines as basis functions with collocation method is considered for numerical treatment of SPDDE. Exponential B-splines are piecewise continuous functions and they are procured by multifold convolution of weight functions. To obtain

mathematical expression for exponential B-spline functions, the weights are taken as exponential functions.

This technique has been deployed on a SPDDE with large delay. In this work, the mathematical model of heating systems which in turn results in delay differential equation is discussed and the recent numerical work carried out on SPDDE has been investigated. The considered SPDDE used in signal transmission in control theory. The considered equation is of the form:

$$-\varepsilon y''(x) + a(x)y(x) + b(x)y(x-1) = f(x), \quad x \in \Omega^- \cup \Omega^+,$$

where $\Omega^- = (0,1)$ and $\Omega^+ = (1,2)$

subject to the conditions:

$$y(x) = \phi(x), \quad x \in [-1,0], \quad y(2) = \gamma.$$

Chapter 5, embraces the comparison of exponential and trigonometric B-spline collocation technique. The SPDDE considered is:

$$-\varepsilon y''(x) + a(x)y'(x) + b(x)y(x-1) = f(x), \quad x \in \Omega^*$$

subject to the conditions:

$$y(x) = \phi(x), \quad x \in [-1,0], \quad y(2) = l.$$

Where $a(x) = \begin{cases} a_1(x), & x \in [0,1] \\ a_2(x), & x \in (1,2] \end{cases}$, $f(x) = \begin{cases} f_1(x), & x \in [0,1] \\ f_2(x), & x \in (1,2] \end{cases}$, $\Omega^* = \Omega^- \cup \Omega^+$, $\Omega^- = (0,1)$ and $\Omega^+ = (1,2)$

In this work, the considered equation has been treated with two techniques: cubic trigonometric B-spline collocation method and cubic exponential B-spline method with uniform and Shishkin mesh and the numerical results obtained by both schemes are compared.

In chapter 6, conclusions and results have been established based on the present work. Moreover, further research work in this orientation has been proposed.

Acknowledgments

I would like to express my gratitude to Almighty God for the blessing to acquire education. Then I would like to say sincere thanks to my supervisor Dr. Geeta Arora, Assistant professor, Lovely Professional University for her immense support, enlightenment, and forbearance throughout this work. I am truly grateful to have the opportunity to work with her as a research scholar. She provides directions in programming, use of software, technical writing, presentation style and lessons to tackle challenges in every walk of life. It was an honor for me to work with her. I found her guidance to be extremely valuable.

I would like to thank Dr. Sanjay Mishra for his support to start research work. In addition, I would like to express my gratitude to my friends and all staff members of the Department of Mathematics and the entire staff of Lovely Professional University, Phagwara for their help and support. I want to pay my sincere thanks to all those who helped me to complete my work successfully in any way.

Lastly, but more prominently, I would like to say thanks to my younger sisters, Antardeep Kaur and Manpreet Kaur for all technical support to get this work done. My sincere thanks to my parents who always prompt me to move forward.

Contents

Declaration of Authorship.....	i
Certificate.....	ii
Abstract.....	iii
Acknowledgments.....	ix
Table of Contents.....	xi
List of Tables	xiv
List of Figures	xvi

Table of Contents

Chapter 1.....	1
Introduction	1
1.1 Introduction	1
1.1.1 Singularly perturbed differential equation	1
1.1.2 Delay differential equation	2
1.2 Mathematical modeling.....	7
1.2.1. Tumor expansion model	7
1.2.2. Heating systems as delay model.....	7
1.2.3. Delay model of the biological system	8
1.2.4. Delay model in the treatment of HIV.....	9
1.3 Collocation Method	10
1.4 B-spline	11
1.4.1 Introduction of spline.....	11
1.4.2 B-spline.....	13
1.5 Convergence Analysis	15
1.6 Error Analysis	16
Chapter 2.....	19
Modified cubic B-spline collocation method for numerical solution of second order singularly perturbed delay differential equation	19
2.1 Introduction	19
2.2 Mesh strategy	21
2.3 Modified cubic B-spline method.....	22
2.4 First-exist time problem.....	24
2.4.1 SPDDE from stein model	24
2.4.2 Solution of SPDDE with a small shift by collocation method.....	25
2.4.3 Numerical examples.....	26
2.5 Generalized perturbed delay differential equation.....	27
2.5.1 Description of method for the numerical solution of generalized perturbed delay differential equation	29

2.5.2 Convergence	30
2.5.3 Error analysis.....	31
2.6 Summary	34
Chapter 3.....	48
Trigonometric B–spline collocation method for numerical treatment of singularly perturbed delay differential equations.....	48
3.1 Introduction	48
3.2 Numerical solution of second-order problem	50
3.2.1 Trigonometric cubic B-spline collocation method	51
3.2.2 Convergence analysis.....	54
3.2.3 Numerical analysis of second-order SPDDE.....	56
3.2.4 Discussion and conclusions.....	57
3.3 Numerical treatment of third order SPDDE.....	58
3.3.1 Problem statement of third order SPDDE.....	59
3.3.2 Existence of solution	60
3.3.3 Quintic trigonometric collocation scheme	60
3.3.4 Convergence Analysis	64
3.3.5 Numerical Examples of third order SPDDE	68
3.3.6 Discussion.....	68
Chapter 4.....	79
Exponential B-spline collocation scheme for numerical treatment of singularly perturbed delay differential equations	79
4.1 Introduction	79
4.2 Problem statement.....	81
4.3 Exponential cubic B-spline collocation method.....	82
4.4 Convergence Analysis	86
4.5 Numerical Examples.....	88
4.6 Discussion.....	90
Chapter 5.....	103
A comparison of trigonometric B-spline collocation method and exponential B-spline collocation technique	103

5.1 Introduction	103
5.2 Problem Statement.....	103
5.3 Existence of Solution.....	104
5.4 Selection of mesh.....	104
5.5 Implementation of Collocation Method	105
5.6 Convergence Analysis	109
5.7 Numerical Examples.....	113
5.7.1 Discussion of numerical examples	114
5.8 Conclusion.....	115
Chapter 6.....	128
Conclusion and Future Directions.....	128
6.1 Conclusion.....	128
6.2 Highlights of work	129
6.3 Overall Numerical Work done	131
6.4 Conclusions from our work.....	132
6.5 Suggestions for Future Work	132
References	135
Research publications/Conferences/Workshops attended.....	142

List of Tables

Table 2.1: B-spline basis values.....	22
Table 2.2: Maximum absolute error in solution of Example 2.1 with $\delta = 0.01$	35
Table 2.3: Maximum absolute error in solution of Example 2.1 with $\varepsilon = 0.01$	35
Table 2.4: Solution of Example 2.2 with $\varepsilon = 0.1$ and $\delta = 0.01$	37
Table 2.5: Numerical solution of Example 2.3 with $\varepsilon = 0.01$ and $\delta = 0.01$	38
Table 2.6: Numerical solution of Example 2.3 with $\varepsilon = 0.02$ and $\delta = 0.01$	39
Table 2.7: Numerical solution of Example 2.3 with $\varepsilon = 0.03$ and $\delta = 0.01$	39
Table 2.8: Maximum absolute error of Example 2.3 with $\varepsilon = 0.001$	39
Table 2.9: Solution of Example 2.4 with Shishkin mesh.....	40
Table 2.10: Solution of Example 2.5 with $\tau = 0.2$	41
Table 2.11: Solution of Example 2.5 with $\tau = 0.3$	41
Table 2.12: Solution of Example 2.5 with $\tau = 0.4$	42
Table 2.13: Solution of Example 2.6 with $\tau = 0.4$, $N = 16$ and $\delta = 1$	43
Table 2.14: Solution of Example 2.7 with $\tau = 0.4$, $N = 16$ and $\delta = 1$	43
Table 2.15: Solution of Example 2.9 with $\tau = 0.4$, $N = 8$ and $\varepsilon = 0.1$	44
Table 2.16: Solution of Example 2.10	45
Table 2.17: Maximum absolute error obtained for Example 2.10 with Shishkin mesh and uniform mesh.....	46
Table 2.18: Solution of Example 2.11	47
Table 3.1: The maximum error obtained for $\varepsilon = 0.1$ and for different values of N and δ for Example 3.1.....	69
Table 3.2: The maximum absolute error of Example 3.1 for $\delta = 0.5\varepsilon$	69
Table 3.3: The maximum error obtained for $\varepsilon = 0.1$ for different values of N and δ for Example 3.2	71
Table 3.4: The maximum absolute error of Example 3.2 for $\delta = 0.5\varepsilon$	71
Table 3.5: Maximum absolute error obtained for Example 3.3 for $\varepsilon = 0.1$	72
Table 3.6: Maximum absolute error obtained for Example 3.4 for $\varepsilon = 0.1$ and for different values of N	73
Table 3.7: Maximum absolute error of Example 3.5	75
Table 3.8: Maximum absolute error of Example 3.6	77
Table 4.1: Values of exponential basis.....	84
Table 4.2: Maximum absolute error obtained for Example 4.1	91
Table 4.3: Maximum absolute error obtained for Example 4.1 for different values of ε	92
Table 4.4: Solution of Example 4.1 for $\varepsilon = 0.01$	93
Table 4.5: Maximum absolute error obtained for Example 4.2 for different values of ε	95
Table 4.6: Maximum absolute error obtained for various values of ε for Example 4.2	96
Table 4.7: Approximate solution of Example 4.2 for $\varepsilon = 0.01$	97

Table 4.8: Maximum absolute error obtained for Example 4.3 for diverse values of ϵ	99
Table 4.9: Maximum absolute error obtained for various values of ϵ for Example 4.3	100
Table 4.10: Solution of Example 4.3 for $\epsilon = \mathbf{0.01}$	101
Table 5.1: Maximum absolute error of Example 5.1 by trigonometric B-spline with refined mesh with $\tau_1=0.3, \tau_2=0.15$	116
Table 5.2: Maximum absolute error of Example 5.1 by both schemes with refined mesh	117
Table 5.3: Maximum absolute error of Example 5.1 by both schemes with uniform mesh	118
Table 5.4: Maximum absolute error obtained for Example 5.1 by both schemes and	119
both meshes for $\epsilon=2^{-6}$	119
Table 5.5: Solution of Example 5.2 by trigonometric B-spline by refined mesh with $\tau_1=0.3, \tau_2=0.15$	122
Table 5.6: Maximum absolute error of Example 5.2 by both schemes with refined mesh	123
Table 5.7: Maximum absolute error of Example 5.2 by both schemes with uniform mesh	124
Table 5.8: Maximum absolute error obtained for Example 5.2 by both schemes and both meshes MAE for $\epsilon=2^{-6}$	125
Table 6.1: Summary of the numerical treatments performed on SPDDEs	131

List of Figures

Figure 1.1: Spline template	12
Figure 1.2: 3-D design of car.	13
Figure 1.3: B-spline functions	15
Figure 1.4: Error while considering single term accuracy.....	17
Figure 1.5: Error while considering double term accuracy.....	18
Figure 2.1: Solid lines present cubic B-spline curve and dotted lines show its modified curve	20
Figure 2.2: Solution of Example 2.1 with $\epsilon = 0.01$	36
Figure 2.3: Solution of Example 2.2 with $\epsilon = 0.1$ and $\delta = 0.01$	37
Figure 2.4: Solution of Example 2.2 with $\epsilon = 0.01$ and $\delta = 0.2*\epsilon$	38
Figure 2.5: Solution of Example 2.3 with $\epsilon = .001$	40
Figure 2.6: Solution of Example 2.5 with Shishkin mesh	42
Figure 2.7: Solution of Example 2.8 with $\epsilon = 0.001$ and $\delta = 0.0003$	44
Figure 2.8: Solution of Example 2.9 with Shishkin mesh	45
Figure 2.9: Solution of Example 2.10 with uniform and Shishkin mesh	46
Figure 3.1: Quadratic trigonometric B-spline	49
Figure 3.2: Quintic trigonometric spline curve	58
Figure 3.3: Solution of Example 3.1 for $\epsilon = 0.01$	70
Figure 3.4: Solution of Example 3.2 for $\epsilon = 0.01$	72
Figure 3.5: Solution of Example 3.3 for different values of ϵ and δ	73
Figure 3.6: Solution of Example 3.4	74
Figure 3.7: Graph of solution of Example 3.5 for $N=128$ and $\epsilon = 0.25$	76
Figure 3.8: Graph of solution of Example 3.6 for $N=128$ and $\epsilon = 0.25$	78
Figure 4.1: (a) B spline polynomials of order 2, (b) exponential B splines obtained by convolution	79
Figure 4.2: Solution of Example 4.1 for diverse values of ϵ	94
Figure 4.3: Solution of Example 4.2 at different values of ϵ	98
Figure 4.4: Layer behavior of Example 4.3 for $\epsilon = 0.01$	102
Figure 5.1: Solution of Example 5.1 by trigonometric scheme and refined mesh	119
Figure 5.2: Solution of Example 5.1 by both schemes with refined mesh for $N=64$ and $\epsilon = 0.25$	120
Figure 5.3: Solution of Example 5.1	121
Figure 5.4: Solution of Example 5.2 by exponential scheme for $N=64$ and $\epsilon = 0.25$	125
Figure 5.5: Solution of Example 5.2 by both schemes with refined mesh for $N = 64$ and $\epsilon = 0.25$	126
Figure 5.6: Solution of Example 5.2	127

Dedicated to my parents and sisters-Bikoo & Preet

Chapter 1

Introduction

1.1 Introduction

Numerical treatment of differential equations is of flourish concerns to researchers due to the wide range of application of differential equations in various disciplines such as biosciences, control theory, and physical sciences. Researchers have been investigating different differential equations, which frequently emerge in mathematical modeling of various problems by variety of numerical methods which provide more accurate solution. In addition to the accurate solution other challenges targeted by researchers are handling unusual behavior of solution under certain conditions.

1.1.1 Singularly perturbed differential equation

A singularly perturbed differential equation is an ordinary differential equation in which a variable, known as perturbation parameter, is associated with higher order derivative term. The perturbation parameter (ε) is a positive bijou (small) variable and crackdown in it reduces the order of the differential equation. So, these equations are known as singularly perturbed differential equations (SPDE). One of the examples of a physical system which results in SPDE is, control theory where tiny variables such as capacitance, resistance, inductance and so on raise the order but flip side clampdown (suppression) of these variables decreases the order of the system. Furthermore, the temperament of the restricted solution when $\varepsilon \rightarrow 0$ is entirely divergent as compared to the solution for finite value of ε and the hasty variation in the solution introduces the concept of boundary layer, which is also known as inner region.

This notion of boundary layer was instigate by physicist Ludwing Prandtl (Prandtl, 1905) when he speculated that the frictional reaction was endured in the tiny layer near the surface

of fluid only. The singularly perturbed differential equations emerged in the modeling of divert intricate systems, such as pollution (Pudykiewicz, 1989), problem of polluted water in rivers (Baumert, Braun, Glos, Müller, & Stoyan, 1980), transportation of groundwater (Bear & Verruijt, 1987), mobile media involving electromagnetic field issues (Hahn, Bigeon, & Sabonnadiere, 1987), and production of oil from underground water body (Ewing, 1983) etc.

A lot of work has been reported in the literature for numerical treatment of these equations. For instance, some spline-based methods are proposed by Aziz and Khan (Aziz & Khan, 2002), Jha (Jha, 2012), El-salam (Abd El-Salam, 2013), Akram and Naheed (Akram & Naheed, 2013). These methods were based on the simple technique to divide the domain in the uniform partition and to calculate the approximate solution at these points through method such as the finite element method, collocation method etc, using spline functions. Some differential transformations based on analytical methods were also reported, one such method was presented by Dogan et al. (Doğan, Ertürk, & Akın, 2012) while Mishra and Saini (Mishra & Saini, 2013) proposed a Liouville-Green transform based method. Gupta et al. (Gupta, Srivastava, & Kumar, 2011) and Akram (Akram, 2011) solved these equations by using the spline as basis functions.

1.1.2 Delay differential equation

Differential equations which embrace small parameter (δ) known as shift, delay or retarded are delay differential equations. This small parameter occurs in the argument of the reaction term, convention term or in both because of the involvement of feedback, which is mandatory to avoid an unsteady state. But a definite time is demanded to diagnose the instruction and to react on it in the feedback control. So, modeling of such problems as delay differential equation is a conventional way to interpret the process. For instance, a nonlinear differential equation given by Longtin and Milton (Longtin & Milton, 1988), which describes the simple and complex conduct exhibits in human pupil light reflex involves constant and delayed feedback. Other similar application of delay differential equations exists in optics (Mallet-Paret & Nussbaum, 1989), in the study of HIV infection

(Nelson & Perelson, 2002), in the sensitivity analysis in biosciences (Rihan, 2013), in neural models (Stein, 1967). Hence, a singularly perturbed delay differential equation (SPDDE) involves two small parameters: perturbation as well as delay parameter.

The study of these differential equations is prominent because of their frequent emergence in mathematical modeling of different applications in science and technology such as:

Environmental issues

In the study of major environmental issues like water pollution, appropriate uses of natural resources to save environment such as solar energy. The study of bearing of the population of a system of organism can be well explained by a delay model which is prominent to insight pitfalls in the ecosystem due to human error such as the effect of pollution on the expansion of population of an organic system.

In control theory

The problems involving signal transmission in control theory are affected by time delays and the various causes which hinder the signal propagation such as media of propagation of the signal. The study of these mathematical models enables the technology to expand to have cost-effective techniques and to upgrade the services.

In biosciences

One of the factors which is liable for odd behavior of blood cells or nerves cells is a delay (a retardation) and to rein the problems study of the behavior of cells is essential to tackle the problems in ecology, epidemiology, immunology, physiology and neural network.

In the study of deadly diseases

The study of maladies such as cancer, HIV, tumor and swine flu which are jeopardizing human life in recent decades is significant in order to understand the factors affecting the treatment and the rate at which viral is deteriorating the condition of the patient. All these medical problems are demonstrated by delay differential equations. The study of these

mathematical models enables the scientist to endure factors such as the dose of chemotherapy required for a patient because chemotherapy not only control the expansion of cancer cells but also affect the immunity of the bearer. Similarly, a delay model of hospital enables the medical officer to understand the need of essential precautions to take in the hospital to control the spew of infection to the staff members and to other patients. Likewise, cell proliferation in the expansion of tumor is well explored by a delay model.

In heating systems

In current scenario environmental conditions enforce human being to work on man-made systems to live in a contented environment. So, central heating systems, cooling systems are needed. To adapt the less costly techniques with better performance, the study of these systems can well be elaborated by delay models.

And many more such applications in science and technology. Thus, the major issues that are essential to resolve for mankind triggers the mathematicians to work on numerical treatment on SPDDE.

In past decades, gigantic furtherance has been reported in numerical techniques for the solution of the differential equations and many researchers have proposed various techniques to solve SPDDE. Some spline based methods were given by Kumar and Kadalbajoo (Kumar & Kadalbajoo, 2012), Aggarwal and Sharma (Aggarwal & Sharma, 2008), Chakravarthy et al. (Chakravarthy, Kumar, Rao, & Ghate 2015). Singularly perturbed delay differential equation has been treated using B-spline collocation method. The author had selected Shishkin mesh which is adequate to handle singularly perturbed problems (Kumar & Kadalbajoo, 2012).The mesh is constructed in such a way that more mesh points were created in the boundary layer region than outside of those regions.

An optimized B-spline method has been proposed to solve singularly perturbed differential difference equation with delay as well as advance (Aggarwal & Sharma, 2008). Chakravarthy et al. (Chakravarthy, Kumar, Rao, & Ghate 2015) solved these equations using cubic splines in compression. In this article, the author considered the SPDDE of

second order with a large delay. The uniform mesh was selected to partition the domain and method based on cubic spline in compression was used to estimate the solution of the problem. Yuzbagj and Sezer (Yüzbaşı & Sezer, 2013) proposed an exponential collocation method for numerical treatment of SPDDE. The author discussed the solution of the problem by considering the exponential basic set $\{1, e^{-x}, e^{-2x}, \dots, e^{-Nx}\}$ and solution was of the form $y(x) = \sum_{n=0}^N a_n e^{-nx}$. Some computational schemes were given by File and Reddy (File & Reddy, 2013), Swamy et al. (Swamy, Phaneendra, Babu, & Reddy, 2015), and Kumar (Kumar, 2013). Some other techniques were also used such as asymptotic-fitted method by Andargie and Reddy (Andargie & Reddy, 2012). In the reported work, Taylor's expansion was used to approximate the term containing negative shift. In the new equation, a fitted parameter on the highest order derivative was introduced and its value was determined by using theory of singular perturbation. Uniform mesh was selected and the interval $[0, 1]$ was split into N equal parts. Hp Finite Element Method was proposed by Nicaise and Xenophontos (Nicaise & Xenophontos, 2013) to estimate the solution of second order SPDDE. The solution of boundary value problem decomposed into a smooth part, boundary layer part, an interior/interface layer part and a remainder.

A terminal boundary–value technique was used by File and Reddy (File & Reddy, 2014) to solve the singularly perturbed delay differential equation of second order. A terminal point was introduced into the domain and the actual problem was decomposed into two problems. The introduced terminal point is common to both inner and outer regions. The inner region problem is solved by choosing the transformation and the new differential equation for the inner region is solved by using second order classical finite difference scheme. To solve the outer region problem uniform mesh with constant length has been considered and the classical central finite difference scheme is used. Finally, to obtain the solution of the original problem the two solutions obtained at inner region and outer region are combined. Hybrid initial value method was proposed by Subburayan (Subburayan, 2016a) to solve SPDDE of second order considered with the discontinuous coefficient of derivative term. The considered equation was a second order SPDDE with discontinuous convention coefficient and source term. The proposed scheme was reported to be of second

order convergent. An asymptotic-numerical hybrid method is also reported for the solution of SPDDE by Cengizci (Cengizci, 2017)

Recently, SPDDE with mixed shifts has been treated numerically by Swamy et al. (Swamy, Phaneendra, & Reddy, 2016) by applying Galerkin method with exponential fitting. In that work, endured SPDDE was having the retarded term in the convention term and the used scheme was a successive complementary expansion method that provides the highly accurate numerical solution as compared to the reported schemes in literature.

A fourth order finite difference scheme by File et al. (File, Gadisa, Aga, & Reddy, 2017) was reported for numerical treatment of SPDDE. In that work authors considered reaction-diffusion equation for numerical solution. The considered SPDDE was of second order in which the retarded term exist in reaction term and the applied scheme was fourth order uniformly convergent finite difference method of fourth order. The considered SPDDE was:

$$\varepsilon^2 y''(x) + a(x)y(x - \delta) + b(x)y(x) = f(x) ,$$

under the constraints:

$$y(x) = \emptyset(x) \text{ for } -\delta \leq x \leq 0 \text{ and } y(1) = \beta.$$

Cimen (Cimen, 2017) gave a prior estimation for SPDDE with delay parameter in convention term by considering the following equation :

$$\varepsilon y''(x) + a(x)y'(x) + b(x)y'(x - r) + c(x)y(x - r) = f(x) , x \in \Omega$$

subject to the conditions:

$$y(x) = \emptyset(x) \text{ for } x \in \Omega_0 \text{ and } y(l) = A.$$

In this work, the author focused to elucidate the method to evaluate the first and second order derivative of the solution of SPDDE. Kanth and Murali (Kanth & Murali, 2018) studied a nonlinear SPDDE which was first transformed into a system of linear SPDDE and then the system of linear equations was solved by an exponentially fitted spline method. The considered equation was:

$$\varepsilon y''(x) = g(x, y, y'(x - \delta)) \text{ on } (0,1)$$

subject to the constraint:

$$y(x) = \emptyset(x) \text{ for } -\delta \leq x \leq 0 \text{ and } y(1) = \gamma.$$

Sekar and Tamilselvan (Sekar & Tamilselvan, 2018) considered a class of SPDDE of convection-diffusion type of second order for numerical treatment with integral boundary condition and solved the considered equation:

$$-\varepsilon y''(x) + a(x)y'(x) + b(x)y(x) + c(x)y(x-1) = f(x), x \in \Omega$$

under the boundary conditions:

$$y(x) = \emptyset(x) \text{ for } -1 \leq x \leq 0 \text{ and } y(2) = l + \varepsilon \int_0^2 g(x)y(x)dx$$

by using the finite difference scheme. The proposed scheme was tested on numerical illustrations.

1.2 Mathematical modeling

The singularly perturbed delay differential equations are the result of modeling of numerous problems in science and technology. Some of the models are explained are:

1.2.1. Tumor expansion model

A model which explains the study the tumor expansion was proposed by Cui and Xu (Cui & Xu, 2007). As stated by the authors, the proliferation of tumor occurs due to genetic transmutation of abnormal cells and the rate of extension of these cells is much more than the growth of normal cells. In the presented work, the considered model equation demonstrates the delay between the time required in initializing of the cell division and the time of origination of the daughter cells. By considering $y(t)$ as the radius of tumor at time t and τ as time delay, the obtained delay differential equation was of the form given by:

$$y(t) = f(y(t), y(t-\tau)) \text{ for } t > 0, \text{ and } y(t) = \emptyset(t) \text{ for } -\tau \leq t \leq 0$$

1.2.2. Heating systems as delay model

The operation of thermal heating systems such as solar heating systems, central heating systems and so on is deployed on simple thermal heating systems which are composed of

a heater, storage pipes and pump. The pump circulates the heat transfer fluid from the heater to the storage. The retard in heat transfer comes into view due to the movement of fluid through pipes. The delaying effect of pipes plays an important role in the modeling of heater-storage systems in order to utilize maximum solar energy. A model developed for domestic hot water and for water heating in swimming pools had taken delaying effect of pipes into consideration and it was perceived that application of solar energy has been expanded as compared to the models which disregard the delaying effect of pipes (Kicsiny & Farkas, 2012). The use of delay approach for complex heating systems such as combustion system is an augmentation of delay differential equations. Kicsiny (Kicsiny, 2014) developed one such model to elucidate heating systems with pipes. In his work, thermal engineering systems involving heat and mass transfer, fluid mechanics and science of thermodynamics were inspected. The model was based on the white-box model. It has considered both heat exchange and no heat exchange in the heating system and the delay parameter depends upon time and state of the heating system. This time delay was determined by the rate of flow of fluid through the pump.

1.2.3. Delay model of the biological system

The development of the bearing of the population of a system of organisms can be well explained by its mathematical modeling where delay gives the prominent insight into the dynamic conduct of the system. This time delay appears in a polluted ecosystem which is one of the important factors affecting the expansion of the biological system. So, delay differential equations are the result of mathematical modeling explaining organic structure. The disparity and bifurcation in the system emerges due to the time delay. One of the common bifurcations (the division of system into two parts) is hop bifurcation which refers to the division of the system at a point where the firmness turnaround and periodic solution arises as a particular variable changes its values. One such mathematical model of the singularly biological system is proposed by Zhang et al. (Zhang, Jie, & Meng, 2016) by considering the delay parameter.

By considering τ as the time delay of the transformation of immature organisms into mature organisms, $u(t)$ and $v(t)$ as the densities of the immature and mature organisms, $E(t)$ as capture capability of mature creatures at time t , p as a unit price, c is a unit cost, and m is economic profit. $aE(t)v(t)$ represents the total revenue, and $cE(t)$ denotes the total cost. The delay model of the biological system was given by:

$$\begin{aligned}u(t) &= pv(t) - qu(t - \tau) - d_1u(t) - \phi_1y(t)u(t) \\v(t) &= qu(t - \tau) - d_2v(t) - \beta g^2(t) - E(t)g(t) - \phi_2y(t)g(t) \\ \text{and } y(t) &= \theta - hy(t), 0 = E(t)(pg(t) - c) - m.\end{aligned}$$

1.2.4. Delay model in the treatment of HIV

Treatment of human immunodeficiency virus (HIV) infection is one of the major challenge in recent years due to the rapid spew of ailment, which is referred as occupancy of virus in blood that lessens the immunity of the sufferer. In the initial stage, the viral enter the blood due to outer contacts and increases to the summit. The immune cells known as cytotoxic T cells (CTL) get activated and rein the multiplication of the infection, and level of infection experience a decline to a steady state. The chronic infection (full-blown AIDS) is attained by the patient due to the high-level viral set-in blood. The time delays exist because of finite time is required for infected cells to produce virions and definite time is needed by immune cells to retort the viral contagion. One such mathematical model which includes both time delays was considered for analysis by Pawelek et al. (Pawelek, Liu, Pahlevani, & Rong, 2012). The delay differential equation was as follows:

$$\begin{aligned}\frac{dT^*(t)}{dt} &= k_1V(t - \tau_1)T(t - \tau_1) - \delta T^* - d_xET^* \\ \frac{dE(t)}{dt} &= pT^*(t - \tau_2) - d_EE\end{aligned}$$

where $T(t)$ represents the number of uninfected target cells, $T^*(t)$ is productively infected cells, $V(t)$ are free virus, $E(t)$ denotes effector cells and τ_1, τ_2 are time delays.

1.3 Collocation Method

A differential equation can be solved by using an analytical or numerical method. The analytical exploration of differential equations sometimes is laborious, and it is tough to find the exact solution. So, the advanced numerical methods are obliged to easily get the precise solution of the differential equations. The well-known techniques for approximating the solution of differential equations are finite difference method, finite element method, differential quadrature method and lie symmetry method. Finite difference methods involve the determination of approximate derivatives at partitioned points of the domain. Some common finite difference methods are Euler method, Crank-Nicolson method, implicit methods etc. Collocation is a form of finite element method of approximating the solution of the differential equation by satisfying solution at collocation points, which are the few chosen points in the boundary of the problem. This method involves determining the function by passing a polynomial through selected points. And this polynomial can be determined by any set of basic functions for example B-spline, exponential basis functions or wavelets. B-spline basis functions used in this report will be explained in section 1.4. Collocation method is one of the rapid progressing technique because of some merits over other numerical techniques. One of the considerable conveniences of this technique is that its easiness to apply on an ordinary as well as on partial differential equations. And the other main benefit of the scheme is that it provides a piecewise continuous solution of the differential equations.

Collocation method is used to approximate the solution of the differential equation by many researchers. Some of the reported work is as follows:

Mittal and Jain solved nonlinear parabolic partial differential equations by cubic B-spline collocation scheme. (Mittal & Jain, 2012a) The good Boussinesq equation was solved by Siddiqi and Arshed (Siddiqi & Arshed, 2014). Mohammadi (Mohammadi, 2014) solved Euler-Bernoulli beam models by using sextic B-spline collocation method. Morinishi et al. (Morinishi, Tamano, & Nakabayashi, 2003) used collocation technique for compressible turbulent channel flow. Botella (Botella, 2002) solved Navier-Stokes equation by applying

collocation method. Diffusion problems have been solved using cubic B-spline collocation method by Gupta and Kukreja (Gupta & Kukreja, 2012). Lakestani and Dehghan (Lakestani & Dehghan, 2012) have solved generalized Kuramoto-Sivashinsky equation by using spline collocation method. Dag et al. (Dag, Hepson, & Kacmaz, 2014) solved Burger's equation by cubic trigonometric B-spline collocation technique. Abbas et al. (Abbas, Majid, Ismail, & Rashid, 2014a) proposed a finite difference collocation scheme for the numerical treatment of a one-dimensional wave equation.

Time-dependent HJB equations were solved using multivariate B-splines collocation by Govindarajan et al. (Govindarajan, Visser, & Krishnakumar, 2014). Singularly perturbed differential equations have also been treated using collocation method by Kadalbajoo and Kumar (Kadalbajoo & Kumar, 2008). Kadalbajoo and Gupta (Kadalbajoo & Gupta, 2009) solved singularly perturbed convection-diffusion problem by using parameter uniform B-spline collocation method. Kadalbajoo and Arora (Kadalbajoo & Arora, 2009) used B-spline collocation method for solution of the singular-perturbation problem using artificial viscosity. Rao and Kumar (Rao & Kumar, 2007) applied optimal B-spline collocation method for approximating the solution of self-adjoint singularly perturbed boundary value problems. Nonlinear fractional differential equations have been solved by using spline collocation method by Pedas and Tamme (Pedas & Tamme, 2014). A new approach including semi orthogonal B-spline wavelet collocation scheme was proposed by Sahu and Ray (Sahu & Ray, 2014) to solve Fredholm integral equations of the second kind. Li (Li, 2012) solved fractional differential equations using cubic B-spline wavelet collocation method.

1.4 B-spline

1.4.1 Introduction of spline

Splines are the computational curves which are the piecewise polynomial approximation of the available data and is continuously differentiable to some degree on an interval of the boundary. The concept of splines is used in designing of the ships, enshrining of car

designs, design of buildings, aerospace industry for delineation (designing), constructing, congregating (assembling) different parts of the aircraft and many more. Romans used wooden cuttings for making the fickle(variable) wooden ribs to strengthen their ships hulls. The idea of spline is shown in Figure 1.1(Schoenberg, 1946).

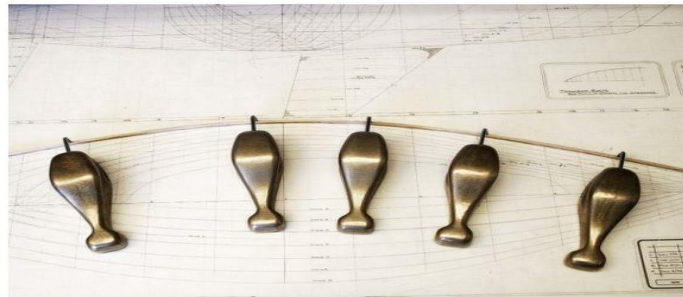


Figure 1.1: Spline template

The concept of spline curves was introduced to have a piecewise smooth polynomial in lieu of having a higher degree polynomial, which is difficult to handle. By combining polynomials of lower degree, a smooth polynomial over a specific domain can be obtained irrespective of the number of points in the segment of the domain. This property of splines enables the researchers to easily work for numerical computations by using computerized algorithms.

One more application of bezier curves (which are specific spline curves), in designing a three-dimensional structure of a car proposed by French engineer Pierre Etienne Bezier. Such a 3-D design of the car was not possible with a set of composite curves. To elucidate internal as well as an external outline of the car design demands a variable surface. Figure 1.2 (Townsend, 2015) shows such design of car by bezier curves.

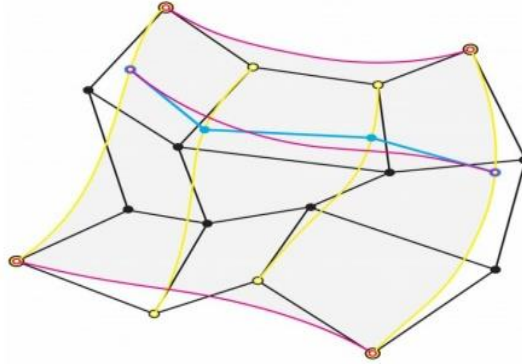


Figure 1.2: 3-D design of car.

In the contemporary time, spline based software such as CAD is broadly used in aerospace engineering for manufacturing of fighter planes and for designing buildings by architectures.

Mathematically, a spline is a piecewise smooth curve characterized by polynomials. To understand this concept, consider a uniform partition of the domain $[a, b]$ as $x_0 < x_1 < x_2 < \dots < x_{N-1} < x_N$ where $x_0 = a$ and $x_N = b$, here x_i 's are referred as knots. A spline function $S(x)$ is defined as:

$$S(x) = \sum_{i=1}^N p_i(x)$$

in domain $[a, b]$, where $p(x)$ is a k^{th} degree polynomial in each subinterval $[x_i, x_{i+1}]$ for $i = 0, 1, 2, \dots, N - 1$ with the characteristic that the polynomial $p(x)$ and its $k - 1$ derivatives are continuous in $[a, b]$.

1.4.2 B-spline

A B-spline is a generalization of the Bezier curves. Schoenberg (Schoenberg, 1946) was the first person who introduced the name B-spline. A B-spline is characterized as a spline function that has minimal support for a given degree, smoothness, and zone partition.

Let us consider partition of domain $[a, b]$ as $x_0 < x_1 < x_2 < \dots < x_{N-1} < x_N$ where $x_0 = a$ and $x_N = b$, here x_i 's are referred to as knots and intervals $[x_i, x_{i+1})$ referred as i th knot

span. The knot partition is said to be uniform or non-uniform partition if the span of knots is equal or unequal respectively. The basis functions are defined as:

$$B_{i,0}(x) = \begin{cases} 1, & \text{if } x_i \leq x < x_{i+1} \\ 0, & \text{otherwise} \end{cases}$$

and $B_{i,j}(x) = \frac{x-x_i}{x_{i+j}-x_i} B_{i,j-1}(x) + \frac{x_{i+j+1}-x}{x_{i+j+1}-x_{i+1}} B_{i+1,j-1}(x)$ where $j = 1, 2, 3, \dots, p$

Then the B-spline curve is defined as:

$$B(x) = \sum_{i=0}^N x_i B_{i,p}(x).$$

In a B-spline, each knot point is associated with the function $B_{i,j}(x)$ which is a polynomial of order k (degree $k - 1$). The shapes of the B-spline functions are as shown below in Figure 1.3.

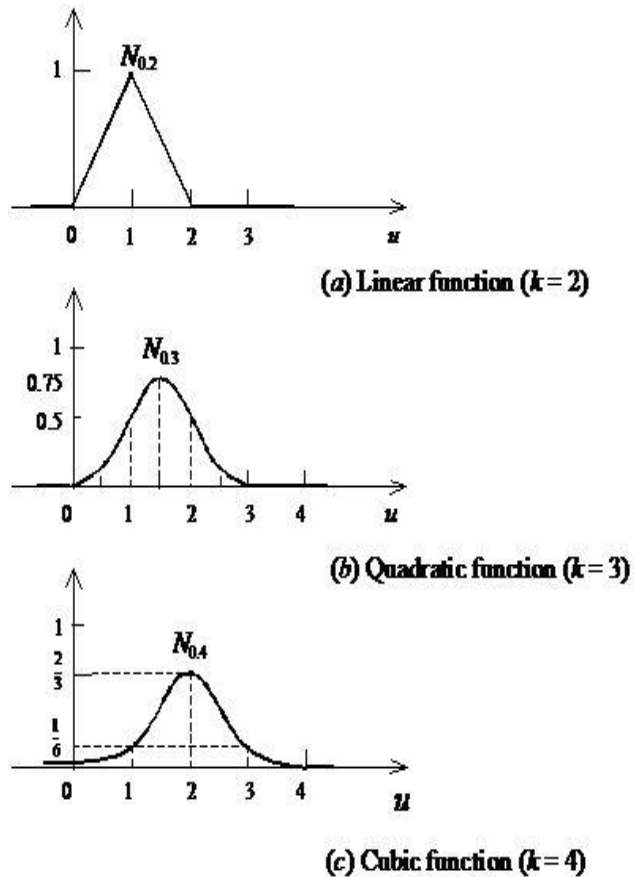


Figure 1.3: B-spline functions

Nowadays, the idea of B-spline has been extended to both rational and non-uniform partitions. The concept of non-uniformly spaced knots along the curve is used in designing of aircrafts as it involves spacing of spline at placing multiple knots in one location in the corner at that point. A new mathematical model to meet all needs of Boeing called Non-Uniform Rational Basis Splines, or NURBS was introduced by combining rational Bezier curves and non-uniform B-Splines.

1.5 Convergence Analysis

Estimation of convergence and its order is prominent to authorize any numerical approach. Convergence measures the closeness of the approximated solution to the exact solution. To

elaborate the meaning of convergence, consider the differential equation of the form $\emptyset(x, y_x) = 0$ with condition $y(0) = y_0$, $0 < x < X$

Any numerical approach used to evaluate the solution of the above equation is convergent if

$$\max_{n \in \{0, 1, \dots, \frac{X}{\Delta x}\}} |Y^n - y^n| \rightarrow 0 \text{ as } \Delta x \rightarrow 0,$$

where Y is exact solution, y is calculated solution and $|Y^n - y^n|$ is absolute error. It means as the step size Δx become smaller, the estimated solution come closer to the true solution, then the applied numerical scheme will be convergent.

The rate of convergence also known as global order of accuracy of a scheme is p , if

$$\max_{n \in \{0, 1, \dots, \frac{X}{\Delta x}\}} |Y^n - y^n| \leq \theta(\Delta x^p) \text{ as } \Delta x \rightarrow 0 \text{ (Jerison, 2007)}$$

A higher order of convergence indicates a faster convergence rate of the numerical method. Convergence analysis of the applied hybrid schemes with truncation error has been covered in this report.

1.6 Error Analysis

To justify the numerical results, it is essential to compare the obtained results with the exact solutions if present or with numerical results computed by the reported numerical approaches in the literature. For numerical treatment of SPDDE, concept of error used in this research work are as follows:

- Absolute error
- Maximum absolute error
- Double mesh principle: As the exact solution of SPDDE is not available, so we used double mesh principle to find the absolute error.

$$E_\epsilon^N = |y_i^N - y_{2i}^{2N}|, 0 \leq i \leq N$$

and $D^N = \max |y_i^N - y_{2i}^{2N}|, 0 \leq i \leq N$

- **Truncation Error**

To find out the order of convergence of a numerical method, truncation error is calculated. In scientific computing and numerical analysis, local truncation error is the error obtained while abbreviating the infinite sum as a finite number.

Figure 1.4 and 1.5 (Fitzpatrick, 2006) shows the truncation error and instability of two methods: Euler's method and fourth order Runge-Kutta method by considering one term and two terms for accuracy (solid curve represents results for a fourth-order Runge-Kutta method and dotted curve for Euler's method plotted against the step-length h).

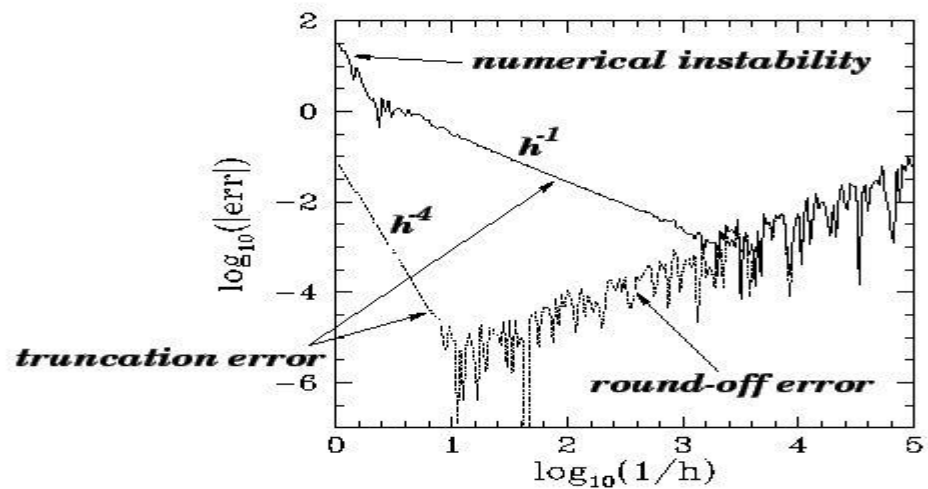


Figure1.4: Error while considering single term accuracy

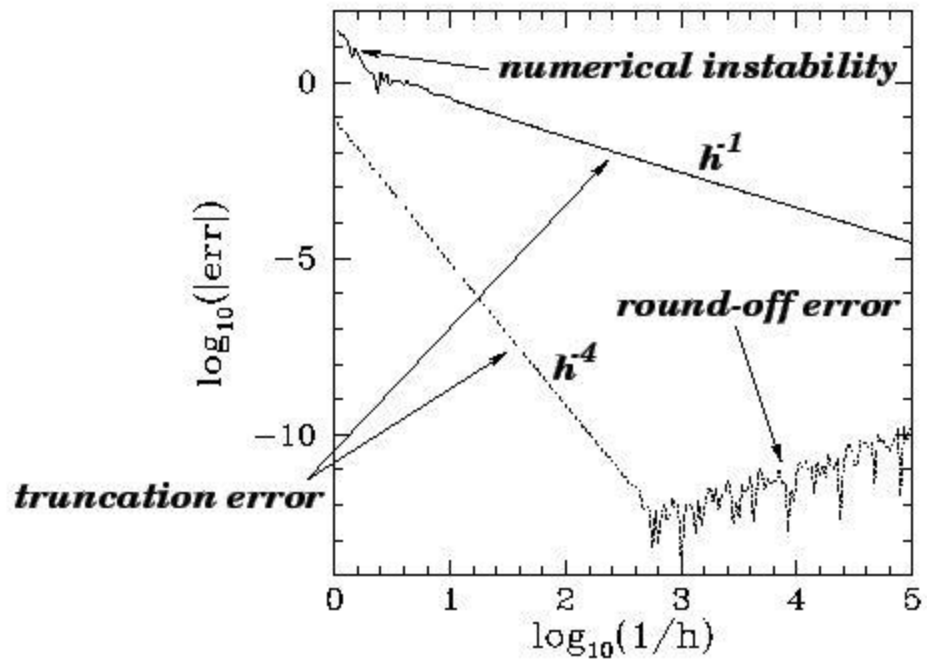


Figure 1.5: Error while considering double term accuracy

Chapter 2

Modified cubic B-spline collocation method for numerical solution of second order singularly perturbed delay differential equation

2.1 Introduction

Many researchers have examined different differential equations with various spline-based techniques. These methods are effectual because of their intelligibility and feasibility. The chief benefit of using these methods is that they are able to approximate the curve up to a certain smoothness. Therefore, the spline-based methods are considered as the premier methods to approximate the solution of differential equations within the domain. This, prompt us for the study of SPDDE by cubic B-spline based numerical method.

The modification in cubic B-spline functions gives different types of shape control tools and the change in the value of nodal point effects the shape of the smooth curve. One of the advantages of weight modification in the basis of B-spline is to obtain fine tuning of the shape of the curve as shown in Figure 2.1 (Juhász & Hoffmann, 2002). This change exerts strong clench (grip) on the positioning of the curve in the convex hull property region (which states that the curve lies within the convex set of its knot points).

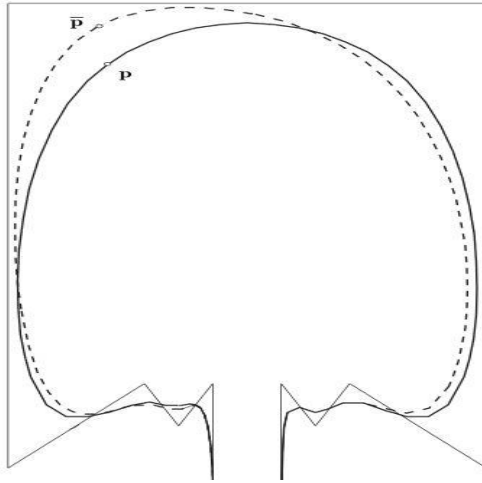


Figure 2.1: Solid lines present cubic B-spline curve and dotted lines show its modified curve

Mathematically, the alteration in the basis functions facilitates the calculation work as the resultant system of the matrix obtained is diagonally dominant and relaxes the calculations on the boundary of the problem. So, in this work, modified B-spline collocation technique has been used to imprecise the solution of SPDDE of second order. The concept of alteration in the basis has been used by many researchers to solve diverse differential equations. Mittal and Jain (Mittal & Jain, 2013) applied this scheme to find the solution of non-linear Fisher's reaction-diffusion equation. Mittal and Bhatia (Mittal & Bhatia, 2014) treated nonlinear Sine-Gordon equation by modified cubic B-spline collocation method. Arora and Singh (Arora & Singh, 2013) solved Burgers' equation by modified cubic-B-spline differential quadrature method. Mittal and Jain (Mittal & Jain, 2012b) applied B-spline collocation method to approximate the solution of non-linear Burger's equation. One dimensional hyperbolic telegraphic equation of second order tested by Mittal and Bhatia (Mittal & Bhatia, 2013) by using third order splines with collocation method. Fisher's equation was numerically treated by Ersoy and Dag (Ersoy & Dag, 2015b) by extended B-spline collocation method.

2.2 Mesh strategy

To imprecise the numerical solution of SPDDE, the domain $0 \leq x \leq l$ is partitioned into a uniform mesh known as Shishkin mesh. (Kumar & Kadalbajoo, 2012) The piecewise uniform mesh is constructed in such a way that more mesh points are generated in the boundary layer region than the points outside these regions. The given domain $[0, l]$ is divided into two sub intervals $[0, \tau]$ and $[\tau, l]$, that results in partition $\{0=x_0 < x_1 < x_2 < \dots < x_N = l\}$ with N as total partition points.

On the boundary layer, $x = 0$ mesh points are given by

$$x_i = \begin{cases} ih_i, & \text{if } i = 0, 1, 2, 3 \dots \dots, \frac{N}{2} \\ \tau + \left(i - \frac{N}{2}\right)h_i, & \text{if } i = \frac{N}{2} + 1, \frac{N}{2} + 2, \dots \dots, N \end{cases}$$

where

$$h_i = \begin{cases} \frac{2\tau}{N}, & \text{if } i = 1, 2, 3 \dots \dots, \frac{N}{2} \\ \frac{2(l - \tau)}{N}, & \text{if } i = \frac{N}{2} + 1, \frac{N}{2} + 2, \dots \dots N \end{cases}$$

On the boundary layer, $x = l$ mesh points are given by

$$x_i = \begin{cases} ih_i, & \text{if } i = 0, 1, 2, 3 \dots \dots, \frac{N}{2} \\ l - \tau + \left(i - \frac{N}{2}\right)h_i, & \text{if } i = \frac{N}{2} + 1, \frac{N}{2} + 2, \dots \dots, N \end{cases}$$

where

$$h_i = \begin{cases} \frac{2(l - \tau)}{N}, & \text{if } i = 1, 2, 3 \dots \dots, \frac{N}{2} \\ \frac{2(\tau)}{N}, & \text{if } i = \frac{N}{2} + 1, \frac{N}{2} + 2, \dots \dots N \end{cases}$$

2.3 Modified cubic B-spline method

An approximation to the solution is $y(x) = \sum_{i=-1}^{N+1} \alpha_i B_i(x)$

where α_i 's are unknown real coefficients and $B_i(x)$'s are the B-spline basis functions. The cubic B-spline B_i for $i = -1, 0, 1, 2, \dots, N + 1$ is as follow:

$$B_j = \frac{1}{h^3} \begin{cases} (x - x_{j-2})^3, & x \in [x_{j-2}, x_{j-1}), \\ (x - x_{j-2})^3 - 4(x - x_{j-1})^3, & x \in [x_{j-1}, x_j), \\ (x_{j+2} - x)^3 - 4(x_{j+1} - x)^3, & x \in [x_j, x_{j+1}), \\ (x_{j+2} - x)^3, & x \in [x_{j+1}, x_{j+2}), \\ 0, & \text{otherwise.} \end{cases}$$

The set of functions $\{B_{-1}, B_0, B_1, \dots, B_N, B_{N+1}\}$, form a basis for the function defined over the region $0 \leq x \leq 1$. At nodal points, the values of $B_i(x)$, $B_i'(x)$, $B_i''(x)$ are given below:

Table 2.1: B-spline basis values

	Nodal Values				
	x_{i-2}	x_{i-1}	x_i	x_{i+1}	x_{i+2}
$B_i(x)$	0	1	4	1	0
$B_i'(x)$	0	3/h	0	-3/h	0
$B_i''(x)$	0	6/h ²	-12/h ²	6/h ²	0

Modified cubic B-spline basis function has been used to solve the singularly perturbed delay differential equation. A diagonal leading system of differential equations is obtained by modifying the cubic B-spline basis function into a new set of basis functions. Below is the procedure of modifying the basis functions:

$$\begin{aligned}
\tilde{B}_0(x) &= B_0(x) + 2B_{-1}(x), \\
\tilde{B}_1(x) &= B_1(x) - B_{-1}(x), \\
\tilde{B}_i(x) &= B_i(x) \text{ for } i = 2, 3, \dots, N-2 \\
\tilde{B}_{N-1}(x) &= B_{N-1}(x) - B_{N+1}(x), \\
\tilde{B}_N(x) &= B_N(x) + 2B_{N+1}(x).
\end{aligned}$$

To approximate the solution of SPDDE using modified cubic B-spline collocation method, the imprecise result defined as:

$$y(x) = \sum_{i=0}^N \alpha_i \tilde{B}_i(x)$$

By using above and the values of $\tilde{B}_i(x)$ at nodal points from Table 2.1 following equation has been obtained:

$$\begin{aligned}
y(x_0) &= 6 \alpha_0 \\
y(x_i) &= \alpha_{i-1} + 4 \alpha_i + \alpha_{i+1}, \quad i = 1, 2, 3, \dots, N-1, \\
y(x_N) &= 6 \alpha_N
\end{aligned}$$

And the value of derivatives $y'(x)$ and $y''(x)$ at nodal points are given as:

$$\begin{aligned}
h y'(x_0) &= -6\alpha_0 + 6\alpha_1, \\
h y'(x_i) &= -3\alpha_{i-1} + 3\alpha_{i+1}, \quad 1 \leq i \leq N-1, \\
h y'(x_N) &= -6\alpha_{N-1} + 6\alpha_N, \\
h^2 y''(x_0) &= 0, h^2 y''(x_i) = 6\alpha_{i-1} - 12\alpha_i + 6\alpha_{i+1}, \quad 1 \leq i \leq N-1, h^2 y''(x_N) = 0
\end{aligned}$$

2.4 First-exist time problem

In this work, second order SPDEs has been considered for numerical treatment using collocation technique with modified cubic B-spline. The endured SPDDE emerge from the model first-exist time problem using formulated by stein (Stein, 1967) describes the regulation of the required time for the causation of action potential in nerve cell by random synaptic inputs in the dendrites. The input of the distribution is taken as a Poisson process with exponential decay between the inputs. The decay between the inputs is exponential and the input of the distribution was taken as a Poisson process (Lange & Miura, 1982) (Lange & Miura, 1994). The problem for expected first-exist time $y(x)$, is given by:

$$\frac{\sigma^2}{2} y'' + (\mu - x)y' + \lambda_I y(x - a_I) + \lambda_E y(x + a_E) - (\lambda_{\lambda E} + \lambda_I)y = -1$$

with the boundary condition:

$$y \equiv 0, \quad x \notin (x_1, x_2).$$

where y is the expected first-exist time and exponential decay between synaptic inputs is given by first-order derivative term $-xy'$. The excitatory and inhibitory synaptic inputs given by undifferentiated terms, modeled as Poisson process with mean rate λ_E and λ_I respectively, the membrane potential a_E and a_I , depend on voltage and are small quantities.

2.4.1 SPDDE from stein model

We considered the following singularly perturbed differential equation with a minute delay

$$\varepsilon^2 y''(x) + a(x)y(x - \delta) + b(x)y(x) = f(x), \quad 0 < x < 1 \quad (2.1)$$

subject to conditions:

$$y(x) = \emptyset(x) \text{ on } -\delta \leq x \leq 0, y(1) = \gamma, \quad (2.2)$$

where $0 < \varepsilon \ll 1$ and $\delta(0 < \delta \leq 1)$. $a(x), b(x), f(x)$ and $\emptyset(x)$ are sufficiently smooth functions and γ is a constant. When the shift δ vanish, sign of $(a(x) + b(x))$ determines

the behavior of the solution of the problem (2.1), (2.2). Positive value of $(a(x) + b(x))$ indicates that the solution of problem shows oscillatory behavior and negative $(a(x) + b(x))$ depicts that the solution shows layer behavior. In particular, the layer behavior of the solution is destroyed when the delay is large, and the solution begins to exhibit oscillation behavior.

In this work, Taylor's series has been used to manage the retarded expression. Then the resultant differential-difference equation becomes:

$$p(x)y'' + q(x)y' + r(x)y(x) = f(x) \quad (2.3)$$

where $p(x) = (\varepsilon^2 + \delta^2/2)a(x)$, $q(x) = -\delta a(x)$, $r(x) = a(x) + b(x)$.

2.4.2 Solution of SPDDE with a small shift by collocation method

Collocation method is applied by electing collocation points selected to concur with nodes and substituting the values of y_i, y_i' and y_i'' at nodal points in equation. This results a system of $N + 1$ linear equations in $N + 1$ variables.

$$t_i^- \alpha_{i-1} + t_i \alpha_i + t_i^+ \alpha_{i+1} = h^2 f_i, \quad 1 \leq i \leq N - 1 \quad (2.4)$$

where

$$t_i^- = 6p(x_i) - 3hq(x_i) + h^2r(x_i),$$

$$t_i = -12p(x_i) + 4h^2r(x_i),$$

$$t_i^+ = 6p(x_i) + 3hq(x_i) + h^2r(x_i)$$

The given boundary conditions become,

$$6\alpha_0 = \phi_0 \text{ and } 6\alpha_N = \gamma.$$

Now we have $N + 1$ linear equations

$$A\alpha=B$$

where $\alpha = [\alpha_0, \alpha_1, \alpha_2, \dots, \alpha_N]^T$ with right hand side $B = [b_0, b_1, b_2, \dots, b_N]^T$ and coefficient matrix given by:

$$A = \begin{bmatrix} 1 & 0 & \dots & \dots & \dots & \dots & \dots & \dots & 0 \\ t_1^- & t_1 & t_1^+ & 0 & \dots & \dots & \dots & \dots & 0 \\ \vdots & \vdots & \vdots & \vdots & \vdots & \vdots & \vdots & \vdots & \vdots \\ \vdots & \vdots & \vdots & \vdots & \vdots & \vdots & \vdots & \vdots & \vdots \\ 0 & \dots & 0 & t_i^- & t_i & t_i^+ & 0 & \dots & 0 \\ \vdots & \vdots & \vdots & \vdots & \vdots & \vdots & \vdots & \vdots & \vdots \\ \vdots & \vdots & \vdots & \vdots & \vdots & \vdots & \vdots & \vdots & \vdots \\ 0 & \dots & \dots & \dots & \dots & 0 & t_{n-1}^- & t_{n-1} & t_{n-1}^+ \\ 0 & \dots & \dots & \dots & \dots & \dots & \dots & 0 & 1 \end{bmatrix}$$

$$B = \left(\frac{\theta_0}{6}, h^2 f_1, \dots, h^2 f_{N-1}, \frac{\gamma}{6} \right)^T$$

2.4.3 Numerical examples

Example 2.1:

$$\varepsilon^2 y''(x) + 0.25y(x - \delta) - y(x) = 1,$$

with restriction

$$y(x) = 1, -\delta \leq x \leq 0, \quad y(1) = 0.$$

The maximum absolute error obtained for Example 2.1 for different values of shift parameter is shown in Table 2.2-2.3 for different values of shift and perturbation parameter, respectively. It is observed that maximum absolute error decreases as ε increases. On the other side, the maximum absolute error decreases and width of layer increases with increase in δ . Figure 2.2 shows the results obtained for this example.

Example 2.2:

$$\varepsilon^2 y''(x) + y(x - \delta) + 2y(x) = 1,$$

with restriction

$$y(x) = 1, -\delta \leq x \leq 0, \quad y(1) = 0.$$

Table 2.4 represents the results obtained for Example 2.2 for distinct values of N. It is observed that the absolute error (Abs. error) decreases with increase in N. Figure 2.3-2.4 shows oscillatory behavior of the solution.

Example 2.3:

$$\varepsilon^2 y''(x) - 2e^{-x}y(x - \delta) - y(x) = 1,$$

with restriction

$$y(x) = 1, -\delta \leq x \leq 0, \quad y(1) = 0.$$

Table 2.5 - 2.8, shows obtained solution and maximum absolute error (Max Abs. Error) obtained for Example 2.3 for different values of shift parameter and ε respectively. It is detected that maximum absolute error decreases as ε increases. Figure 2.5 shows the results obtained for this example.

2.5 Generalized perturbed delay differential equation

Consider the following general boundary value problem:

$$\varepsilon y''(x) + a(x)y'(x - \delta_1) + b(x)y(x - \delta_2) + c(x)y(x) = f(x), \quad 0 < x < l,$$

with restrictions:

$$y(x) = \phi(x) \text{ on } -\delta \leq x < 0 \text{ where } \delta = \max(\delta_1, \delta_2) \text{ and } y(l) = \gamma,$$

where $0 < \varepsilon \ll 1$ and δ_1 and δ_2 are delay parameters. $a(x), b(x), c(x)$ and $f(x)$ are sufficiently smooth functions on $[0, l]$ and $\phi(x)$ is a smooth function on $[-\delta, 0)$.

For the different values of parameters there exist four different types of perturbed delay differential equations as follows:

Type 1: Considering $\delta_1 = \delta_2 = \delta$ and $l = 1$, the problem becomes:

$$\varepsilon y''(x) + a(x)y'(x - \delta) + b(x)y(x - \delta) + c(x)y(x) = f(x), \quad 0 < x < 1,$$

under restrictions:

$$y(x) = \phi(x) \text{ on } -\delta \leq x < 0 \text{ and } y(1) = \gamma,$$

This system of equation exhibits layer on the left side or right side of domain depending on the sign of $a(x)$. If $a(x) > 0$, the layer exits on the left side otherwise on the right side.

Type 2: Considering $\delta_1=0, \delta_2=1, l=2$, and $c(x) = 0$, problem becomes:

$$\varepsilon y''(x) + a(x)y'(x) + b(x)y(x - 1) = f(x), \quad 0 < x < 2,$$

under restrictions:

$$y(x) = \phi(x) \text{ on } -1 \leq x < 0 \text{ and } y(2) = \gamma,$$

above system exhibits boundary layer at $x = 0$ if $a(x) \geq 0$ and if $a(x) < 0$ then system exhibits boundary layer at $x = 2$.

Type 3: Considering $\delta_2=\delta, a(x)=0$ and $l=1$, problem reduces to

$$\varepsilon y''(x) + b(x)y(x - \delta) + c(x)y(x) = f(x), \quad 0 < x < 1,$$

under restrictions:

$$y(x) = \phi(x) \text{ on } -\delta \leq x < 0 \text{ and } y(1)=\gamma,$$

Type 4: Considering $\delta_1=\delta, b(x) = 0$ and $l=1$, problem reduces to

$$\varepsilon y''(x) + a(x)y'(x - \delta) + c(x)y(x) = f(x), \quad 0 < x < 1,$$

under restrictions:

$$y(0) = \phi(x) \text{ on } -\delta \leq x < 0 \text{ and } y(1) = \gamma$$

2.5.1 Description of method for the numerical solution of generalized perturbed delay differential equation

To approximate the retarded argument in the considered equation following Taylor's series is used:

$$y'(x - \delta_1) \approx y'(x) - \delta_1 y''(x)$$

and

$$y(x - \delta_2) \approx y(x) - \delta_2 y'(x) + \left(\frac{\delta_2^2}{2}\right) y''(x)$$

On substituting above Taylor's series approximations, equation (2.5) and (2.6) leads to:

$$\begin{aligned} \varepsilon y''(x) + a(x)[y'(x) - \delta_1 y''(x)] + b(x) \left[y(x) - \delta_2 y'(x) + \left(\frac{\delta_2^2}{2}\right) y''(x) \right] \\ + c(x)y(x) = f(x) \end{aligned}$$

$$\text{or } p(x)y''(x) + q(x)y'(x) + r(x)y(x) = f(x) \quad (2.7)$$

$$\text{where } p(x) = \varepsilon - \delta_1 a(x) + \left(\frac{\delta_2^2}{2}\right) b(x), q(x) = a(x) - \delta_2 b(x), r(x) = b(x) + c(x)$$

Collocation method is applied by selecting collocation points selected to concur with nodes and substituting the values of y_i , y'_i and y''_i at nodal points in equation (2.7). This gives a system of N-1 linear equations in N+1 variables.

$$t_i^- \alpha_{i-1} + t_i \alpha_i + t_i^+ \alpha_{i+1} = h^2 f_i, \quad 1 \leq i \leq N - 1$$

where

$$t_i^- = 6p(x_i) - 3hq(x_i) + h^2 r(x_i),$$

$$t_i = -12p(x_i) + 4h^2 r(x_i),$$

$$t_i^+ = 6p(x_i) + 3hq(x_i) + h^2r(x_i)$$

The given boundary conditions become, $6\alpha_0 = \phi_0$ and $6\alpha_N = \gamma$.

Using these values, matrix system of form $AX = B$ has been obtained which is set of $N + 1$ linear equations in $N + 1$ variables $X = [\alpha_0, \alpha_1, \alpha_2, \dots, \alpha_N]^T$ with right hand side $B = [b_0, b_1, b_2, \dots, b_N]^T$ and the coefficient matrix is given by:

$$A = \begin{bmatrix} 1 & 0 & \dots & \dots & \dots & \dots & \dots & 0 \\ t_1^- & t_1 & t_1^+ & \dots & \dots & \dots & \dots & 0 \\ \vdots & \vdots & \vdots & \vdots & \vdots & \vdots & \vdots & \vdots \\ \vdots & \vdots & \vdots & \vdots & \vdots & \vdots & \vdots & \vdots \\ 0 & \dots & 0 & t_i^- & t_i & t_i^+ & 0 & \dots \\ \vdots & \vdots & \vdots & \vdots & \vdots & \vdots & \vdots & \vdots \\ \vdots & \vdots & \vdots & \vdots & \vdots & \vdots & \vdots & \vdots \\ 0 & \dots & \dots & \dots & \dots & t_{n-1}^- & t_{n-1} & t_{n-1}^+ \\ 0 & \dots & \dots & \dots & \dots & \dots & 0 & 1 \end{bmatrix}$$

2.5.2 Convergence

To find the rate of convergence, a procedure has been examined to detect truncation error. By using $y(x_i)$ and $y'(x_i)$, a relation in $y(x_i)$ and $y'(x_i)$ at points x_{i-1}, x_i, x_{i+1} can be obtained as

$$h[Y_N'(x_{i-1}) + 4Y_N'(x_i) + Y_N'(x_{i+1})] = 3[y(x_{i+1}) - y(x_{i-1})]$$

Now using $E(y(x_i)) = y(x_{i+1})$ the above relation can be re-written as

$$(E^{-1} + 4 + E)hY_N'(x_i) = 3(E - E^{-1})y(x_i)$$

or

$$hY_N'(x_i) = \left[\frac{3(E - E^{-1})}{(E^{-1} + 4 + E)} \right] y(x_i)$$

Now substituting $E = e^{hD}$ and expand it in powers of hD , following is obtained:

$$Y'_N(x_i) = y(x_i) - \frac{1}{30} h^4 y^{(4)}(x_i) + O(h^6)$$

So, the local truncation error is $T_i(h_i) = h^4 \left[\frac{1}{30} y^{(4)}(x_i) \right] + O(h^6)$

Let $Y = (y_1, y_2, y_3, \dots, y_{n-1})^t$ and if $\bar{Y} = (\bar{y}_1, \bar{y}_2, \bar{y}_3, \dots, \bar{y}_{n-1})^t$ is the exact solution. We

know that $A\bar{Y} - T(h) = C$, where C is a constant and $T(h)$ is local truncation error.

So, we have $A(\bar{Y} - Y) = T(h)$. Re-writing truncation error in form of error equation

$$AE = T(h)$$

where $E = \bar{Y} - Y = (e_1, e_2, e_3, \dots, e_{n-1})^T$.

The element wise error is $e_j = \sum_{i=0}^n \bar{m}_{k,i} T_i(h)$, for $j = 0, 1, 2, 3, \dots, n$ implies the result

that $e_j \leq \frac{kh^2}{|L_i|}$ where k is a constant independent of h .

So, it is concluded that our method is almost second-order convergent.

2.5.3 Error analysis

To validate the coherence of the scheme, eight test examples have been solved. The results have been achieved using double mesh principle $E_\epsilon^N = \max |y_i^N - y_{2i}^{2N}|, 0 \leq i \leq N$ to calculate maximum absolute error.

Example 2.4:

$$\epsilon y''(x) + (1+x)y'(x-\delta) + \exp(-2x)y(x-\delta) - 2\exp(-x)y(x) = 0,$$

subject to restriction

$$y(x) = 1, \text{ for } -\delta \leq x < 0 \text{ and } y(1) = 0$$

with boundary layer on left side. Table 2.9 shows the results obtained for example 1 with Shishkin mesh and values of parameters used are $\varepsilon = 0.1$, $\delta = 0.01$, $\tau = 0.2$ and N varies from 64 to 1024. It is observed that absolute error decrease as the value of N increases.

Example 2.5:

$$\varepsilon y''(x) - (1 + x)y'(x - \delta) + \exp(-2x)y(x - \delta) - \exp(-x)y(x) = 0,$$

subject to restriction

$$y(x) = 1, \text{ for } -\delta \leq x < 0 \text{ and } y(1) = -1$$

has boundary layer on $x = 1$. Table 2.10-2.12 shows the results for example 2.5 which are obtained by using Shishkin mesh with the different values of the transition parameter with $\varepsilon = 0.1$, $\delta = 0.01$. Figure 2.6 shows the graph of solution of example 2.5 with $N = 256$ with boundary layer on right side.

Example 2.6:

$$\varepsilon y''(x) - 3y'(x) + y(x - 1) = 0,$$

under the boundary restrictions:

$$y(x) = 1 \text{ on } -1 \leq x < 0 \text{ and } y(2) = 2.$$

This example has boundary layer at $x = 2$ with large delay. Table 6 depicts the results for example 3 by using Shishkin mesh for different values of ε with $N = 16$, $\delta = 1$, $\tau = 0.4$.

Example 2.7:

$$\varepsilon y''(x) - 2y'(x) + 5y(x - 1) = 0,$$

with the conditions:

$$y(x) = 1 \text{ on } -1 \leq x < 0 \text{ and } y(2) = 2.$$

Tables 2.14 show the results for 2.7.

Example 2.8:

$$\varepsilon y''(x) + 0.25y(x - \delta) - y(x) = 1,$$

subject to the constraints,

$$\text{value of } y \text{ is } 1 \text{ on } -\delta \leq x < 0 \text{ and } y(1)=0.$$

Example 2.9:

$$\varepsilon y''(x) - 0.25y(x - \delta) - y(x) = 1,$$

subject to the constraints,

$$\text{value of } y \text{ is } 1 \text{ on } -\delta \leq x < 0 \text{ and } y(1)=0.$$

Two examples 2.8 and 2.9 are considered from type (c) with layer and oscillation behavior. Figure 2.7 shows the graph of example 2.7 and table 2.15 shows the results for example 2.9 for different values of delta. Shishkin mesh along fixed value for τ , ε and N have been used for this research work. It is observed that solution improves as the value of delta decreases. Figure 2.8 shows the graph of example 2.8. The graph shows the layer behavior of the solution obtained using Shishkin mesh where the value of $\varepsilon = 0.01$, $\delta=0.001$, N= 32 and $\tau =0.4$.

Example 2.10:

$$\varepsilon y''(x) + y'(x - \delta) - y(x) = 0, x \in [0,1]$$

subject to the restrictions:

$$y(0) =1 \text{ and } y(1) =1$$

Example 2.11:

$$\varepsilon y''(x) - e^x y'(x - \delta) - xy(x) = 0,$$

subject to the restrictions:

$$y(0) = 1 \text{ and } y(1) = 1$$

Both examples given above are with boundary layer on left side. Table 2.16 and 2.17 shows the results of the solution obtained for example 2.10 and 2.11 respectively. In these tables results obtained by uniform mesh and Shishkin mesh are presented with $\tau = 0.4$ (for Shishkin mesh), $\varepsilon = 0.1$ and $\delta = 0.01$. Figure 2.9 shows the graph of Example 2.11 that depicts the solution obtained by using Shishkin mesh and uniform mesh for $N=512$, $\varepsilon = 0.1$ and $\delta = 0.01$. Maximum absolute error obtained using Shishkin mesh and uniform mesh for Example 2.11 has been compared in Table 2.18 for different values of ε with $\delta = 0.001$, $\tau = 0.4$ (for Shishkin mesh), $N=64$ and 128 . It has been observed that the maximum absolute error obtained with Shishkin mesh is less than maximum absolute error obtained with uniform mesh.

2.6 Summary

Due to the application in neurobiology, the considered differential equations trigger the researchers to solve them by distinctive methods. In this chapter, modified cubic B-spline basis functions have been used to solve SPDDE with collocation method. The convergence analysis of the applied scheme has been discussed to test the stability of the method. Boundary of the problem has been partitioned into uniform mesh and piecewise uniform mesh (Shishkin mesh). The result obtained by both meshes has been compared. The presented scheme is easy to use and readily adapted for computer implementation. Based on results obtained, it can be concluded that the proposed method is significant for the solution of second order singularly perturbed differential equations with small shift and for a general SPDDE. It is spotted that the solution obtained using Shishkin mesh improves for large values of N and with a decrease in value of delay. It can be concluded that the method is easy to apply on a variety of SPDDE.

Table 2.2: Maximum absolute error in solution of Example 2.1 with $\delta = 0.01$

ε	N=64	N=128	N=256	N=512
0.01	0.163803	0.033685	0.007710	0.001530
0.02	0.091470	0.021261	0.004989	0.000993
0.03	0.055668	0.013340	0.003144	0.000619

Table 2.3: Maximum absolute error in solution of Example 2.1 with $\varepsilon = 0.01$

δ	N=64	N=128	N=256	N=512
0.200	0.008089	0.001885	0.001160	0.001120
0.020	0.137142	0.030440	0.007072	0.001407
0.002	0.174330	0.032699	0.007367	0.001457

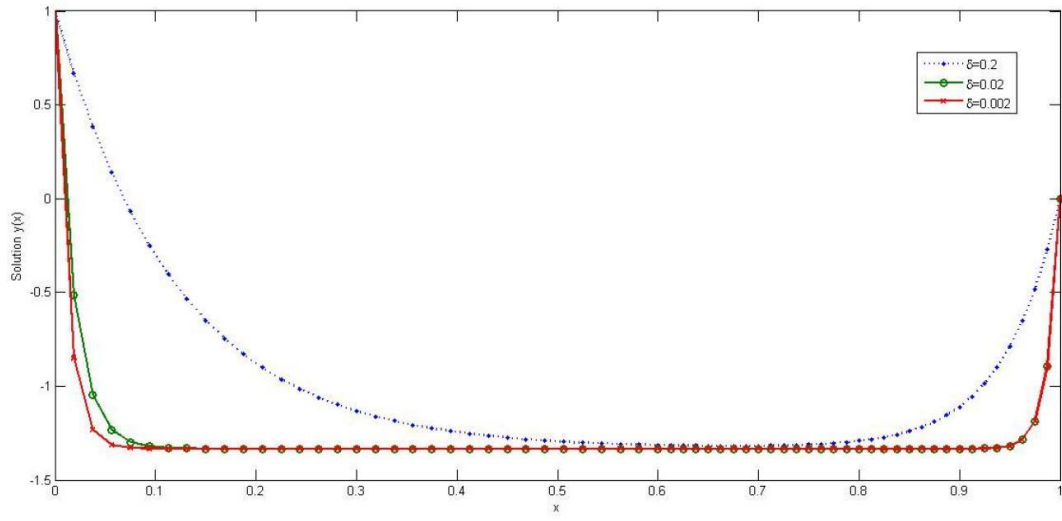


Figure 2.2: Solution of Example 2.1 with $\epsilon = 0.01$

Table 2.4: Solution of Example 2.2 with $\varepsilon = 0.1$ and $\delta = 0.01$

x	N=256	Abs. error	N=512	Abs. error	N=1024	Abs. error	N=2048
0.00	1.000000	0.000000	1.000000	0.000000	1.000000	0.000000	1.000000
0.15	-0.105350	0.003949	-0.108060	0.001232	-0.109010	0.000289	-0.109300
0.30	0.365294	0.007073	0.369878	0.002489	0.371486	0.000881	0.372367
0.45	0.783901	0.007589	0.778667	0.002355	0.776742	0.000430	0.776312
0.60	-0.530560	0.006353	-0.526600	0.002398	-0.525130	0.000925	-0.524200
0.70	1.235750	0.018900	1.227880	0.011030	1.222860	0.006010	1.216850
0.80	0.993411	0.004122	0.991080	0.001791	0.990118	0.000829	0.989289
0.90	-0.879030	0.019991	-0.869690	0.010657	-0.864590	0.005555	-0.859040
1.00	0.000000	0.000000	0.000000	0.000000	0.000000	0.000000	0.000000

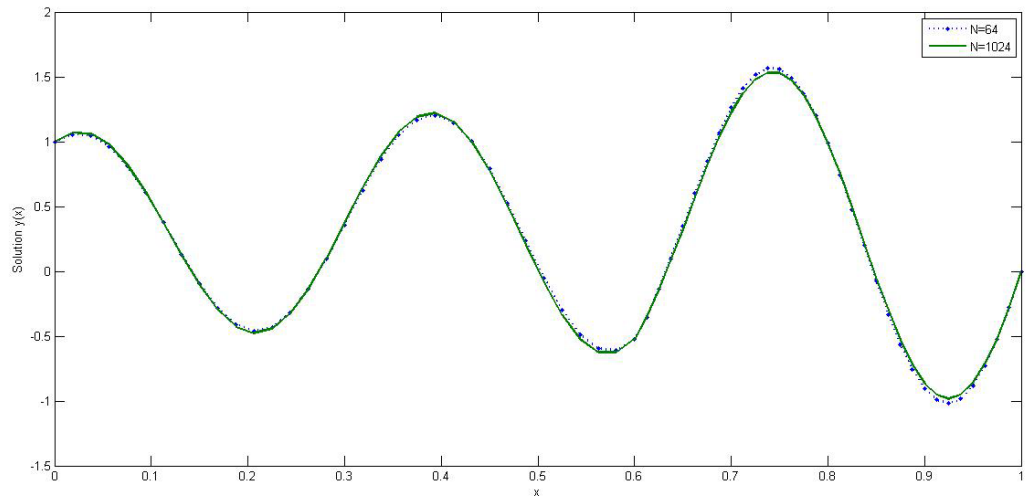


Figure 2.3: Solution of Example 2.2 with $\varepsilon = 0.1$ and $\delta = 0.01$

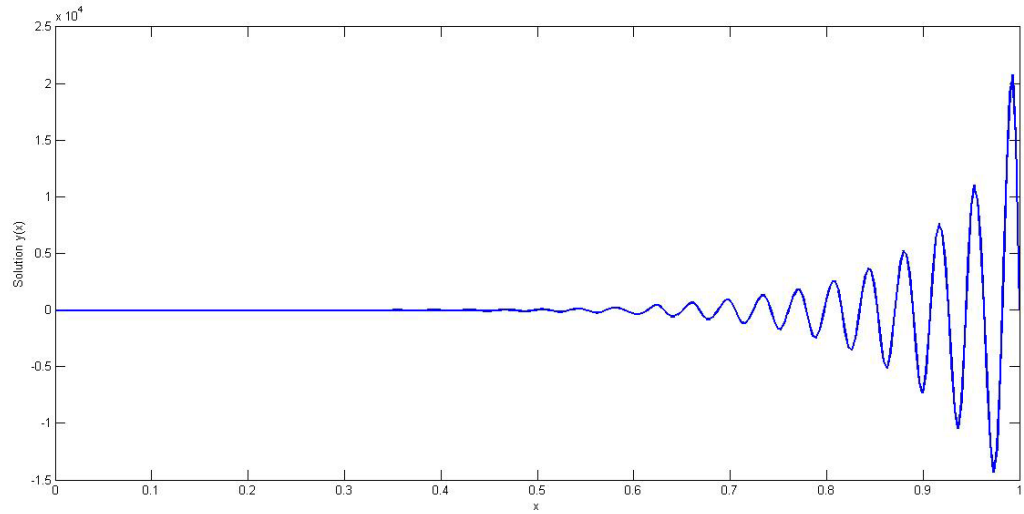


Figure 2.4: Solution of Example 2.2 with $\varepsilon = 0.01$ and $\delta = 0.2*\text{epsilon}$

Table 2.5: Numerical solution of Example 2.3 with $\varepsilon = 0.01$ and $\delta = 0.01$

x	N=128	N=256	N=512	N=1024	N=2048
0.10	-0.354220	-0.357110	-0.357390	-0.357390	-0.357390
0.20	-0.380600	-0.380610	-0.380610	-0.380610	-0.380610
0.30	-0.404400	-0.404400	-0.404400	-0.404400	-0.404400
0.40	-0.429040	-0.428970	-0.428880	-0.428830	-0.428800
0.55	-0.465600	-0.465600	-0.465600	-0.465600	-0.465600
0.70	-0.502960	-0.502960	-0.502960	-0.502960	-0.502960
0.85	-0.540270	-0.540270	-0.540270	-0.540270	-0.540280
1.00	0.000000	0.000000	0.000000	0.000000	0.000000
Max Abs. Error	0.003169	0.000275	8.6E-05	3.1E-05	

Table 2.6: Numerical solution of Example 2.3 with $\varepsilon = 0.02$ and $\delta = 0.01$

x	N=128	N=256	N=512	N=1024	N=2048
0.10	-0.357400	-0.357400	-0.357390	-0.357390	-0.357390
0.20	-0.380620	-0.380620	-0.380620	-0.380620	-0.380620
0.30	-0.404400	-0.404400	-0.404400	-0.404400	-0.404400
0.40	-0.429400	-0.429310	-0.429250	-0.429220	-0.429200
0.55	-0.465610	-0.465610	-0.465610	-0.465610	-0.465610
0.70	-0.502960	-0.502960	-0.502960	-0.502960	-0.502960
0.85	-0.540220	-0.540210	-0.540210	-0.540200	-0.540200
1.00	0.000000	0.000000	0.000000	0.000000	0.000000
Max Abs. Error	0.000199	0.000114	5.4E-05	1.9E-05	

Table 2.7: Numerical solution of Example 2.3 with $\varepsilon = 0.03$ and $\delta = 0.01$

x	N=128	N=256	N=512	N=1024	N=2048
0.10	-0.356630	-0.356520	-0.356490	-0.356480	-0.356480
0.20	-0.380630	-0.380630	-0.380630	-0.380630	-0.380630
0.30	-0.404420	-0.404420	-0.404420	-0.404420	-0.404420
0.40	-0.429730	-0.429650	-0.429590	-0.429560	-0.429550
0.55	-0.465610	-0.465610	-0.465610	-0.465610	-0.465610
0.70	-0.502950	-0.502950	-0.502950	-0.502950	-0.502950
0.85	-0.539150	-0.539110	-0.539100	-0.539100	-0.539100
1.00	0.000000	0.000000	0.000000	0.000000	0.000000
Max Abs. Error	0.000182	9.8E-05	4.4E-05	1.4E-05	

Table 2.8: Maximum absolute error of Example 2.3 with $\varepsilon = 0.001$

δ	N=128	N=256	N=512
0.00100	0.020636	0.007791	0.001744
0.00010	0.002844	0.000428	2E-06
0.00001	0.004215	0.000420	1E-06

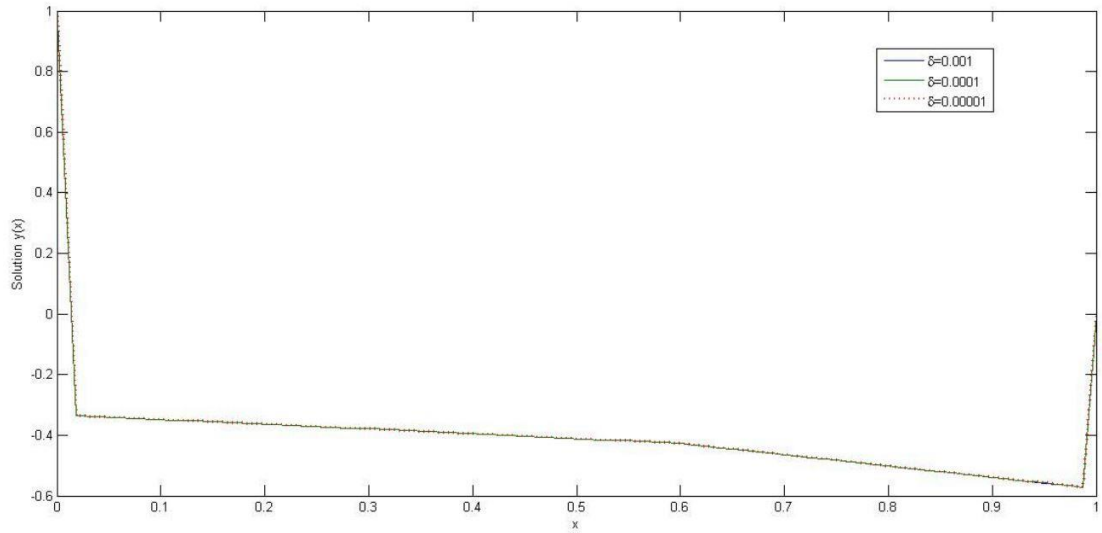


Figure 2.5: Solution of Example 2.3 with $\varepsilon = .001$

Table 2.9: Solution of Example 2.4 with Shishkin mesh

x_i	N=64	Absolute Error	N=128	Absolute Error	N=256	Absolute Error	N=512	Absolute Error	N=1024
0.00	1.000000	0.000000	1.000000	0.000000	1.000000	0.000000	1.000000	0.000000	1.000000
0.05	0.718136	0.001462	0.717282	0.000608	0.716851	0.000177	0.716832	0.000158	0.716674
0.10	0.492861	0.002857	0.491266	0.001262	0.490446	0.000442	0.490273	0.000269	0.490004
0.15	0.306881	0.004481	0.304444	0.002044	0.303198	0.000798	0.302766	0.000366	0.302400
0.20	0.145823	0.006466	0.142375	0.003018	0.140630	0.001273	0.139842	0.000485	0.139357
0.40	0.047802	0.002239	0.046598	0.001035	0.046010	0.000447	0.045739	0.000176	0.0455629
0.60	0.015469	0.000719	0.015089	0.000339	0.014902	0.000152	0.014812	6.19E-05	0.0147500
0.80	0.004554	0.000210	0.004445	0.000101	0.004390	4.64E-05	0.004363	1.94E-05	0.0043439
1.00	0.000000	0.000000	0.000000	0.000000	0.000000	0.000000	0.000000	0.000000	0.000000

Table 2.10: Solution of Example 2.5 with $\tau = 0.2$

x_i	N=32	N=64	N=128	N=256
0.000	1.000000	1.000000	1.000000	1.000000
0.175	0.981658	0.981784	0.981815	0.981828
0.350	0.956725	0.956838	0.956867	0.956885
0.525	0.930907	0.930992	0.931017	0.931031
0.700	0.904432	0.904455	0.904486	0.904514
0.775	0.857557	0.857375	0.857356	0.857352
0.850	0.729837	0.729702	0.729694	0.729689
0.925	0.328554	0.331384	0.332097	0.33228
1.000	-1.00000	-1.00000	-1.00000	-1.00000

Table 2.11: Solution of Example 2.5 with $\tau = 0.3$

x_i	N=32	N=64	N=128	N=256
0.00	1.000000	1.000000	1.000000	1.000000
0.20	0.978269	0.978431	0.978469	0.978483
0.40	0.949264	0.949399	0.949425	0.949432
0.60	0.920099	0.920077	0.920038	0.920010
0.80	0.883276	0.881791	0.880975	0.880532
0.85	0.781700	0.779887	0.778996	0.778539
0.90	0.563645	0.562602	0.561956	0.561568
0.95	0.081295	0.083020	0.083179	0.083056
1.00	-1.00000	-1.00000	-1.00000	-1.00000

Table 2.12: Solution of Example 2.5 with $\tau = 0.4$

x_i	N=32	N=64	N=128	N=256
0.00	1.000000	1.000000	1.000000	1.000000
0.15	0.984917	0.985011	0.985036	0.985045
0.30	0.964160	0.964248	0.964278	0.964291
0.45	0.942001	0.942099	0.942145	0.942162
0.60	0.920521	0.920735	0.920878	0.920940
0.70	0.893295	0.893252	0.893326	0.893351
0.80	0.818751	0.818189	0.818131	0.818112
0.90	0.507499	0.509355	0.509869	0.509992
1.00	-1.000000	-1.000000	-1.000000	-1.000000

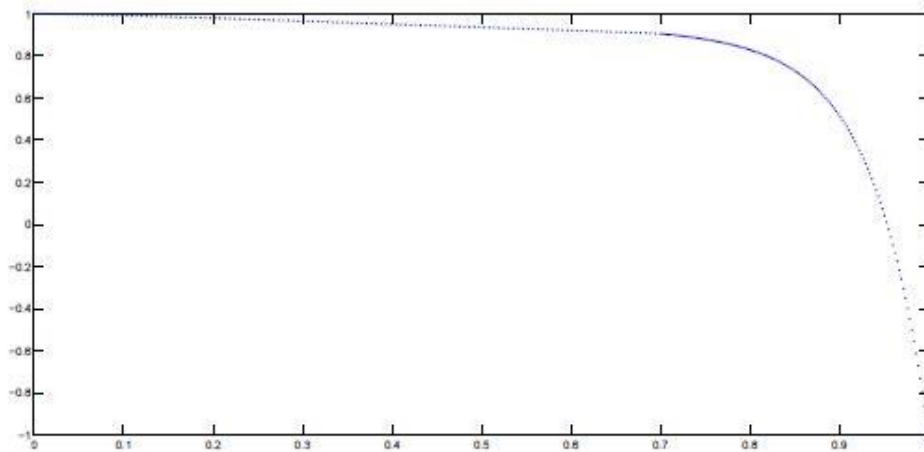


Figure 2.6: Solution of Example 2.5 with Shishkin mesh

Table 2.13: Solution of Example 2.6 with $\tau = 0.4$, $N = 16$ and $\delta = 1$

x_i	$\varepsilon=0.1$	$\varepsilon=0.01$	$\varepsilon=0.001$	$\varepsilon=0.0001$	$\varepsilon=0.00001$
0.00	1.000000	1.000000	1.000000	1.000000	1.000000
0.15	0.869165	0.871692	0.871951	0.871977	0.871979
0.30	0.709945	0.714641	0.715121	0.715170	0.715174
0.45	0.517010	0.523305	0.523950	0.524015	0.524021
0.60	0.285557	0.292629	0.293356	0.293428	0.293435
1.70	0.0149903	0.0218526	0.0225581	0.0226287	0.0226355
1.80	-0.288102	-0.282380	-0.281791	-0.281732	-0.281726
1.90	-0.625973	-0.622489	-0.62213	-0.622094	-0.622091
2.00	-1.000000	-1.000000	-1.000000	-1.000000	-1.000000

Table 2.14: Solution of Example 2.7 with $\tau = 0.4$, $N = 16$ and $\delta = 1$

x_i	$\varepsilon=0.1$	$\varepsilon=0.01$	$\varepsilon=0.001$	$\varepsilon=0.0001$	$\varepsilon=0.00001$
0.00	1.00000	1.00000	1.00000	1.00000	1.00000
0.15	1.12978	1.12985	1.12985	1.12985	1.12985
0.30	1.26161	1.26179	1.26181	1.26182	1.26181
0.45	1.39263	1.39295	1.39298	1.39298	1.39298
0.60	1.51904	1.51942	1.51946	1.51946	1.51946
1.70	1.64009	1.64041	1.64044	1.64045	1.64045
1.80	1.76126	1.76152	1.76154	1.76155	1.76155
1.90	1.88169	1.88185	1.88186	1.88187	1.88187
2.00	2.00000	2.00000	2.00000	2.00000	2.00000

Table 2.15: Solution of Example 2.9 with $\tau=0.4$, $N=8$ and $\varepsilon=0.1$

x_i	$\delta=0.01$	$\delta=0.02$	$\delta=0.03$	$\delta=0.04$	$\delta=0.05$
0.00	1.000000	1.000000	1.000000	1.000000	1.000000
0.10	0.497865	0.499426	0.501045	0.502721	0.504453
0.20	0.104346	0.106637	0.109028	0.111517	0.114101
0.30	-0.180856	-0.178557	-0.176135	-0.173591	-0.170927
0.40	-0.379150	-0.377316	-0.375347	-0.373245	-0.371011
0.55	-0.492079	-0.490994	-0.489776	-0.488425	-0.486941
0.70	-0.474446	-0.474157	-0.473754	-0.473236	-0.472605
0.85	-0.307344	-0.307507	-0.307599	-0.307621	-0.307571
1.00	0.000000	0.000000	0.000000	0.000000	0.000000
Maximum absolute error	0.049830	0.051659	0.053628	0.055730	0.057964

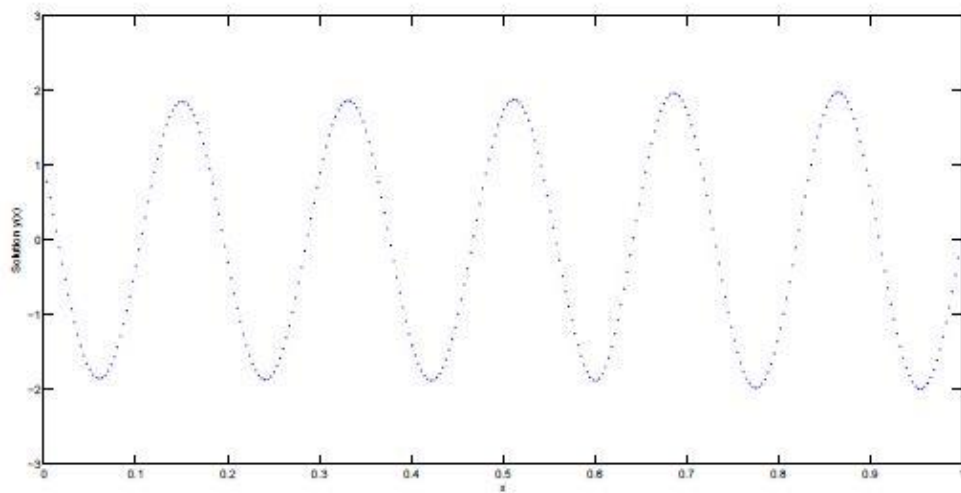


Figure 2.7: Solution of Example 2.8 with $\varepsilon = 0.001$ and $\delta = 0.0003$

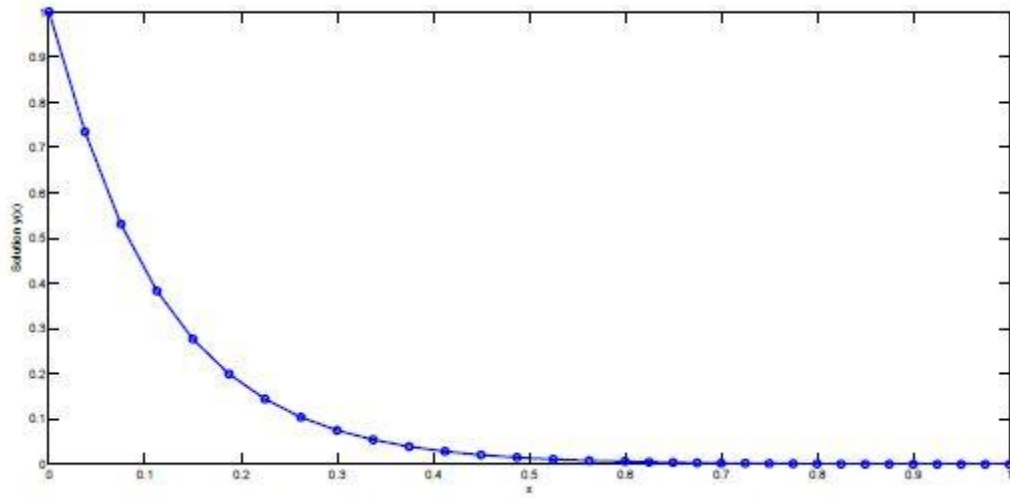


Figure 2.8: Solution of Example 2.9 with Shishkin mesh

Table 2.16: Solution of Example 2.10

Shishkin mesh			Uniform mesh				
x_i	N=128	N=256	N=512	x_i	N=128	N=256	N=512
0.00	1.000000	1.000000	1.000000	0.000	1.000000	1.000000	1.000000
0.10	0.623968	0.623855	0.623466	0.125	0.579792	0.579727	0.579599
0.20	0.542317	0.542186	0.541751	0.250	0.530084	0.530070	0.529922
0.30	0.552180	0.551969	0.551555	0.375	0.568156	0.568134	0.567963
0.40	0.592818	0.592516	0.592160	0.500	0.631718	0.631689	0.631490
0.55	0.662997	0.660353	0.662931	0.625	0.707679	0.707641	0.707421
0.70	0.758543	0.758613	0.758585	0.750	0.793958	0.793918	0.793690
0.85	0.870742	0.870786	0.870808	0.875	0.891020	0.890983	0.890850
1.00	1.000000	1.000000	1.000000	1.000	1.000000	1.000000	1.000000

Table 2.17: Maximum absolute error obtained for Example 2.10 with Shishkin mesh and uniform mesh

	$\varepsilon=0.03$	$\varepsilon=0.05$	$\varepsilon=0.07$	$\varepsilon=0.09$
Max absolute error with Shishkin mesh	0.008304	0.003848	0.002234	0.001484
Max absolute error with uniform mesh	0.010972	0.005341	0.003147	0.002084

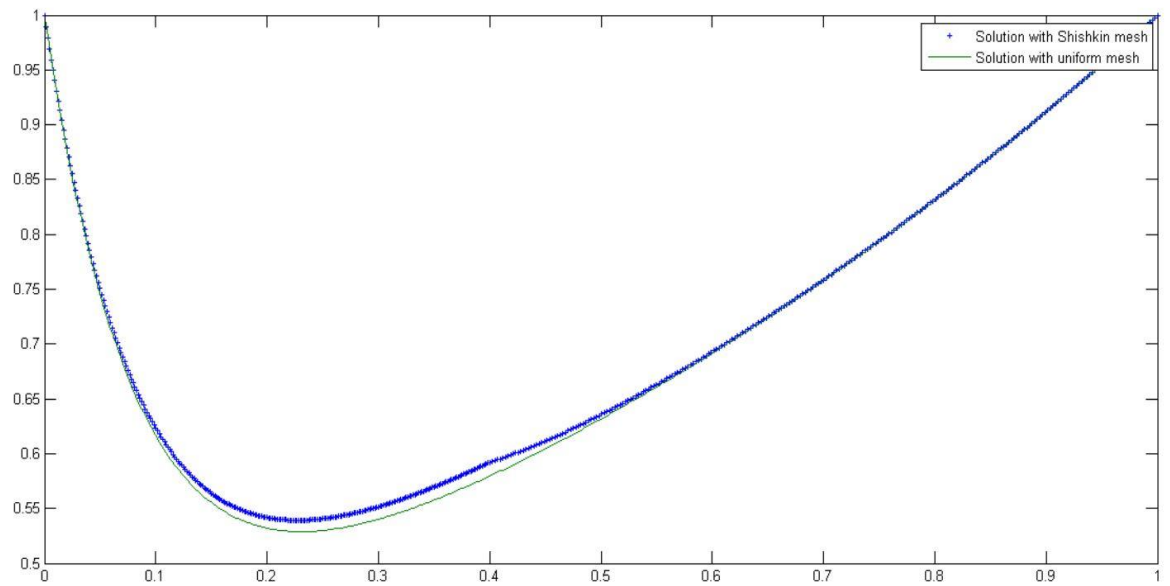


Figure 2.9: Solution of Example 2.10 with uniform and Shishkin mesh

Table 2.18: Solution of Example 2.11

Shishkin mesh				Uniform mesh			
x_i	N=128	N=256	N=512	x_i	N=128	N=256	N=512
0.00	1.000000	1.000000	1.000000	0.000	1.000000	1.000000	1.000000
0.15	0.980245	0.980253	0.980256	0.125	0.972976	0.972991	0.973008
0.30	0.948972	0.948983	0.948989	0.250	0.926161	0.926179	0.926199
0.45	0.910997	0.911033	0.911053	0.375	0.862754	0.862775	0.862800
0.60	0.873931	0.874157	0.874269	0.500	0.791566	0.791585	0.791593
0.70	0.845383	0.845627	0.845733	0.625	0.729398	0.729410	0.729398
0.80	0.820320	0.820559	0.820650	0.750	0.705082	0.705073	0.705049
0.90	0.818859	0.819058	0.819127	0.875	0.767318	0.767265	0.767232
1.00	1.000000	1.000000	1.000000	1.000	1.000000	1.000000	1.000000

Chapter 3

Trigonometric B–spline collocation method for numerical treatment of singularly perturbed delay differential equations

3.1 Introduction

Trigonometric spline functions were introduced by Schoenberg (Schoenberg, 1964) and then the divert aspect of these functions were studied by many researchers (Koch, Lyche, Neamtu, & Schumaker, 1995) (Lyche & Winther, 1979). These functions have been given surveillance in recent years due to their application in the geometric modeling of the surfaces. These functions are used in developing geometric models such as CAGD (computer-aided graphic design) and are piecewise in the space $\{1, \cos(x), \sin(x), \dots, \cos(kx), \sin(kx)\}$.

Definition of trigonometric spline function: In the partition of the domain $[a, b]$ with the knot points $x_1, x_2, x_3, \dots, x_N$, a trigonometric spline function $TS(x)$ of order N fulfill the following constraints:

- i) $TS(x)$ is a periodic function and is continuously differentiable $4N$ times.
- ii) In each sub-interval $[x_i, x_{i+1}]$, the function $TS(x)$ satisfy the differential equation:

$$D^2(D^2 + 1)^2 \dots (D^2 + n^2)^2 y = 0$$

The first order trigonometric functions (Lange & Miura, 1982) are given by:

$$TS_{1,i}(x) = \begin{cases} 1, & \text{for } x_i \leq x < x_{i+1} \\ 0, & \text{otherwise} \end{cases}$$

And the τ ordered trigonometric i^{th} function for $\tau \geq 2$ is given by:

$$TS_{\tau,i}(x) = \sin\left(\frac{x - x_i}{2}\right) B_{\tau-1,i}(x) + \sin\left(\frac{x_{i+\tau} - x}{2}\right) B_{\tau-1,i+1}(x)$$

$$\text{where } B_{\tau-1,\gamma}(x) = \begin{cases} \frac{T_{\tau-1,\gamma}(x)}{\sin\left(\frac{x_{\gamma+\tau+1}-x_{\gamma}}{2}\right)}, & x_{\gamma} < x_{\gamma+\tau-1} \\ 0, & x_{\gamma} = x_{\gamma+\tau-1} \end{cases} \text{ for } \gamma = i \text{ or } \gamma = i + 1$$

Figure 3.1 (Hussain, Abbas, & Irshad, 2017) shows quadratic trigonometric B-spline.

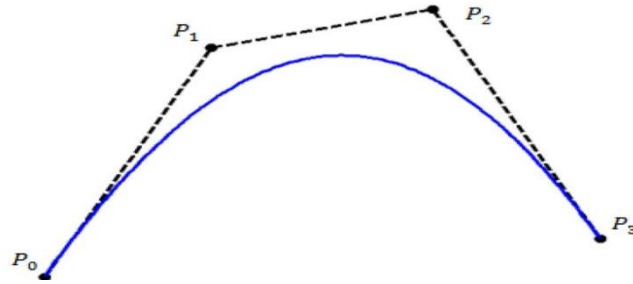


Figure 3.1: Quadratic trigonometric B-spline

In the present time, researchers are working on the solution of many differential equations by numerical schemes based on trigonometric B-spline functions. Nonclassical diffusion problems are treated by Abbas et al. (Abbas, Majid, Ismail, & Rashid, 2014b) by applying numerical method using cubic trigonometric B-spline. Zin et al. (Zin, Majid, Ismail, & Abbas, 2014) solved the wave equation by cubic trigonometric B-spline with finite difference approach. Tamsir et al. (Tamsir, Dhiman, & Srivastava, 2018) simulated the Fisher's reaction-diffusion equations by cubic trigonometric B-spline differential quadrature method. Irk and Keshkin (Irk & Keskin, 2016) approximated solution of the regularized long wave equation by applying Galerkin finite element method. Collocation finite difference scheme based on cubic trigonometric B-spline is used to find numerical solution of the hyperbolic problems by Abbas et al. (Abbas, Majid, Ismail, & Rashid, 2014a). Yaseen and Abbas (Yaseen & Abbas, 2018) presented a numerical technique based on finite difference formulation and cubic trigonometric B-splines to find the solution of time-fractional telegraph equation. Yaseen et al. (Yaseen, Abbas, Ismail, & Nazir, 2017) used cubic trigonometric B-spline collocation approach for numerical solution of the fractional sub-diffusion equations. Alshomrani et al. (Alshomrani, Pandit, Alzahrani, Alghamdi, & Jiwari, 2017) proposed a numerical algorithm based on modified cubic

trigonometric B-spline functions for computational modeling of hyperbolic-type wave equations.

Dag et al. (Dag, Hepson, & Kacmaz, 2014) used cubic trigonometric B-spline collocation method for numerical treatment of Burgers' equation. Arora and Joshi (Arora & Joshi 2016) compared the imprecise numerical solution of one dimensional (1D) hyperbolic telegraph equation with appropriate primary and limiting conditions by two different basis: B-spline and trigonometric B-spline functions with differential quadrature method. A computational approach presented by Arora and Joshi (Arora & Joshi 2018) by using modified trigonometric cubic B-spline for numerical solution of Burgers' equation in one and two dimensions.

So, trigonometric B-spline collocation technique has been considered to simulate SPDDE. A second order SPDDE is solved by trigonometric cubic B-spline collocation method while a third order SPDDE is numerically treated by quintic trigonometric B-spline collocation scheme.

3.2 Numerical solution of second-order problem

Consider the singularly perturbed delay differential equation of the form:

$$Ly \equiv \varepsilon y''(x) + a(x)y(x - \delta) + b(x)y(x) = f(x), 0 < x < 1 \quad (3.1)$$

subject to the boundary conditions:

$$y(x) = \phi(x), \quad x \in [-\delta, 0] \text{ and } y(1) = \gamma$$

where $0 < \varepsilon \ll 1$ and $\phi(x)$ is sufficiently smooth on $[-1, 0]$ and γ is a given constant which is independent of ε .

Delay term is managed by using expression given by:

$$y(x - \delta) = y(x) - \delta y'(x)$$

On substituting above delay term relation in equation (3.1), following equation has been obtained:

$$\varepsilon y''(x) - a(x)\delta y'(x) + (a(x) + b(x))y(x) = f(x)$$

Re-writing above equation following is achieved:

$$p(x)y''(x) + q(x)y'(x) + s(x)y(x) = f(x) \quad (3.2)$$

where $p(x) = \varepsilon$, $q(x) = -a(x)\delta$ and $s(x) = a(x) + b(x)$

3.2.1 Trigonometric cubic B-spline collocation method

The approximate solution of the considered problem is obtained by using the cubic trigonometric B-spline collocation method. The set of functions $\{T_{-1}, T_0, T_1, \dots, T_N, T_{N+1}\}$ form a basis for functions defined over the interval $[0,1]$. Let $\{0 \equiv x_0 < x_1 < x_2 < \dots < x_N \equiv 1\}$ be the partitioned of the domain. The length of each sub intervals is given by h where $h = x_{i+1} - x_i$, $i = 0, 1, 2, \dots, N - 1$.

An approximation to the solution can be expressed in terms of trigonometric B-splines as

$$y(x) = \sum_{i=-1}^{N+1} \alpha_i T_i(x)$$

where α_i 's are unknown coefficients to be determined using the constraint that $y(x)$ satisfies the considered problem at $N+1$ collocation points as well as the boundary conditions and $T_i(x)$'s are the trigonometric B-spline basis functions.

Now, by using trigonometric cubic B-spline basis functions and their values at the nodal points, the value of $y(x)$ and its first and second order derivative can be expressed in terms of α_i 's as:

$$y(x_i) = k_1 \alpha_{i-1} + k_2 \alpha_i + k_1 \alpha_{i+1}$$

$$y'(x_i) = k_3 \alpha_{i-1} + k_4 \alpha_{i+1}$$

$$y''(x_i) = k_5 \alpha_{i-1} + k_6 \alpha_i + k_5 \alpha_{i+1}$$

where $k_1 = \sin^2\left(\frac{h}{2}\right) \csc(h) \csc\left(\frac{3h}{2}\right)$,

$$k_2 = \frac{2}{1+2\cos(h)},$$

$$k_3 = -\frac{3}{4} \csc\left(\frac{3h}{2}\right),$$

$$k_4 = \frac{3}{4} \csc\left(\frac{3h}{2}\right),$$

$$k_5 = \frac{3 \left((1 + 3 \cos(h)) \cos^2\left(\frac{h}{2}\right) \right)}{16 \left(2 \cos\left(\frac{h}{2}\right) + \cos\left(\frac{3h}{2}\right) \right)},$$

$$k_6 = -\frac{3 \cot^2\left(\frac{h}{2}\right)}{2 + 4 \cos(h)}$$

To apply the collocation technique, collocation points are selected in such a way that they concur with the nodal points. On substituting the values of y_i , y_i' and y_i'' at nodal points in equation (3.2) we get a system of $N + 1$ linear equations in $N + 3$ unspecified variables as:

$$E_i^l \alpha_{i-1} + E_i \alpha_i + E_i^r \alpha_{i+1} = f_i, \quad 0 \leq i \leq N \quad (3.3)$$

where

$$E_i^l = p(x)k_5 + q(x)k_3 + s(x)k_1,$$

$$E_i = p(x)k_6 + s(x)k_2$$

$$E_i^r = p(x)k_5 + q(x)k_4 + s(x)k_1$$

Now, to obtain a system with the number of variables equal to the number of equations, boundary conditions have been used to calculate the value of two unknowns α_{-1} and α_{n+1} .

When $i = 0$ in equation (3.3) there exist an unspecified variable α_{-1} and similarly, for $i = n$ in equation (3.3) variable α_{n+1} exists.

From boundary conditions, equation given below has been obtained:

$$\alpha_{-1} = \frac{\phi_0 - k_2 \alpha_0 - k_1 \alpha_1}{k_1} \text{ and } \alpha_{n+1} = \frac{\gamma - k_1 \alpha_{n-1} - k_2 \alpha_n}{k_1}$$

By using the value of α_{-1} and α_{n+1} in the above system, following equation is obtained:

$$\alpha_0 \left(\frac{-k_2}{k_1} E_0^l + E_0 \right) + \alpha_1 (E_0^r - E_0^l) = f_0 - \frac{\phi E_0^l}{k_1} \quad (3.4)$$

and

$$\alpha_{n-1} (E_n^l - E_n^r) + \alpha_n \left(E_n - \frac{k_2}{k_1} E_n^r \right) = f_n - \frac{\gamma E_n^r}{k_1} \quad (3.5)$$

Now we have $N + 1$ linear equations in $N + 1$ variables which can be expressed as matrix system: $AY = B$ where $Y = [\alpha_0, \alpha_1, \alpha_2, \dots, \alpha_N]^T$.

The coefficient matrix A is given by

$$A = \begin{bmatrix} E_0 - \frac{k_2}{k_1} E_0^l & E_0^r - E_0^l & \cdots & \cdots & \cdots & \cdots & \cdots & 0 \\ E_1^l & E_1 & E_1^r & \cdots & \cdots & \cdots & \cdots & 0 \\ \vdots & \vdots & \vdots & \vdots & \vdots & \vdots & \vdots & \vdots \\ \vdots & \vdots & \vdots & \vdots & \vdots & \vdots & \vdots & \vdots \\ 0 & \cdots & 0 & E_i^l & E_i & E_i^r & 0 & \cdots \\ \vdots & \vdots & \vdots & \vdots & \vdots & \vdots & \vdots & \vdots \\ \vdots & \vdots & \vdots & \vdots & \vdots & \vdots & \vdots & \vdots \\ 0 & \cdots & \cdots & \cdots & \cdots & E_i^l & E_{n-1} & E_{n-1}^r \\ 0 & \cdots & \cdots & \cdots & \cdots & \cdots & E_n^l - E_n^r & E_n - \frac{k_2}{k_1} E_n^r \end{bmatrix}$$

$$B = \begin{bmatrix} f(x_0) - E_0^l \left(\frac{\phi_0}{k_1} \right) \\ f(x_1) \\ \vdots \\ \vdots \\ \vdots \\ f(x_{n-1}) \\ f(x_n) - \gamma \left(\frac{E_n^r}{k_1} \right) \end{bmatrix}$$

3.2.2 Convergence analysis

Consider an assumption that the function $y(x)$ is a function with continuous derivatives over the entire domain $[0, 1]$. The tri-diagonal system of the matrix defined above is:

$AY = B$ where $A = (m_{i,j})$, $0 \leq i, j \leq N$ is a tridiagonal matrix with

$$m_{i,i-1} = E_i^l, m_{i,i} = E_i \text{ and } m_{i,i+1} = E_i^r \text{ for } i = 1, 2, 3, 4, \dots, N-1$$

$$m_{0,0} = E_0, m_{0,1} = E_0^r, m_{N-1,N} = E_N \text{ and } m_{N,N} = E_N^r$$

with local truncation error

$$T_i(h_i) = h^2 \left[\left(\frac{k_2}{2(2k_1 + k_2)} \right) \left(\frac{k_3 + k_4}{2k_1 + k_2} \right) y' \right] + O(h^3)$$

and

$$Y = (y_1, y_2, y_3, \dots, y_{n-1})^T$$

Also if $\bar{Y} = (\bar{y}_1, \bar{y}_2, \bar{y}_3, \dots, \bar{y}_{n-1})^T$ is the exact solution and the local truncation error is

$$T(h) = (T_1(h_1), T_2(h_2), T_3(h_3), \dots, T_{n-1}(h_{n-1}))^T$$

Also, it is known that $A\bar{Y} - T(h) = C$, where C is any constant.

Hence it can be said that $A(\bar{Y} - Y) = T(h)$

The choice of h is made sufficiently small, so that matrix A is irreducible and monotone. Thus A^{-1} exists.

$$\text{The error equation can be written as } AE = T(h) \quad (3.6)$$

$$\text{where } E = \bar{Y} - Y = (e_1, e_2, e_3, \dots, e_{n-1})^T$$

$$\text{Hence from equation (3.6), } E = A^{-1}T(h) \quad (3.7)$$

From the theory of matrices it is known that if $A = m_{k,i}$ then $\sum_{i=0}^n m_{k,i} S_i = 1$

where $m_{k,i}$ is the $(k,i)^{\text{th}}$ element of the A^{-1} .

$$\text{Here we have } S_i = \sum_{j=1}^{n-1} m_{i,j} = h^0 B_i,$$

where

$$B_i = \begin{cases} p(x_i)(k_5 + k_6) + q(x_i)(k_4) + s(x_i)(k_1 + k_2) & \text{for } i = 0 \\ p(x_i)(2k_5 + k_6) + q(x_i)(k_3 + k_4) + s(x_i)(2k_1 + k_2) & \text{for } i = 1, 2, 3, \dots, N-1 \\ p(x_i)(k_5 + k_6) + q(x_i)(k_4) + s(x_i)(k_1 + k_2) & \text{for } i = N \end{cases}$$

Therefore,

$$\sum_{i=0}^n m_{k,i} \leq \frac{1}{\min(S_i)} \leq \frac{1}{|B_i|}$$

Thus, from the equation (3.7), the element-wise error is $e_j = \sum_{i=0}^n m_{k,i} T_i(h)$, for

$j = 0, 1, 2, 3, \dots, n$ implies the result that:

$$e_j \leq \frac{kh^2}{|B_i|}$$

where k is a constant independent of h .

Therefore, $\|E\| = O(h^2)$

This concludes that order of convergence is two for the uniform mesh.

3.2.3 Numerical analysis of second-order SPDDE

Example 3.1:

$$\varepsilon y''(x) - 2y(x - \delta) - y(x) = 1$$

subject to the boundary conditions:

$$y(x) = 1, -\delta \leq x \leq 0 \quad \text{and} \quad y(1) = 0.$$

This example illustrates the behavior of SPDDE with the left layer. The maximum absolute error obtained for this example for diverse values of delay parameter and for different values of the perturbed parameter is presented in table 3.1 and 3.2, respectively. The results are compared with the existing method and it is found that results by present method are better as compared to the discussed method. The conduct of the solution is presented in Figure 3.2.

Example 3.2:

Consider

$$\varepsilon y''(x) + 0.25y(x - \delta) - y(x) = 1$$

subject to the boundary conditions:

$$y(x) = 1, -\delta \leq x \leq 0 \quad \text{and} \quad y(1) = 0$$

This example is a SPDDE with left layer and the behavior of the solution obtained for different values of delay parameters is shown in Figure 3.8. The maximum absolute error obtained for various values of delay parameter and for different values of the perturbed parameter is presented in table 3.3 and 3.4 respectively.

Example 3.3:

Consider

$$\varepsilon y''(x) + 0.25y(x - \delta) + y(x) = 1$$

under restriction:

$$y(x) = 1, -\delta \leq x \leq 0 \quad \text{and} \quad y(1) = 0$$

The oscillation behavior of the obtained solution of example 3.3 is presented for four different values of δ in Figure 3.8. In table 3.5, the maximum absolute error calculated for this example for different values of delay parameter is presented.

Example 3.4:

Consider

$$\varepsilon y''(x) + y(x - \delta) + 2y(x) = 1$$

under restriction:

$$y(x) = 1, -\delta \leq x \leq 0 \quad \text{and} \quad y(1) = 0$$

The solution of example 3.4 shows oscillation behavior which is presented in Figure 3.8 for three different values of perturbation parameter and the maximum absolute error found for this example for different values of delay δ and N is presented in table 3.6.

3.2.4 Discussion and conclusions

A numerical approach based on trigonometric cubic B-spline function with collocation method has been used to determine the solution of SPDDE. Uniform mesh has been used to partition the domain. The presented scheme is applied on four numerical examples and the results obtained are shown in tables. Graphs are also plotted for the solution. The results obtained are better than the results obtained by the reported method. The rate of convergence of the presented scheme is calculated as two by application of truncation error. It can be deduced that the given method is easy and efficient to apply on SPDDE.

3.3 Numerical treatment of third order SPDDE

For numerical treatment of third order differential equations, cubic B-spline function-based scheme do not provide good numerical results when applied on some differential equations because the third order derivatives of cubic spline functions become constant. So, higher order B-spline functions are required to approximate the solution of higher order differential equations.

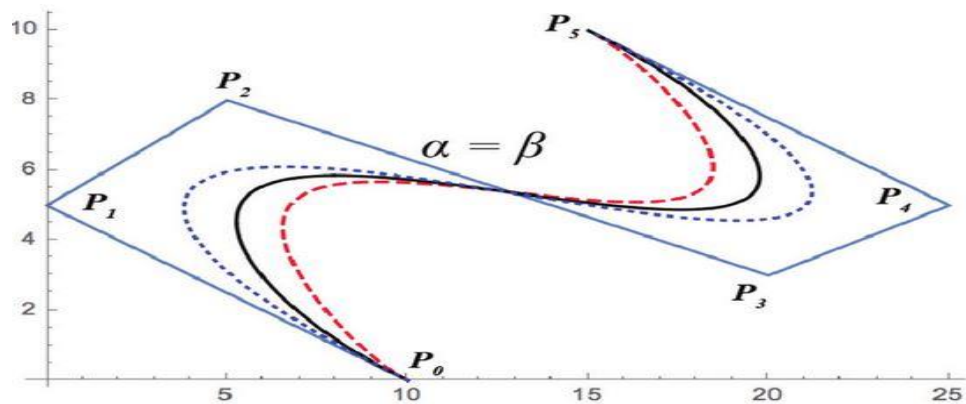


Figure 3.2: Quintic trigonometric spline curve

Figure 3.2 (Misro, Ramli, & Ali, 2017) shows Quintic trigonometric spline curve which is a polynomial curve of degree five. Quintic B-spline function-based scheme is engaging researchers to obtain the numerical solution of differential equations with greater accuracy as compared to the cubic B-spline function. Many researchers have worked with this function-based scheme. Mittal and Arora (Mittal & Arora, 2010) used this scheme to approximate the solution of the Kuramoto–Sivashinsky equation. Irk and Dag (Irk & Dag, 2011) solved the generalized nonlinear Schrodinger equation by applying this collocation scheme. A second order mixed boundary value problem was solved by Lag and Xu (Lang & Xu, 2012) by B-spline collocation method. Arshed (Arshed, 2017) proposed numerical solution of time-fractional super diffusion fourth-order differential equation by Quintic B-spline collocation method. A quintic B-spline finite-element method has been presented by Saka (Saka, 2012) for numerical solution of the nonlinear Schrödinger equation. Zakaria

et al. (Zakaria, Hassan, Hamid, Majid, & Ismail, 2017) presented solution of Boussinesq equation by using both quintic B-spline and quintic trigonometric B-spline interpolation methods. Siddiqi and Arshed (Siddiqi & Arshed, 2013) used quintic B-Spline collocation method for the numerical solution of fourth-order parabolic partial differential equations. Saka et al. (Saka, Dag, & Irk, 2008) used the same method for numerical treatment of the RLW equation.

3.3.1 Problem statement of third order SPDDE

The problem is to find solution $y \in Y = C^1(\bar{\Omega}) \cap C^2(\Omega) \cap C^3(\Omega^*)$ so that it satisfies the following equation:

$$-\varepsilon y'''(x) + a(x)y''(x) + b(x)y'(x) + c(x)y(x) + d(x)y'(x-1) = f(x), \quad x \in \Omega^* \quad (3.8)$$

with boundary conditions:

$$y(x) = \phi(x), \quad x \in [-1, 0], \quad y'(2) = \gamma$$

where ε is very-very small positive number and $a(x), f(x)$ are discontinuous functions as shown below (Subburayan & Mahendran, 2018):

$$a(x) = \begin{cases} a_1(x), & x \in [0, 1] \\ a_2(x), & x \in (1, 2] \end{cases} \text{ and } f(x) = \begin{cases} f_1(x), & x \in [0, 1] \\ f_2(x), & x \in (1, 2] \end{cases}$$

The functions $a(x)$ and $f(x)$ are sufficiently smooth and bounded on Ω^* , $b(x), c(x)$ and $d(x)$ are sufficiently smooth on $\bar{\Omega}$, where $\Omega^* = \Omega^+ \cup \Omega^-$, $\Omega^- = (0, 1)$, $\Omega^+ = (1, 2)$ and $\Omega = (0, 2)$.

To tackle the delay parameter Taylor's series up to second order accuracy is used as

$$y'(x-1) = y'(x) - y''(x)$$

Following equation is obtained using the above value in equation (3.8),

$$P(x)y'''(x) + Q(x)y''(x) + R(x)y'(x) + S(x)y(x) = f(x) \quad (3.9)$$

where $P(x) = -\varepsilon$, $Q(x) = a(x) - d(x)$, $R(x) = b(x) + d(x)$ and $S(x) = c(x)$.

3.3.2 Existence of solution

Theorem: The equation (3.8) has solution $\bar{y} = (y_1, y_2)$ where $y_1 \in C^0(\bar{\Omega}) \cap C^1(\Omega \cup \{2\})$ and $y_2 \in C^0(\bar{\Omega}) \cap C^1(\Omega) \cap C^2(\Omega^*)$.

Proof: As discussed by Subburayan and Mahendran (Subburayan & Mahendran, 2018).

3.3.3 Quintic trigonometric collocation scheme

Quintic trigonometric B-spline with collocation scheme is used for numerical solution of the considered SPDDE. Let the partitioned of the domain be $\{0 \equiv x_0 < x_1 < x_2 < \dots < x_N \equiv 2\}$, where $h = x_{i+1} - x_i$. The set of functions $\{T_{5,-2}(x), T_{5,-1}(x), \dots, T_{5,N+2}(x)\}$ form the basis for functions defined over the interval $[0, 2]$. The approximated solution is considered as:

$$y(x) = \sum_{i=-2}^{N+2} \alpha_i T_{5,i}(x)$$

where $T_{5,i}(x)$ the trigonometric B-spline basis function of fifth order as described in (Zakaria, Hassan, Hamid, Majid, & Ismail, 2017) and α_i are unknown coefficients to be determined.

At the nodal points x_i , the function $y(x)$ and its derivatives are determined as:

$$y(x_i) = k_1 c_{i-2} + k_2 c_{i-1} + k_3 c_i + k_2 c_{i+1} + k_1 c_{i+2},$$

$$y'(x_i) = k_4 c_{i-2} + k_5 c_{i-1} + k_6 c_{i+1} + k_7 c_{i+2}$$

$$y''(x_i) = k_8 c_{i-2} + k_9 c_{i-1} + k_{10} c_i + k_9 c_{i+1} + k_8 c_{i+2},$$

$$y'''(x_i) = k_{11} c_{i-2} + k_{12} c_{i-1} + k_{13} c_{i+1} + k_{14} c_{i+2}$$

where the constants k_i for quintic trigonometric B-spline are as follows: *sec*

$$k_1 = \frac{\sin\left(\frac{h}{4}\right)^4}{\sin(h) \sin\left(\frac{3h}{2}\right) \sin(2h) \sin\left(\frac{5h}{2}\right)},$$

$$k_2 = \frac{5+8\cosh}{4 \cosh \cos\left(\frac{h}{2}\right)(1+2 \cos(h))(1+2\cosh+2\cos(2h))},$$

$$k_3 = \frac{5+6 \cos(h) \operatorname{sech} \sec\left(\frac{h}{2}\right)^2}{4+8 \cos(h)+8 \cos(2h)},$$

$$k_4 = \frac{-5\sin\left(\frac{h}{2}\right)^2}{4 \sin\left(\frac{3h}{2}\right) \sin(2h) \sin\left(\frac{5h}{2}\right)},$$

$$k_5 = \frac{-5(1+4\cosh)\operatorname{cosec}\left(\frac{h}{2}\right) \sec(h)}{8(1+2 \cos(h))(1+2 \cos(h)+2 \cos(2h))},$$

$$k_6 = \frac{5(1+4 \cos(h))\operatorname{cosec}\left(\frac{h}{2}\right) \sec(h)}{8(1+2 \cos(h))(1+2 \cos(h)+2 \cos(2h))},$$

$$k_7 = \frac{5\sin\left(\frac{h}{2}\right)^2}{4 \sin\left(\frac{3h}{2}\right) \sin(2h) \sin\left(\frac{5h}{2}\right)},$$

$$k_8 = \frac{5(3+5 \cos(h))}{16\cos(h)(1+2 \cos(h))(1+2 \cos(h)+2 \cos(2h))\sin(h)^2},$$

$$k_9 = \frac{5(3+\cos(h)+4 \cos(2h))}{32 \cos(h) \cos\left(\frac{h}{2}\right)(1+2 \cos(h))(1+2 \cos(h)+2 \cos(2h))\sin\left(\frac{h}{2}\right)^2},$$

$$k_{10} = \frac{-5(2+5 \cos(h)+2 \cos(2h))}{8\cos(h)(1+2 \cos(h)+2 \cos(2h))\sin(h)^2},$$

$$k_{11} = \frac{-5(-1+25 \cos(h))}{128 \cos(h) \cos\left(\frac{h}{2}\right)(1+2 \cos(h))(1+2 \cos(h)+2 \cos(2h))\sin\left(\frac{h}{2}\right)^3},$$

$$k_{12} = \frac{-5(1-27 \cos(h))+2 \cos(2h)}{64\cos(h)(1+2 \cos(h))(1+2 \cos(h)+2 \cos(2h))\sin\left(\frac{h}{2}\right)^3},$$

$$k_{13} = \frac{5(1-27 \cos(h)+2 \cos(2h))}{64\cos(h)(1+2 \cos(h))(1+2 \cos(h)+2 \cos(2h))\sin\left(\frac{h}{2}\right)^3},$$

$$k_{14} = \frac{5(-1+25 \cos(h))}{128 \cos(h) \cos\left(\frac{h}{2}\right)(1+2 \cos(h))(1+2 \cos(h)+2 \cos(2h))\sin\left(\frac{h}{2}\right)^3}$$

Now, by substituting the values of y_i , y'_i , y''_i and y'''_i at nodal points in equation (3.9), a system of $N + 1$ linear equations in $N + 5$ unspecified variables have been obtained as:

$$W_1^i \alpha_{i-2} + W_2^i \alpha_{i-1} + W_3^i \alpha_i + W_4^i \alpha_{i+1} + W_5^i \alpha_{i+2} = f_i, \quad 0 \leq i \leq N \quad (3.10)$$

where

$$W_1^i = k_{11}P(x) + k_8Q(x) + k_4R(x) + k_1S(x),$$

$$W_2^i = k_{12}P(x) + k_9Q(x) + k_5R(x) + k_2S(x),$$

$$W_3^i = k_{10}Q(x) + k_3S(x),$$

$$W_4^i = k_{13}P(x) + k_9Q(x) + k_6R(x) + k_2S(x),$$

$$W_5^i = k_{14}P(x) + k_8Q(x) + k_7R(x) + k_1S(x),$$

To calculate the values of $N + 5$ unknown variables, the two given boundary conditions and two extra conditions as following are used:

$$(i) \quad y_0 = \emptyset \quad (ii) \quad y'(2) = \gamma \quad \text{and} \quad (iii) \quad y''(0) = 0, \quad (iv) \quad y''(2) = 0$$

The variables α_{-1} , α_{-2} , α_{N+1} and α_{N+2} will be calculated by using above four conditions.

By solving the system of equations $y_0 = \emptyset$ and $y''(0) = 0$, values of α_{-2} and α_{-1} has been obtained as:

$$\alpha_{-2} = \frac{Lk_2 - Rk_9}{k_8k_2 - k_1k_9} = A_1 \text{ (say)}$$

$$\text{and } \alpha_{-1} = \frac{Rk_8 - Lk_1}{k_8k_2 - k_1k_9} = A_2$$

where $L = -k_{10}\alpha_0 - k_9\alpha_1 - k_8\alpha_2$ and $R = \emptyset - k_3\alpha_0 - k_2\alpha_1 - k_1\alpha_2$

Similarly, by solving the system of equations $y'(2) = \gamma$ and $y''(2) = 0$, values of α_{N+2} and α_{N+1} has been obtained as below:

$$\alpha_{N+1} = \frac{L_1 k_7 - R_1 k_8}{k_9 k_7 - k_8 k_6} = A_3$$

$$\text{and } \alpha_{N+2} = \frac{R_1 k_9 - L_1 k_6}{k_9 k_7 - k_8 k_6} = A_4$$

where $L_1 = -k_8 \alpha_{N-2} - k_9 \alpha_{N-1} - k_{10} \alpha_N$ and $R_1 = \gamma - k_4 \alpha_{N-2} - k_5 \alpha_{N-1}$

Substituting these values in equation (3.10) for $i = 0, 1, N - 1$ and $i = N$, following equations have been obtained:

$$\alpha_0 W_3^0 + \alpha_1 W_4^0 + \alpha_2 W_5^0 = f_0 - A_1 W_1^0 - A_2 W_2^0 \quad (3.11)$$

$$\alpha_0 W_2^1 + \alpha_1 W_3^1 + \alpha_2 W_4^1 + \alpha_3 W_5^1 = f_1 - A_2 W_1^1 \quad (3.12)$$

$$\alpha_{N-3} W_1^{N-1} + \alpha_{N-2} W_2^{N-1} + \alpha_{N-1} W_3^{N-1} + \alpha_N W_4^{N-1} = f_{N-1} - A_3 W_5^{N-1} \quad (3.13)$$

and

$$\alpha_{N-2} W_1^N + \alpha_{N-1} W_2^N + \alpha_N W_3^N = f_n - A_3 W_4^N - A_4 W_5^N \quad (3.14)$$

Now, considering equations (3.9) and (3.11) to (3.14) for $i = 2, 3, \dots, N - 2$, a system of order $N + 1$, $A\alpha = B$ is obtained with $N + 1$ variables and where $\alpha = [\alpha_0, \alpha_1, \alpha_2, \dots, \dots, \alpha_N]^T$ A is pentadiagonal matrix given by

$$A = \begin{bmatrix} W_3^0 & W_4^0 & W_5^0 & \dots & \dots & \dots & \dots & 0 \\ W_2^1 & W_3^1 & W_4^1 & W_5^1 & \dots & \dots & \dots & 0 \\ W_1^2 & W_2^2 & W_3^2 & W_4^2 & W_5^2 & \vdots & \vdots & \vdots \\ \vdots & \vdots & \vdots & \vdots & \vdots & \vdots & \vdots & \vdots \\ 0 & \dots & W_1^i & W_2^i & W_3^i & W_4^i & W_5^i & \dots \\ \vdots & \vdots & \vdots & \vdots & \vdots & \vdots & \vdots & \vdots \\ \vdots & \vdots & \vdots & W_1^{N-2} & W_2^{N-2} & W_3^{N-2} & W_4^{N-2} & W_5^{N-2} \\ 0 & \dots & \dots & \dots & W_1^{N-1} & W_2^{N-1} & W_3^{N-1} & W_4^{N-1} \\ 0 & \dots & \dots & \dots & \dots & W_1^N & W_2^N & W_3^N \end{bmatrix}$$

B=

$$(f(x_0) - A_1 W_1^0 - A_2 W_2^0, f(x_1) - A_2 W_1^1, f(x_2), \dots, f(x_{N-2}), f(x_{n-1}) - A_3 W_5^{N-1}, f(x_n) - A_3 W_4^N - A_4 W_5^N)^T$$

3.3.4 Convergence Analysis

Here C has been assumed as a non-specific positive constant independent of δ, ε and N , which may capture different values at different points.

Lemma 3.1

If the functions $a(x), b(x), c(x), d(x)$ and $f(x)$ are sufficiently smooth and are independent of ε , then the solution y of (3.8) satisfies (Kumar & Kadalbajoo, 2012)

$$|y^{(k)}(x)| \leq C \left(1 + \varepsilon^{-k} e^{-\frac{\alpha x}{\varepsilon}} \right), k = 0, 1, 2 \dots$$

For proof of this lemma, one can follow procedure similar to as given in article by Kellogg and Tsan (Kellogg & Tsan, 1978).

Lemma 3.2

Hall error estimation: If $f(x) \in C^2[0,1]$ and $y(x) \in C^4[0,1]$, then $\|D^j(y - Y)\| \leq \lambda_j \|y^4\| h^{4-j}, j = 0, 1, 2, \dots$ where λ_j are the constants (Hall, 1968).

Lemma 3.3

If A is diagonally dominant by rows and $\alpha = \min_i(|a_{i,i}| - \sum_{i \neq j} |a_{i,j}|)$. Then $\|A^{-1}\| < \frac{1}{\alpha}$ (Varah, 1975).

Lemma 3.4

The trigonometric B-splines $T_{5,-2}, T_{5,-1}, \dots, T_{5,N+2}$, satisfy the inequality

$$\sum_{i=-1}^{N+1} |T_{5,i}(x)| \leq 10, 0 \leq x \leq 2.$$

Proof: The result can be proved similarly as proved by Kadalbajoo and Aggarwal (Kadalbajoo & Aggarwal, 2005)

Theorem 3.1

Let $S(x)$ be the approximation obtained by collocation method to the solution $y(x)$ of boundary value problem (3.8). If $f \in C^2[0,1]$, then the error estimate is given by

$$\sup_{\varepsilon} \max_i |y(x_i) - S(x_i)| \leq CN^{-1} \ln^3 N, \text{ where } 0 \leq i \leq N \text{ and } 0 < \varepsilon \leq 1.$$

Proof: Consider $Y(x)$ be the unique spline interpolate to the solution $y(x)$ of SPDDE given in (3.8) given by $y(x) = \sum_{i=-2}^{N+2} \alpha_i T_{5,i}(x)$ and the estimated error is given by

$$|y(x) - S(x)|$$

Now using Hall error estimation as defined in Lemma 3.2 has resulted in the following estimation:

$$\begin{aligned} |Ly(x_i) - LY(x_i)| &= |-\varepsilon||y'''(x_i) - Y'''(x_i)| + |a(x) - d(x)||y''(x_i) - Y''(x_i)| \\ &\quad + |b(x) + d(x)||y'(x_i) - Y'(x_i)| + |c(x)||y(x_i) - Y(x_i)| \\ &\leq (c_{\varepsilon} \lambda_3 h + (\|a(x)\| + \|b(x)\|) \lambda_2 h^2 + (\|b(x)\| + \|d(x)\|) \lambda_1 h^3 + \|c(x)\| \lambda_0 h^4) \|y^4\| \end{aligned}$$

Using Lemma 3.1, results in the following:

$$\begin{aligned}
|Ly(x_i) - LY(x_i)| &\leq (c_\varepsilon \lambda_3 h + (\|a(x)\| + \|b(x)\|)\lambda_2 h^2 \\
&\quad + (\|b(x)\| + \|d(x)\|)\lambda_1 h^3 \\
&\quad + \|c(x)\|\lambda_0 h^4) C \left(1 + \varepsilon^{-k} e^{-\frac{\alpha x}{\varepsilon}}\right) \quad (3.15)
\end{aligned}$$

where $\varepsilon^{-1} \leq C \ln N$.

$$\text{Thus, } |Ly(x_i) - LY(x_i)| \leq CN^{-1} \ln^3 N$$

$$\text{Therefore, the result is } |Ly(x_i) - LY(x_i)| = |f(x_i) - LY(x_i)| \leq CN^{-1} \ln^3 N \quad (3.16)$$

Now consider the SPDDE as:

$$LY(x) = \bar{f}(x_i) \text{ with restrictions } Y(x_0) = \phi(0), Y(x_N) = \gamma.$$

$A\bar{\alpha} = \bar{B}$ is a linear system of equations obtained from the above problem, which follows that

$$A(\alpha - \bar{\alpha}) = B - \bar{B} \quad (3.17)$$

$$\text{where } B - \bar{B} = [f(x_0) - \bar{f}(x_0), f(x_1) - \bar{f}(x_1), \dots, f(x_N) - \bar{f}(x_N)]^T$$

$$\text{By using (11), } \|B - \bar{B}\| \leq CN^{-1} \ln^3 N \quad (3.18)$$

The matrix A is strictly diagonal dominant for sufficiently small values of h and

$$|a_{i,i}| - (|a_{i,i-1}| + |a_{i,i+1}|) = \begin{cases} F(x_0), & \text{for first row} \\ L(x_N), & \text{for last row} \\ M(x_i), & \text{otherwise} \end{cases}$$

where, for first row, for last row, otherwise

$$F(x_0) = -(k_{13} + k_{14})P(x_0) + (k_{10} - k_9 - k_8)Q(x_0) - (k_6 + k_7)R(x_0) + (k_3 - k_2 - k_1)S(x_0),$$

$$L(x_N) = -(k_{11} + k_{12})P(x_N) + (k_{10} - k_9 - k_8)Q(x_N) + (k_5 - k_4)R(x_N) + (k_6 - k_2 - k_1)S(x_N),$$

$$M(x_i) = -\varepsilon A' + (a(x_i) - d(x_i))A'' - (b(x_i) + d(x_i))A''' + c(x_i)A'''' ,$$

$$\text{And } A' = k_{11} + k_{10} + k_{13} + k_{14}, A'' = k_{10} - 2k_8 - 2k_9, A''' = k_4 + k_5 + k_6 + k_7, A'''' = k_3 - 2k_1 - 2k_2$$

It is apparent, that A is strictly diagonally dominant and by using Lemma 3.3, it is concluded that

$$\|A^{-1}\| \leq C \tag{3.19}$$

Now combining (3.17) and (3.18) with approximate solution, $y(x) = \sum_{i=-2}^{N+2} \alpha_i T_{5,i}(x)$, we get:

$$|\alpha - \bar{\alpha}| \leq CN^{-1} \ln^3 N, 0 \leq i \leq N$$

Similarly, estimating $|\alpha_i - \bar{\alpha}_i|$ from the boundary and assumed conditions as defined in section 4 results in, $\max |\alpha_i - \bar{\alpha}_i| \leq CN^{-1} \ln^3 N$, for $-2 \leq i \leq N + 2$ (3.20)

Now by using Lemma 3.4 and equation 3.20 to estimate $|S(x) - Y(x)|$, following is obtained:

$$|S(x) - Y(x)| = \sum_{i=-2}^{N+2} (\alpha_i - \bar{\alpha}_i) T_{5,i}(x)$$

it results in $|S(x) - Y(x)| \leq CN^{-1} \ln^3 N$, which leads to outcome of theorem with triangle inequality.

$$\sup(\varepsilon) \max(i) |y(x_i) - S(x_i)| \leq CN^{-1} \ln^3 N, \text{ where } 0 \leq i \leq N \text{ and } 0 < \varepsilon \leq 1.$$

Hence the theorem is proved.

3.3.5 Numerical Examples of third order SPDDE

To validate the proposed scheme two examples are considered for numerical solution. The double mesh principle is used to calculate the maximum absolute error and $D^N = \max |y_i^N - y_{2i}^{2N}|$ where $1 \leq i \leq N$.

Example 3.5:

$$-\varepsilon y'''(x) + a(x)y''(x) + b(x)y'(x) + c(x)y(x) + d(x)y'(x-1) = f(x)$$

$$y(x) = 1 + x, \quad x \in [-1, 0], \quad y'(2) = 2$$

where $a_1 = 16, a_2 = 10, b(x) = 0, c(x) = -1, d(x) = -1, f_1(x) = 1, f_2(x) = -1$

Example 3.6:

$$-\varepsilon y'''(x) + a(x)y''(x) + b(x)y'(x) + c(x)y(x) + d(x)y'(x-1) = f(x)$$

$$y(x) = 1 + x, \quad x \in [-1, 0], \quad y'(2) = 2$$

where $a_1 = 10 + \exp(x^2), a_2 = 10 + \exp(-x), b(x) = 3, c(x) = -1, d(x) = -1, f_1(x) = 1, f_2(x) = -1$.

Table 3.7 and 3.8 represents the maximum absolute error obtained for different values of N for example 3.5 and 3.6, where figures 3.7 and 3.8 show the solution of these examples.

3.3.6 Discussion

Third order SPDDE with large delay is considered with discontinuous convection-diffusion coefficient and source term. With the uniform partition of the domain, the solution is approximated by quintic trigonometric B-spline basis by collocation technique. Discussion of convergence is carried out by the hall's theorem and method is first order convergent. It is concluded from the numerical results that maximum absolute error declines as

N increases. So, it can be concluded that the presented scheme is efficient to simulate the SPDDE.

Table 3.1: The maximum error obtained for $\varepsilon = 0.1$ and for different values of N and δ for Example 3.1

δ	N=100	N=200	N=400
0.03	5.7e-005	5.0e-006	4.0e-006
0.05	3.9e-005	2.5e-005	5.0e-006
0.09	7.1e-003	1.4e-005	3.0e-006
Results by Swamy et al. (Swamy, Phaneendra, Babu, & Reddy, 2015)			
0.03	3.1674e-003	1.6058e-003	8.0837e-004
0.05	8.7514e-003	4.7344e-003	2.4561e-004
0.09	3.0784e-003	1.5660e-003	7.9000e-004

Table 3.2: The maximum absolute error of Example 3.1 for $\delta = 0.5\varepsilon$

ε	$N = 2^{-4}$	$N = 2^{-5}$	$N = 2^{-6}$	$N = 2^{-7}$
2^{-4}	2.906e-003	7.13e-004	1.82e-004	4.00e-005
2^{-5}	5.226e-003	1.262e-003	3.14e-004	7.80e-005
2^{-6}	1.071e-002	2.485e-003	6.110e-004	1.520e-004
Results by Swamy et al. (Swamy, Phaneendra, Babu, & Reddy, 2015)				
2^{-4}	2.1118e-002	1.1692e-002	6.1941e-003	3.1887e-003
2^{-5}	2.7872e-002	1.6023e-002	8.6367e-003	4.4957e-003
2^{-6}	3.5711e-002	2.1293e-002	1.1869e-002	6.2731e-003

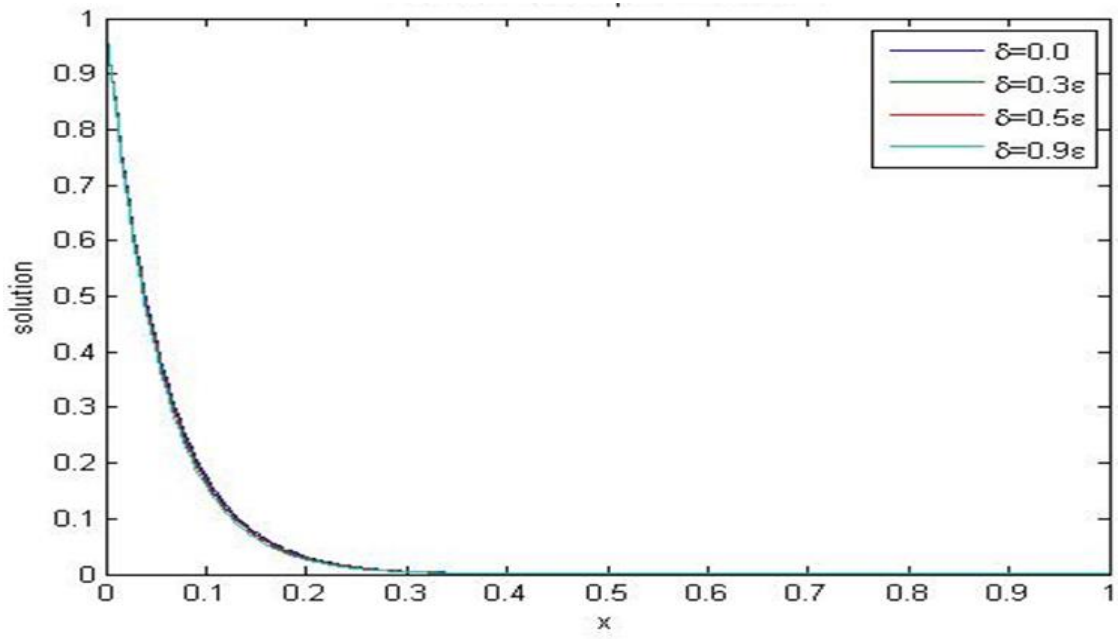


Figure 3.3: Solution of Example 3.1 for $\epsilon = 0.01$

Table 3.3: The maximum error obtained for $\epsilon = 0.1$ for different values of N and δ for Example 3.2

δ	N=100	N=200	N=400
0.03	3.3e-005	6.1e-005	9.0e-006
0.05	2.5e-005	5.0e-006	1.8e-005
0.09	6.0e-006	7.0e-006	2.1e-005
Results by Swamy et al. (Swamy, Phaneendra, Babu, & Reddy, 2015)			
0.03	2.1999e-003	1.1041e-003	5.5315e-004
0.05	2.2012e-003	1.1049e-003	5.5345e-004
0.09	2.1999e-003	1.1038e-003	5.5289e-004

Table 3.4: The maximum absolute error of Example 3.2 for $\delta = 0.5\epsilon$

ϵ	$N = 2^{-4}$	$N = 2^{-5}$	$N = 2^{-6}$	$N = 2^{-7}$
2^{-4}	5.95e-004	1.56e-004	3.9e-005	8.00e-006
2^{-5}	1.152e-003	2.88e-004	7.4e-005	1.8e-005
2^{-6}	2.233e-003	5.48e-004	1.43e-004	3.30e-005
Results by Swamy et al. (Swamy, Phaneendra, Babu, & Reddy, 2015)				
2^{-4}	1.8632e-002	9.6189e-003	4.8865e-003	2.4643e-003
2^{-5}	2.8161e-002	1.4818e-002	7.6255e-003	3.8713e-003
2^{-6}	3.7958e-002	2.0967e-002	1.0977e-002	5.6273e-003

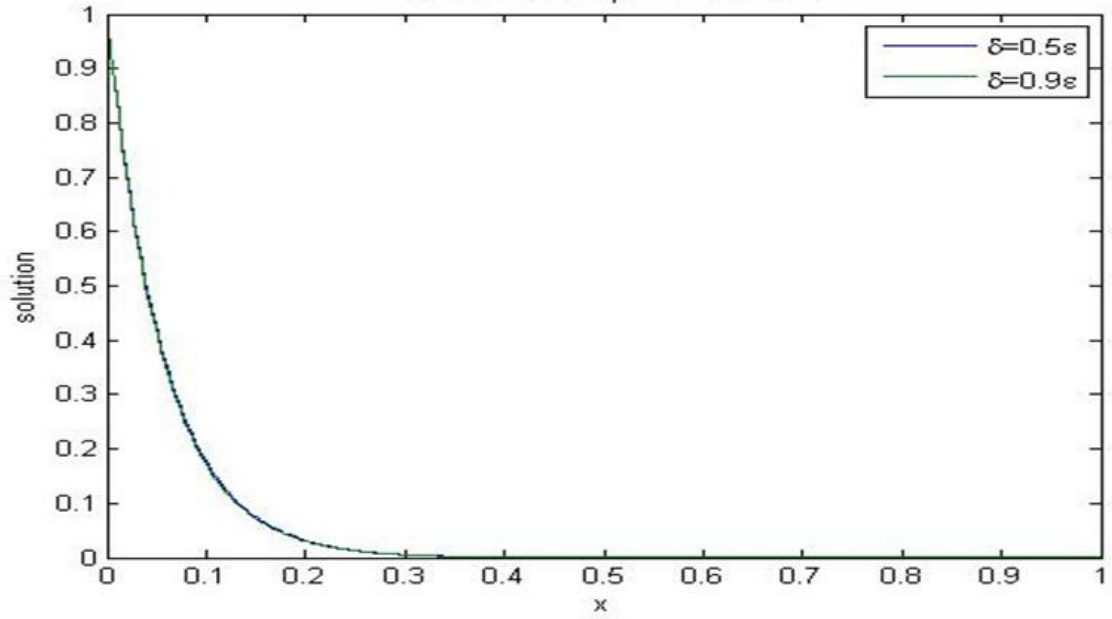


Figure 3.4: Solution of Example 3.2 for $\varepsilon = 0.01$

Table 3.5: Maximum absolute error obtained for Example 3.3 for $\varepsilon = 0.1$

δ	N=100	N=200	N=400
0.03	1.18e-003	6.8e-004	3.0e-004
0.05	1.04e-003	3.5e-004	2.87e-003
0.09	1.03e-003	9.2e-004	5.9e-004
Results by Swamy et al. (Swamy, Phaneendra, Babu, & Reddy, 2015)			
0.03	2.5991e-003	1.2872e-003	6.4039e-004
0.05	2.6270e-003	1.3013e-003	6.47505e-004
0.09	2.6813e-003	1.3289e-003	6.6139e-004

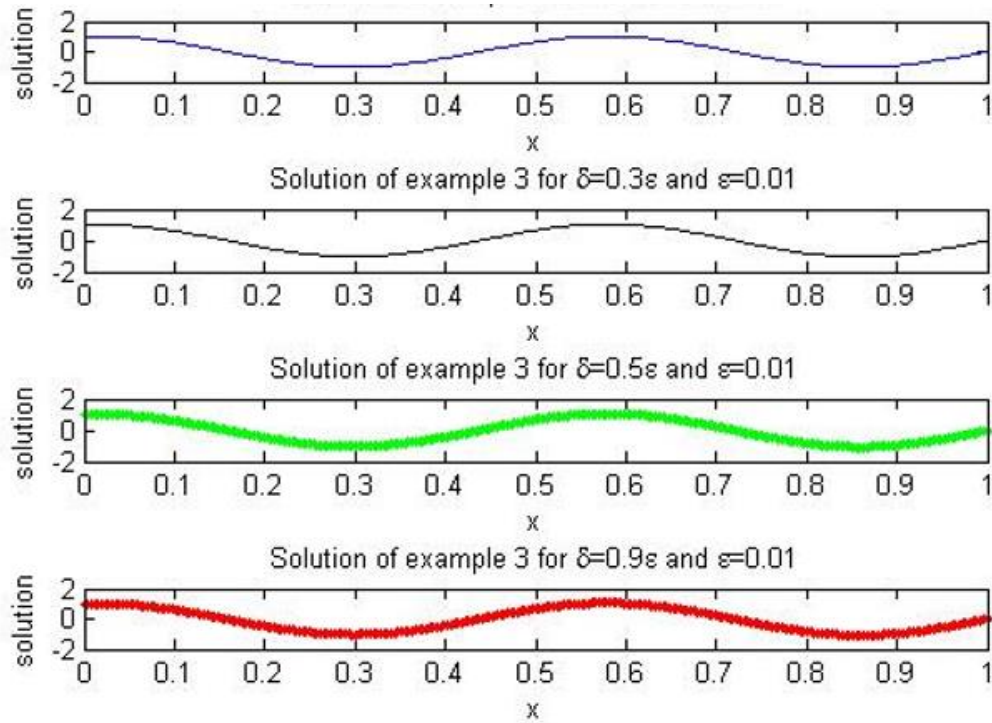


Figure 3.5: Solution of Example 3.3 for different values of ϵ and δ

Table 3.6: Maximum absolute error obtained for Example 3.4 for $\epsilon = 0.1$ and for different values of N

δ	N=100	N=200	N=400
0.03	8.8e-004	1.4e-004	2.53e-004
0.05	7.6e-004	1.6e-004	3.3e-004
0.09	8.3e-004	2.8e-004	2.11e-004
Results by Swamy et al. (Swamy, Phaneendra, Babu, & Reddy, 2015)			
0.03	1.5929e-002	7.4850e-003	3.6202e-003
0.05	1.5470e-002	7.2782e-003	3.5209e-003
0.09	2.1396e-002	1.0097e-002	4.8916e-003

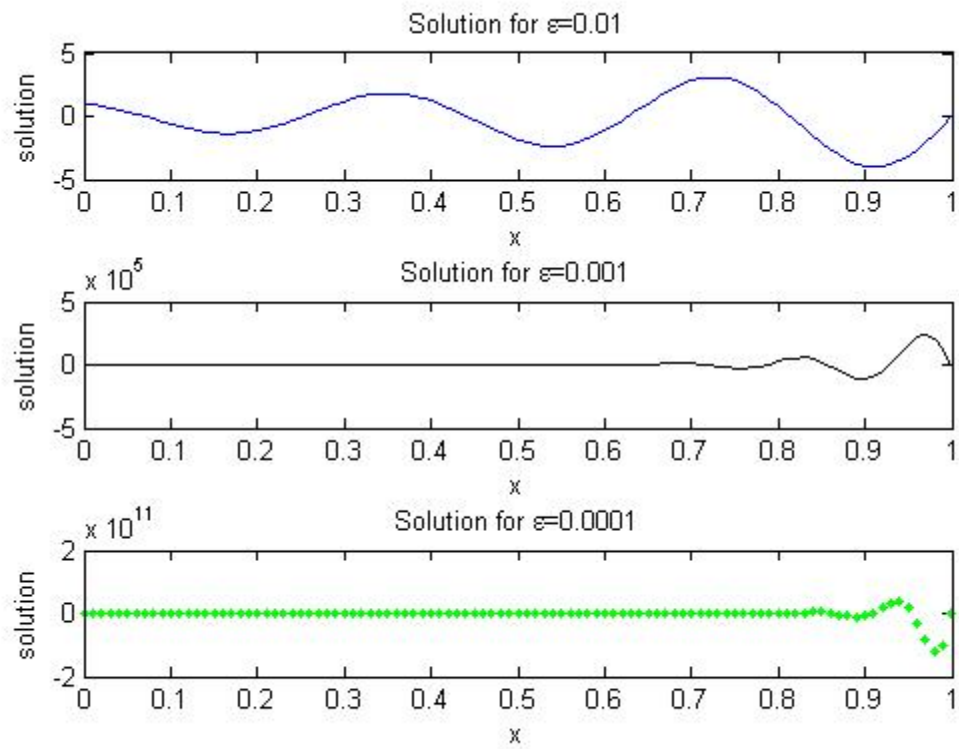


Figure 3.6: Solution of Example 3.4

Table 3.7: Maximum absolute error of Example 3.5

ε	N=16	N=32	N=64	N=128	N=256	N=512	N=1024
$\varepsilon = 2^{-6}$	1.29E+00	1.08E+00	1.41E-01	6.13E-03	2.69E-04	2.46E-02	1.93E-01
$\varepsilon = 2^{-7}$	1.10E+00	1.04E+00	1.18E-01	2.00E-03	1.38E-06	8.69E-09	7.16E-08
$\varepsilon = 2^{-8}$	1.00E+00	1.01E+00	1.04E-01	7.20E-04	8.63E-07	1.29E-11	7.84E-18
$\varepsilon = 2^{-9}$	9.52E-01	9.98E-01	9.69E-02	5.81E-04	1.41E-07	1.22E-13	2.29E-23
$\varepsilon = 2^{-10}$	9.26E-01	9.90E-01	9.31E-02	6.46E-04	1.24E-07	4.94E-15	1.81E-27
$\varepsilon = 2^{-11}$	9.13E-01	9.86E-01	9.12E-02	6.71E-04	1.19E-07	1.95E-15	1.05E-30
$\varepsilon = 2^{-12}$	9.06E-01	9.84E-01	9.03E-02	6.82E-04	1.15E-07	1.10E-15	1.16E-30
$\varepsilon = 2^{-13}$	9.03E-01	9.83E-01	8.98E-02	6.87E-04	1.12E-07	7.29E-16	2.74E-31
$\varepsilon = 2^{-14}$	9.01E-01	9.83E-01	8.96E-02	6.89E-04	1.11E-07	5.61E-16	1.82E-31
$\varepsilon = 2^{-15}$	9.00E-01	9.83E-01	8.94E-02	6.90E-04	1.10E-07	4.82E-16	1.38E-31
$\varepsilon = 2^{-16}$	9.00E-01	9.83E-01	8.94E-02	6.91E-04	1.10E-07	4.44E-16	1.17E-31
$\varepsilon = 2^{-17}$	9.00E-01	9.82E-01	8.93E-02	6.91E-04	1.10E-07	4.25E-16	1.07E-31
$\varepsilon = 2^{-18}$	9.00E-01	9.82E-01	8.93E-02	6.91E-04	1.09E-07	4.15E-16	1.02E-31
$\varepsilon = 2^{-19}$	9.00E-01	9.82E-01	8.93E-02	6.91E-04	1.09E-07	4.11E-16	9.97E-32
$\varepsilon = 2^{-20}$	9.00E-01	9.82E-01	8.93E-02	6.91E-04	1.09E-07	4.08E-16	9.85E-32
$\varepsilon = 2^{-21}$	9.00E-01	9.82E-01	8.93E-02	6.91E-04	1.09E-07	4.07E-16	9.79E-32
$\varepsilon = 2^{-22}$	9.00E-01	9.82E-01	8.93E-02	6.91E-04	1.09E-07	4.07E-16	9.76E-32
$\varepsilon = 2^{-23}$	9.00E-01	9.82E-01	8.93E-02	6.91E-04	1.09E-07	4.06E-16	9.75E-32

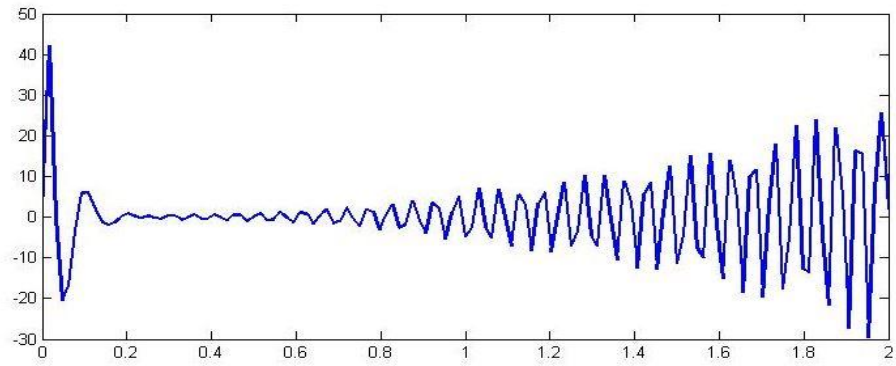


Figure 3.7: Graph of solution of Example 3.5 for $N=128$ and $\varepsilon = 0.25$

Table 3.8: Maximum absolute error of Example 3.6

ε	N=16	N=32	N=64	N=128	N=256	N=512	N=1024
$\varepsilon = 2^{-6}$	3.37E+00	7.46E-01	7.90E-02	6.84E-03	2.04E-04	1.67E-02	2.48E-01
$\varepsilon = 2^{-7}$	3.13E+00	5.87E-01	8.32E-02	2.23E-03	5.57E-06	5.61E-09	9.54E-06
$\varepsilon = 2^{-8}$	3.01E+00	5.16E-01	8.74E-02	9.33E-04	7.23E-07	1.02E-11	4.45E-18
$\varepsilon = 2^{-9}$	2.95E+00	4.83E-01	8.79E-02	4.20E-04	7.41E-08	1.49E-13	2.19E-23
$\varepsilon = 2^{-10}$	2.92E+00	4.67E-01	8.78E-02	2.06E-04	4.57E-08	1.67E-15	1.34E-27
$\varepsilon = 2^{-11}$	2.91E+00	4.59E-01	8.77E-02	1.91E-04	6.42E-08	2.49E-15	1.68E-29
$\varepsilon = 2^{-12}$	2.90E+00	4.55E-01	8.76E-02	1.97E-04	7.28E-08	1.85E-15	3.69E-31
$\varepsilon = 2^{-13}$	2.90E+00	4.53E-01	8.76E-02	1.98E-04	7.57E-08	1.42E-15	2.65E-31
$\varepsilon = 2^{-14}$	2.90E+00	4.52E-01	8.75E-02	1.99E-04	7.69E-08	1.21E-15	2.34E-31
$\varepsilon = 2^{-15}$	2.89E+00	4.52E-01	8.75E-02	2.00E-04	7.74E-08	1.10E-15	1.96E-31
$\varepsilon = 2^{-16}$	2.89E+00	4.51E-01	8.75E-02	2.00E-04	7.76E-08	1.05E-15	1.74E-31
$\varepsilon = 2^{-17}$	2.89E+00	4.51E-01	8.75E-02	2.00E-04	7.78E-08	1.02E-15	1.63E-31
$\varepsilon = 2^{-18}$	2.89E+00	4.51E-01	8.75E-02	2.00E-04	7.78E-08	1.01E-15	1.57E-31
$\varepsilon = 2^{-19}$	2.89E+00	4.51E-01	8.75E-02	2.00E-04	7.78E-08	1.00E-15	1.54E-31
$\varepsilon = 2^{-20}$	2.89E+00	4.51E-01	8.75E-02	2.00E-04	7.79E-08	1.00E-15	1.53E-31
$\varepsilon = 2^{-21}$	2.89E+00	4.51E-01	8.75E-02	2.00E-04	7.79E-08	1.00E-15	1.52E-31
$\varepsilon = 2^{-22}$	2.89E+00	4.51E-01	8.75E-02	2.00E-04	7.79E-08	9.99E-16	1.52E-31
$\varepsilon = 2^{-23}$	2.89E+00	4.51E-01	8.75E-02	2.00E-04	7.79E-08	9.99E-16	1.52E-31

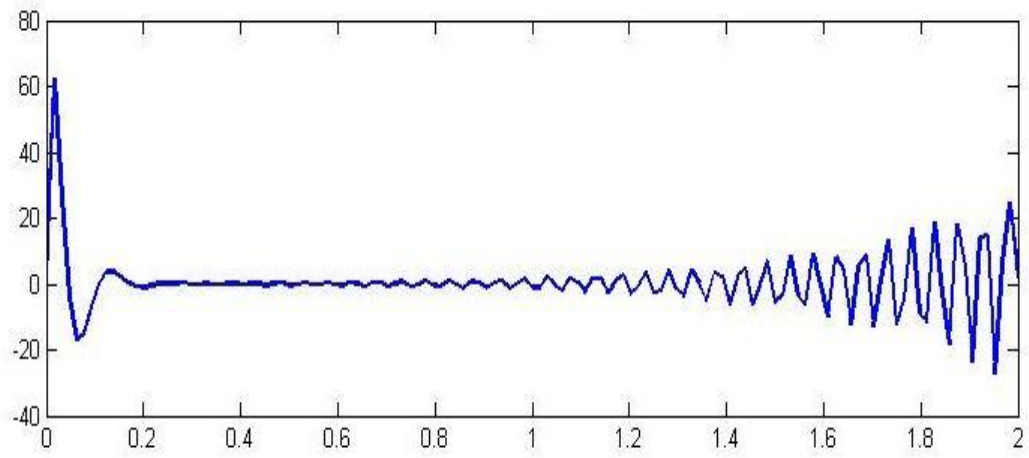


Figure 3.8: Graph of solution of Example 3.6 for $N=128$ and $\varepsilon = 0.25$

Chapter 4

Exponential B-spline collocation scheme for numerical treatment of singularly perturbed delay differential equations

4.1 Introduction

Definition: Exponential B-splines

The piecewise continuous basic spline functions (Asahi, Ichige, & Ishii, 2002) can be procured by multifold convolution of functions $\omega^i(x)$ for $i=1,2,3,\dots,n$ s.t $\gamma^n(x) = \omega^1 \circledast \dots \circledast \omega^n(x)$, where \circledast denotes convolution integral operation.

The weight functions $\omega^i(x)$ are defined as following:

- i) For central basic spline, these are defined in the domain $[-1/2,1/2)$ and vanish in other region
- ii) For shift basic spline, these weights are defined in $[0,1)$
- iii) For polynomial B-spline, the $\omega^i(x)$ functions are the rectangular functions of height 1.

To illustrate the exponential B-spline basis consider Figure 4.1 (Asahi, Ichige, & Ishii, 2002), which shows the exponential B splines obtained by convolution.

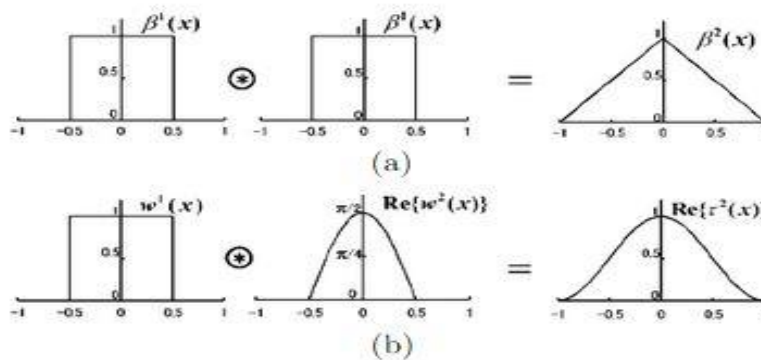


Figure 4.1: (a) B spline polynomials of order 2, (b) exponential B splines obtained by convolution

Now, to obtain the mathematical expression for exponential B-spline functions the weights will be considered as exponential functions $\omega_1^{\mu_1} \exp(\mu_i x)$, $\mu_i \in \mathcal{C}$ and $\omega_1^{\mu_1} \in \mathcal{C}$ is a normalization factor.

The vector $\vec{\mu}_r = (\mu_1, \mu_2, \dots, \mu_r)^T$ and then the exponential B-spline function can be demonstrated as:

$$T^{\vec{\mu}_r}(x) = \sum_{k \in \mathbb{Z}} d^{\vec{\mu}_r}[k] \sigma^{\vec{\mu}_r}(x - k)$$

where $d^{\mu_r}[k] = \delta[k] - e^{\mu_r} \delta[k - 1]$ is single discrete difference function ($\delta[k]$ is Kronector's delta function), $d^{\vec{\mu}_r}[k] = d^{\mu_1} * d^{\mu_2} * \dots * d^{\mu_n}[k]$ is multiple discrete difference function, $\sigma^{\vec{\mu}_r}(\cdot)$ is the continuous exponential truncated power given by:

$$\sigma^{\mu_1}(x) = \begin{cases} \omega^1 \left(x - \frac{1}{2}\right), & x \in [0, \infty) \\ 0, & \text{otherwise} \end{cases}$$

Then the recursively relation is expressed as $\sigma^{\vec{\mu}_r}(x) = \int_0^\infty \omega^r \left(x - \frac{1}{2}\right) \sigma^{\vec{\mu}_r-1}(x - x_1) dx_1$.

So, the expanded exponential B-spline function is given by:

$$T_m^{\vec{\mu}_r}(x) = T^{\vec{\mu}_r} \left(\frac{x}{m}\right) = \lambda_m^{\vec{\mu}_r} \sum_{k \in \mathbb{Z}} d^{\vec{\mu}_r}[k] \sigma^{\vec{\mu}_r} \left(\frac{x}{m} - mk\right)$$
 with m as positive integer

And $\lambda_m^{\vec{\mu}_r} = m \prod_{r=1}^n \frac{\sinh\left(\frac{\mu_r}{2m}\right)}{\sinh\left(\frac{\mu_r}{2}\right)} \exp\left(-\frac{m-1}{2m} \mu_r\right)$ is the scalar function.

In recent years many researchers have worked on exponential B-spline function for numerical solution of the differential equations such as: Mohammadi (Mohammadi, 2013) presented an exponential B-spline collocation method for approximating solution of convection-diffusion equation with Dirichlet's type boundary conditions. Hepson et al. (Hepson, Korkmaz, & Dag, 2017) proposed exponential B-spline collocation method for approximating numerical solutions of the Gardner equation. Burger's equation was treated by Ersoy et al. (Ersoy, Dag, & Adar, 2016) by exponential B-spline collocation method. Ersoy and Dag (Ersoy & Dag, 2016) numerically treated Kuramoto-Sivashinsky equation

together with Crank Nicolson scheme by using exponential cubic B-spline collocation method. Dag and Ersoy (Dag & Ersoy, 2016) applied exponential B-spline collocation method to approximate the numerical solution of Fisher's equation. Ersoy and Dang (Ersoy, Korkmaz, & Dag 2016) proposed exponential B-Spline collocation method for numerical solutions of Boussinesq systems for water waves. Numerical solutions of the Korteweg-de Vries (KdV) equation was approximated by Ersoy and Dag (Ersoy & Dag, 2015a) by the exponential cubic B-spline algorithm by reducing the problem into a system of algebraic equations which were solved by using a variant of Thomas algorithm.

The exponential B-spline Galerkin method was used by Gorgulu et al. (Gorgulu, Dag, & Irk, 2016) to get the numerical solution of the Burgers' equation. Gorgulu et al. (Gorgulu, Dag, & Irk, 2017) solved solitary waves of RLW equation by exponential B-spline Galerkin method. Apart from numerical solution of differential equations, exponential B-spline interpolation is technique used in image compression, digital zooming, computed tomography (CT), magnetic resonance imaging (MRI) (Gupta, Lee, & Lee, 2007). A novel efficient technique was proposed by Fahmy and Fahmy (Fahmy & Fahmy, 2012) for spatial image compression by applications of exponential B-spline functions due to the extra degrees of freedom inherited by the arbitrary choice of exponential B-spline parameters.

4.2 Problem statement

Consider following perturbed delay differential equation:

$$-\varepsilon y''(x) + a(x)y(x) + b(x)y(x - 1) = f(x), \quad x \in \Omega^- \cup \Omega^+, \quad (4.1)$$

subject to the conditions

$$y(x) = \phi(x), \quad x \in [-1, 0], \quad y(2) = \gamma,$$

where $a(x) \geq \alpha_1 > \alpha > 0, \beta_0 \leq b(x) \leq \beta < 0, \alpha_1 + \beta_0 > \eta > 0, \Omega^- = (0,1)$ and $\Omega^+ = (1,2)$. Also, the functions $a(x), b(x)$ and $f(x)$ are sufficiently smooth on $\bar{\Omega}$ where $\bar{\Omega} = [0,2]$.

This type of SPDDE (4.1) showcase layer compartment at $x = 0$ and at $x = 2$, and existence of solution of such equations are well explained in article by Schmitt (Schmitt, 1969). Furthermore, this type of boundary value problem transpires (emerges) in control theory where the problems involving signal transmission are tangled by the sequel of time delays (Kaufmann, Kaufmann, Pamboukian, & Moraes, 2012). Some of the root causes liable for emerge of these time delays are ascertained such as media of propagation of signal and excellence of appliance used while some of the causes are ambiguous. For the readers concerned in such variational problems can refer (Él'sgol'c, 1964).

Taylor's series up to second order accuracy is used to handle the delay term.

$$y(x - 1) = y(x) - y'(x) + \frac{y''(x)}{2}$$

By using the above relation in equation (4.1), following equation is obtained

$$P(x)y''(x) + Q(x)y'(x) + R(x)y(x) = f(x) \quad (4.2)$$

where

$$P(x) = \varepsilon - \frac{b(x)}{2}, Q(x) = -b(x) \text{ and } R(x) = b(x) + a(x)$$

4.3 Exponential cubic B-spline collocation method

The domain is partitioned into a uniform mesh with each sub intervals of length $1/N$ and the resultant partition is $\{0 \equiv x_0 < x_1 < x_2 < \dots < x_N \equiv 2\}$ where N is the total number of partition points.

An approximation to the solution is considered as:

$$y(x) = \sum_{i=-1}^{N+1} \alpha_i EB_i(x) \quad (4.3)$$

where α_i 's are the unknown real coefficients and $EB_i(x)$'s are the exponential B-spline basis functions.

The set of functions $\{EB_{-1}(x), EB_0(x), EB_1(x), \dots, EB_{N+1}(x)\}$ form the basis for functions defined over the interval $[0, 2]$. To know more about exponential B-spline function one can refer (Ersoy & Dag, 2016).

The exponential B-splines, EB_i at the partition points together with the simulate points $x_{-3}, x_{-2}, x_{-1}, x_{N+1}, x_{N+2}, x_{N+3}$ outside the domain $[0, 1]$ can be defined as:

$$EB_i = \begin{cases} b_2 \left((x_{i-2} - x) - \frac{1}{p} (\sinh(p(x_{i-2} - x))) \right), & [x_{i-2}, x_{i-1}], \\ a_1 + b_1(x_i - x) + c_1 \exp(p(x_i - x)) + d_1 \exp(-p(x_i - x)), & [x_{i-1}, x_i], \\ a_1 + b_1(x - x_i) + c_1 \exp(p(x - x_i)) + d_1 \exp(-p(x - x_i)), & [x_i, x_{i+1}], \\ b_2 \left((x - x_{i+2}) - \frac{1}{p} (\sinh(p(x - x_{i+2}))) \right), & [x_{i+1}, x_{i+2}], \\ 0, & \text{otherwise.} \end{cases}$$

where

$$a_1 = \frac{pch}{phc - s},$$

$$b_1 = \frac{p}{2} \left[\frac{c(c-1) + s^2}{(phc - s)(1-c)} \right],$$

$$b_2 = \frac{p}{2(phc - s)},$$

$$c_1 = \frac{1}{4} \left[\frac{\exp(-ph)(1-c) + s(\exp(-ph)-1)}{(phc-s)(1-c)} \right],$$

$$d_1 = \frac{1}{4} \left[\frac{\exp(ph)(c-1) + s(\exp(ph)-1)}{(phc-s)(1-c)} \right],$$

and $c = \cosh(ph)$, $s = \sinh(ph)$, p is the free parameter.

Table 4.1: Values of exponential basis

x	x_{i-2}	x_{i-1}	x_i	x_{i+1}	x_{i+2}
$EB_i(x)$	0	$\frac{s-ph}{2(phc-s)}$	1	$\frac{s-ph}{2(phc-s)}$	0
$EB'_i(x)$	0	$\frac{p(c-1)}{2(phc-s)}$	0	$\frac{p(c-1)}{2(phc-s)}$	0
$EB''_i(x)$	0	$\frac{p^2s}{2(phc-s)}$	$\frac{-p^2s}{phc-s}$	$\frac{p^2s}{2(phc-s)}$	0

Now by using values of $EB_i(x)$, $EB'_i(x)$ and $EB''_i(x)$ at nodal points from Table 4.1, $y(x)$ and its first and second order derivative can be expressed as:

$$y(x_i) = m_1 a_{i-1} + a_i + m_1 a_{i+1}$$

$$y'(x_i) = m_2 a_{i+1} - m_2 a_{i-1}$$

$$y''(x_i) = m_3 a_{i-1} - 2m_3 a_i + m_3 a_{i+1}$$

where $m_1 = \frac{s-ph}{2(phc-s)}$, $m_2 = \frac{p(c-1)}{2(phc-s)}$, $m_3 = \frac{p^2s}{2(phc-s)}$

By substituting the values of y_i , y'_i and y''_i at nodal points in equation (4.2), a system of $N+1$ linear equations in $N+3$ unspecified variables has been obtained as:

$$E_i^l \alpha_{i-1} + E_i \alpha_i + E_i^r \alpha_{i+1} = f_i, \quad 0 \leq i \leq N \quad (4.4)$$

where

$$E_i^l = P(x)m_1 - Q(x)m_2 + R(x)m_3$$

$$E_i = P(x) - 2R(x)m_3$$

$$E_i^r = P(x)m_1 + Q(x)m_2 + R(x)m_3$$

The variables α_{-1} and α_{N+1} exists when $i = 0$ and $i = N$ will be considered in equation (4.4). To eliminate these variables, boundary conditions $y(x_0) = \phi_0$ and $y(x_N) = \gamma$ are used that results in:

$$\alpha_{-1} = \frac{\phi_0 - \alpha_0 - m_1 \alpha_1}{m_1} \text{ and } \alpha_{N+1} = \frac{\gamma - \alpha_N - m_1 \alpha_{N-1}}{m_1}$$

Substituting these values in equation (4.4) for $i=0$ and $i=N$ results in:

$$\alpha_0 \left(E_0 - \frac{1}{m_1} E_0^l \right) + \alpha_1 (E_0^r - E_0^l) = f_0 - \frac{\phi_0 E_0^l}{m_1} \quad (4.5)$$

and

$$\alpha_{N-1} (E_N^l - E_N^r) + \alpha_N \left(E_N - \frac{1}{m_1} E_N^r \right) = f_N - \frac{\gamma E_N^r}{m_1} \quad (4.6)$$

The $N+1$ equations in $N+1$ variables lead to system of linear equations $A\alpha=B$ where $\alpha = [\alpha_0, \alpha_1, \alpha_2, \dots, \alpha_N]^T$.

The tri-diagonal matrix A is given by

$$\begin{bmatrix} \frac{-1}{m_1} E_0^l + E_0 & E_0^r - E_0^l & \cdots & \cdots & \cdots & \cdots & \cdots & \cdots & 0 \\ E_1^l & E_1 & E_1^r & \cdots & \cdots & \cdots & \cdots & \cdots & 0 \\ \vdots & \vdots & \vdots & \vdots & \vdots & \vdots & \vdots & \vdots & \vdots \\ \vdots & \vdots & \vdots & \vdots & \vdots & \vdots & \vdots & \vdots & \vdots \\ 0 & \cdots & 0 & E_i^l & E_i & E_i^r & 0 & \cdots & \cdots \\ \vdots & \vdots & \vdots & \vdots & \vdots & \vdots & \vdots & \vdots & \vdots \\ \vdots & \vdots & \vdots & \vdots & \vdots & \vdots & \vdots & \vdots & \vdots \\ 0 & \cdots & \cdots & \cdots & \cdots & E_{N-1}^l & E_{N-1} & E_{N-1}^r & \cdots \\ 0 & \cdots & \cdots & \cdots & \cdots & \cdots & E_N^l - E_N^r & E_N - \frac{1}{m_1} E_N^r & \cdots \end{bmatrix}$$

and the right-hand side is a column matrix B, given by

$$\begin{bmatrix} f(x_0) - E_0' \left(\frac{\phi_0}{m_1} \right) \\ f(x_1) \\ f(x_2) \\ \vdots \\ \vdots \\ \vdots \\ f(x_{N-1}) \\ f(x_N) - \gamma \left(\frac{E_N'}{m_1} \right) \end{bmatrix}$$

4.4 Convergence Analysis

In this section, a procedure is narrated to discuss the convergence analysis of the method by truncation error. It is assumed that the function $y(x)$ be the function with continuous derivatives over the entire domain $[0,1]$.

Now using the approximated relation of $Y_N(x_i)$, $Y_N'(x_i)$, the following relationship has been obtained:

$$m_1 Y_N'(x_{i-1}) + Y_N'(x_i) + m_1 Y_N'(x_{i+1}) = m_2 [y_N(x_{i+1}) + y_N(x_{i-1})] \quad (4.7)$$

Using the operator $E(y(x_i)) = y_N(x_{i+1})$ in equation (4.7) results in

$$(m_1 E^{-1} + 1 + m_1 E) Y_N'(x_i) = m_2 (E - E^{-1}) y_N(x_i)$$

Hence,

$$Y_N'(x_i) = \left[\frac{m_2 (E - E^{-1})}{(m_1 E^{-1} + 1 + m_2 E)} \right] y_N(x_i)$$

On using $E = e^{hD}$ and expand it in powers of hD , the following is obtained.

$$Y_N'(x_i) = \left[\frac{m_2 (e^{hD} - e^{-hD})}{(m_1 e^{-hD} + 1 + m_2 e^{hD})} \right] y_N(x_i)$$

$$= \frac{2m_2 h}{\lambda} y'_N(x_i) + h^2 \left[\frac{-2m_2(m_2 - m_1)}{\lambda^2} \right] + O(h^3)$$

where $\lambda = m_1 + m_2 + 1$

Therefore, the truncation error is: $h^2 \left[\frac{-2m_2(m_2 - m_1)}{\lambda^2} \right] + O(h^3)$

Now the obtained system of equations $AY = B$ where $A = (t_{i,j})$, $0 \leq i, j \leq N$ which is a tridiagonal matrix with

$$t_{i,i-1} = E_i^l, t_{i,i} = E_i \text{ and } t_{i,i+1} = E_i^r \text{ for } i=1,2,3,4,\dots,N-1$$

$$t_{0,0} = E_0, t_{0,1} = E_0^r, t_{N-1,N} = E_N \text{ and } t_{N,N} = E_N^r$$

with local truncation error $T_i(h_i) = h^2 \left[\frac{-2m_2(m_2 - m_1)}{\lambda^2} \right] + O(h^3)$

And $Y = (y_1, y_2, y_3, \dots, y_{n-1})^T$

Also if $\bar{Y} = (\bar{y}_1, \bar{y}_2, \bar{y}_3, \dots, \bar{y}_{n-1})^T$ is the exact solution and the local truncation error is $T(h) = (T_1(h_1), T_2(h_2), T_3(h_3), \dots, T_{n-1}(h_{n-1}))^T$, then as it is known $A\bar{Y} - T(h) = C$, where C is any constant.

So, result is $A(\bar{Y} - Y) = T(h)$

The error equation can be written as $AE = T(h)$ (4.8)

where $E = \bar{Y} - Y = (e_1, e_2, e_3, \dots, e_{n-1})^T$

Hence from equation (4.8), $E = A^{-1}T(h)$ (4.9)

A is irreducible and monotone for small h .

Thus A^{-1} exists.

From the theory of matrices, it is known that $\sum_{i=0}^n \bar{t}_{k,i} S_i = 1$

where $\overline{t_{k,l}}$ is the $(k,i)^{\text{th}}$ element of the A^{-1} .

Here we have $S_i = \sum_{j=1}^{n-1} t_{i,j} = h^0 B_i$,

$$\text{where } B_i = \begin{cases} P(x_i)(1 + m_1) - Q(x_i)(m_2) + R(x_i)(-m_3), & \text{for } i = 0 \\ P(x_i)(1 + 2m_1), & \text{for } i = 1, 2, 3, \dots, N - 1 \\ P(x_i)(1 + m_1) + Q(x_i)(m_2) - R(x_i)(-m_2), & \text{for } i = N \end{cases}$$

Therefore, $\sum_{i=0}^n \overline{t_{k,l}} \leq \frac{1}{\min(S_i)} \leq \frac{1}{|B_i|}$

Thus from the equation (4.9), the element-wise error is $e_j = \sum_{i=0}^n \overline{t_{k,l}} T_i(h)$, for $j = 0, 1, 2, 3, \dots, N$ implies the result that:

$$e_j \leq \frac{kh^2}{|B_i|}$$

where k is a constant independent of h .

Therefore, $\|E\| = O(h^2)$

This concludes that our method is second order convergent for the uniform mesh.

4.5 Numerical Examples

Example 4.1:

Consider a SPDDE as:

$$-\varepsilon y''(x) + 5y(x) - y(x - 1) = 1,$$

under the conditions:

$$y(x)=1, x \in [-1,0], y(2)=2.$$

The maximum error obtained for this example is presented in Table 4.2 for $\varepsilon = 2^{-4}, 2^{-5}, \dots, 2^{-23}$ and the value of D^N is compared by the results obtained by the reported scheme. It is observed from the results that with an increase in the value of N from 16 to

256 the maximum absolute error diminishes while for $N = 512$ the obtained error again escalates. In Table 3, the maximum error obtained is shown for $\varepsilon = 0.01, 0.001$ and 0.0001 and it is found that as the value of perturbation parameter sinks, the absolute error increases. The obtained solution by the presented scheme is given in Table 4 for some selected nodal points in the domain for $\varepsilon = 0.01$ and for diverse values of N . The layer conduct of the approximated solution for different values of perturbation parameter ε is presented in Figure 4.2.

Example 4.2:

Consider equation given by:

$$-\varepsilon y''(x) + (x + 5)y(x) - y(x - 1) = 1,$$

under the conditions:

$$y(x)=1, x \in [-1,0], y(2) =2.$$

The layer behavior of the approximated solution of this example is presented in Figure 4.3. And the maximum error obtained for this example presented in Table 4.5 for different values of ε and N . It is perceived that as the value of N enriches from 16 to 256, maximum absolute error contracts but for $N = 512$, a fluctuation in the error is spotted. In Table 4.6, maximum error obtained is shown for $\varepsilon = 0.01, 0.001$ and 0.0001 . The calculated solution is presented in Table 4.7 for some nodal points in the domain.

Example 4.3:

We have considered SPDDE:

$$-\varepsilon y''(x) + 2y(x) - 2y(x - 1) = 1,$$

under the conditions:

$$y(x)=1, x \in [-1,0], y(2) =2.$$

The behavior of the solution of this example is found to be of layer type as presented in Figure 4.3. The maximum error obtained for this example is presented in Table 4.8 and 4.9 for various values of ε and N . From the results obtained in Table 4.8, it can be deduced that maximum absolute error depletes with up-gradation in total number of partition points for $\varepsilon = 2^{-5}, 2^{-7}, 2^{-13}$ but for all other values of ε , the absolute error decreases from $N = 16$ to 128 and then deviates. The calculated solution is presented in Table 4.10 for various values of N .

4.6 Discussion

We have considered a boundary value problem for one type of SPDDEs. To find an approximate solution for this type of problem, we have used an exponential B-spline collocation method. The method is shown to be of second order convergent. The proposed scheme has been applied in three numerical examples and result has been compared with the existing schemes and it is found that our results are better than the reported results in the literature. Some recent work reported to solve the SPDDE is also reviewed. The behavior of the approximated solution is presented as graphs for all considered problems. From the results, it can be surmised that the discussed method of exponential B-spline can obtain results of required accuracy.

Table 4.2: Maximum absolute error obtained for Example 4.1

ε	N=16	N=32	N=64	N=128	N=256	N=512
2^{-4}	6.4760E-03	1.6120E-03	3.6600E-04	8.5000E-05	7.9000E-05	3.0800E-04
2^{-5}	5.8860 E-03	1.4680E-03	3.3400E-04	7.4000E-05	7.6000E-05	3.0500E-04
2^{-6}	6.1710 E-03	1.5370E-03	3.4900E-04	7.4000E-05	8.4000E-05	2.8100E-04
2^{-7}	6.3200 E-03	1.5740E-03	3.6000E-04	7.7000E-05	8.4000E-05	3.1400E-04
2^{-8}	6.3970E-03	1.5930E-03	3.6300E-04	8.0000E-05	6.9000E-05	3.1500E-04
2^{-9}	6.4370E-03	1.6020E-03	3.6300E-04	7.9000E-05	5.7000E-05	2.8100E-04
2^{-10}	6.4550 E-03	1.6060E-03	3.6700E-04	8.4000E-05	8.6000E-05	2.8700E-04
2^{-11}	6.4650E-03	1.6100E-03	3.6600E-04	8.1000E-05	7.1000E-05	3.0700E-04
2^{-12}	6.4710E-03	1.6100E-03	3.6600E-04	7.9000E-5	5.8000E-5	3.0600E-04
2^{-13}	6.4730E-03	1.6110E-03	3.6700E-04	7.8000E-05	4.7000E-05	2.9200E-04
2^{-14}	6.4740E-03	1.6110E-03	3.6800E-04	7.9000E-05	6.3000E-05	3.4200E-04
2^{-15}	6.4750E-03	1.6110E-03	3.6800E-04	7.6000E-05	8.2000E-05	3.2900E-04
2^{-16}	6.4760E-03	1.6110E-03	3.6600E-04	8.1000E-05	9.3000E-05	3.4400E-04
2^{-17}	6.4750E-03	1.6120E-03	3.6600E-04	8.3000E-05	8.6000E-05	3.1700E-04
2^{-18}	6.4750E-03	1.6110E-03	3.6700E-04	8.1000E-05	8.7000E-05	3.1400E-04
2^{-19}	6.4750E-03	1.6120E-03	3.6800E-04	8.4000E-05	5.7000E-05	3.2600E-04
2^{-20}	6.4760E-03	1.6100E-03	3.6900E-04	7.4000E-05	7.2000E-05	3.1300E-04
2^{-21}	6.4750E-03	1.6120E-03	3.6500E-04	7.8000E-05	4.3000E-05	3.3900E-04
2^{-22}	6.4760E-03	1.6110E-03	3.6700E-04	7.8000E-05	5.4000E-05	3.1400E-04
2^{-23}	6.4760E-03	1.6110E-03	3.6700E-04	8.6000E-05	7.8000E-05	3.3500E-04

D ^N by our method	6.4760 E-03	1.6120E-03	3.6800E-04	8.6000E-05	9.3000E-05	3.4400E-04
D ^N in (Subburayan & Ramanujam, 2013)	1.2175 E-01	5.2206E-02	1.8447E-02	6.5158E-03	2.1589E-03	6.5625E-04

Table 4.3: Maximum absolute error obtained for Example 4.1 for different values of ε

ε	N=16	N=32	N=64	N=128	N=256
0.01	6.2770E-03	1.5640E-03	3.5500E-04	7.8000E-05	7.0000E-05
0.001	6.4550E-03	1.6070E-03	3.6600E-04	8.0000E-05	6.8000E-05
0.0001	6.4740E-03	1.6100E-03	3.6700E-04	8.1000E-05	6.8000E-05

Table 4.4: Solution of Example 4.1 for $\varepsilon = 0.01$

x_i	N=16	N=32	N=64	N=128	N=256	N=512
0.000	1.000000	1.000000	1.000000	1.000000	1.000000	1.000000
0.250	0.707339	0.707643	0.707723	0.707737	0.707745	0.707753
0.500	0.531473	0.531983	0.532117	0.532142	0.532154	0.532169
0.750	0.430268	0.431084	0.431296	0.431339	0.431354	0.431375
1.000	0.384337	0.385787	0.386158	0.386238	0.386261	0.386279
1.250	0.398841	0.401538	0.40222	0.402373	0.402412	0.40242
1.500	0.522984	0.527685	0.528865	0.529131	0.529195	0.529169
1.750	0.911869	0.918146	0.91971	0.920065	0.920143	0.920073
2.000	2.000000	2.000000	2.000000	2.000000	2.000000	2.000000

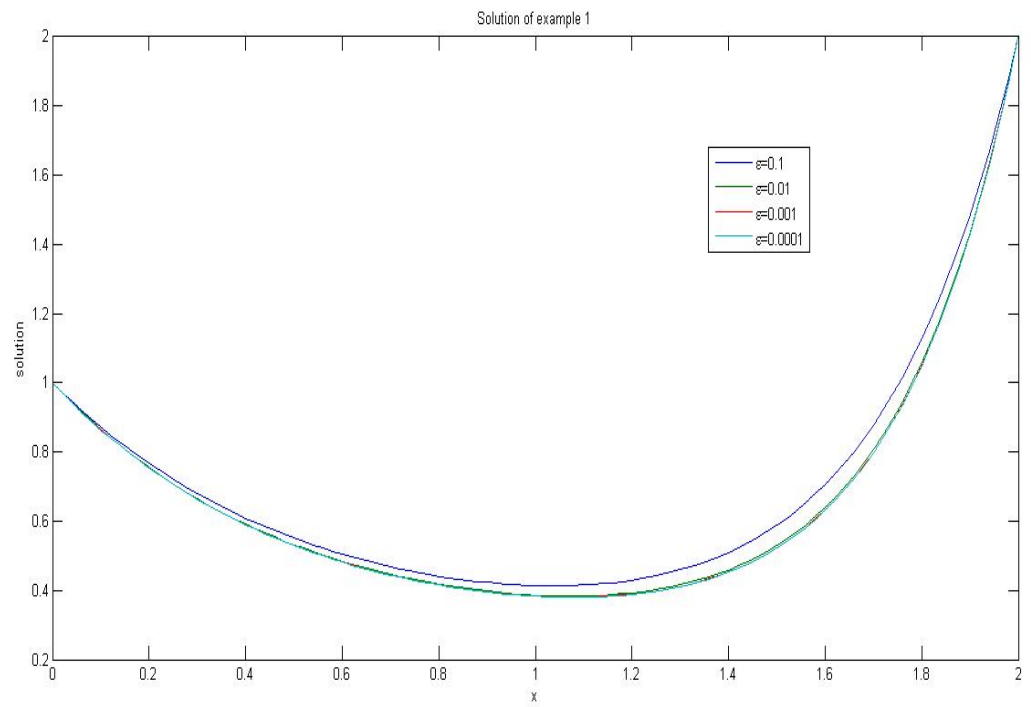


Figure 4.2: Solution of Example 4.1 for diverse values of ϵ .

Table 4.5: Maximum absolute error obtained for Example 4.2 for different values of ε

ε	N=16	N=32	N=64	N=128	N=256	N=512
2^{-4}	7.6480E-03	1.8930E-03	4.3900E-04	1.1700E-04	1.7000E-05	1.9000E-05
2^{-5}	8.2800E-03	2.0440E-03	4.7600E-04	1.2600E-04	2.5000E-05	2.1000E-05
2^{-6}	8.6270E-03	2.1260E-03	4.9700E-04	1.3200E-04	1.8000E-05	2.0000E-05
2^{-7}	8.8090E-03	2.1700E-03	5.0600E-04	1.3100E-04	2.5000E-05	2.7000E-05
2^{-8}	8.9020E-03	2.1930E-03	5.1300E-04	1.3500E-04	2.5000E-05	3.0000E-05
2^{-9}	8.9490E-03	2.2030E-03	5.1600E-04	1.3600E-04	2.7000E-05	1.4000E-05
2^{-10}	8.9730E-03	2.2100E-03	5.1600E-04	1.3600E-04	3.7000E-05	1.6000E-05
2^{-11}	8.9850E-03	2.2120E-03	5.1700E-04	1.3600E-04	2.6000E-05	3.3000E-05
2^{-12}	8.9910E-03	2.2140E-03	5.1800E-04	1.3600E-04	2.6000E-05	1.9000E-05
2^{-13}	8.9940E-03	2.2130E-03	5.1900E-04	1.3700E-04	2.1000E-05	2.0000E-05
2^{-14}	8.9960E-03	2.2150E-03	5.1800E-04	1.3400E-04	3.1000E-05	1.0000E-05
2^{-15}	8.9970E-03	2.2140E-03	5.1700E-04	1.3800E-04	2.3000E-05	1.6000E-05
2^{-16}	8.9970E-03	2.2150E-03	5.1800E-04	1.3800E-04	2.5000E-05	1.4000E-05
2^{-17}	8.9970E-03	2.2160E-03	5.1700E-04	1.3800E-04	2.4000E-05	4.3000E-05
2^{-18}	8.9970E-03	2.2150E-03	5.1600E-04	1.3800E-04	2.3000E-05	1.9000E-05
2^{-19}	8.9970E-03	2.2150E-03	5.1700E-04	1.3700E-04	2.7000E-05	1.9000E-05
2^{-20}	8.9970E-03	2.2150E-03	5.1800E-04	1.3600E-04	2.3000E-05	1.9000E-05
2^{-21}	8.9970E-03	2.2140E-03	5.1900E-04	1.3700E-04	3.0000E-05	2.0000E-05
2^{-22}	8.9970E-03	2.2160E-03	5.1800E-04	1.3400E-04	3.4000E-05	1.6000E-05
2^{-23}	8.9970E-03	2.2150E-03	5.1900E-04	1.3500E-04	3.0000E-05	2.4000E-05

D^N by our method	8.9970E-03	2.2160E-03	5.1900E-04	1.3800E-04	3.0000E-05	4.3000E-05
D^N in (Subburayan & Ramanujam, 2013)	1.6717E-01	7.4650E-02	2.7140E-02	9.3384E-03	3.1724E-03	9.6871E-04

Table 4.6: Maximum absolute error obtained for various values of ϵ for Example 4.2

ϵ	N=16	N=32	N=64	N=128	N=256
0.01	8.7570E-03	2.1580E-03	5.0400E-04	1.2900E-04	2.6000E-05
0.001	8.9730E-03	2.2090E-03	5.1700E-04	1.3800E-04	2.7000E-05
0.0001	8.9950E-04	2.2140E-03	5.1900E-04	1.3700E-04	2.0000E-05

Table 4.7: Approximate solution of Example 4.2 for $\varepsilon = 0.01$

x_i	N=16	N=32	N=64	N=128	N=256	N=512
0.000	1.000000	1.000000	1.000000	1.000000	1.000000	1.000000
0.250	0.687818	0.688021	0.688076	0.688082	0.68808	0.688086
0.500	0.493245	0.493629	0.493731	0.49375	0.493756	0.493753
0.750	0.375968	0.376655	0.376834	0.376871	0.376879	0.376885
1.000	0.314159	0.315527	0.315876	0.315954	0.315972	0.315979
1.250	0.308449	0.311315	0.312036	0.312203	0.312243	0.312251
1.500	0.405000	0.410684	0.412099	0.412428	0.412504	0.412527
1.750	0.777506	0.786263	0.788421	0.788925	0.789054	0.789072
2.000	2.000000	2.000000	2.000000	2.000000	2.000000	2.000000

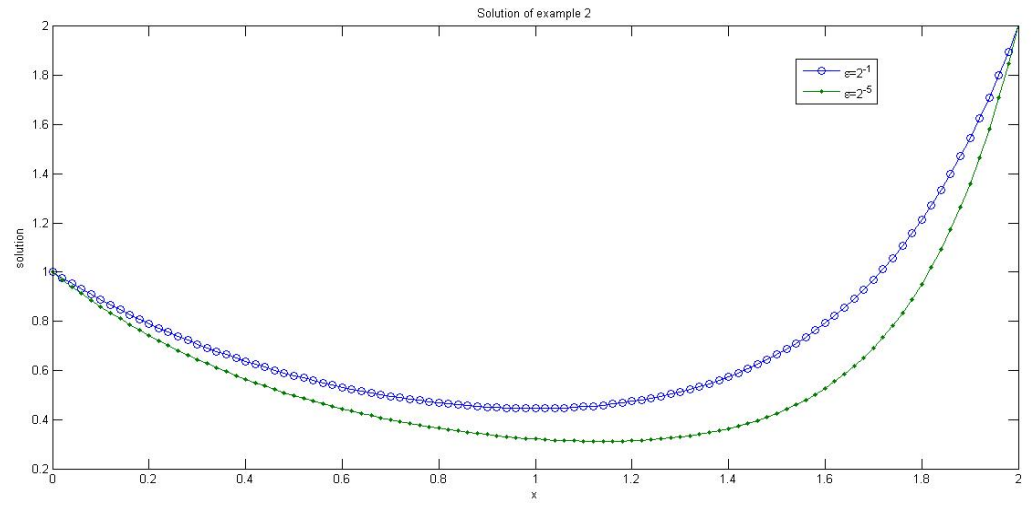


Figure 4.3: Solution of Example 4.2 at different values of ϵ .

Table 4.8: Maximum absolute error obtained for Example 4.3 for diverse values of ε

ε	N=16	N=32	N=64	N=128	N=256	N=512
2^{-4}	8.0000E-04	2.2000E-04	4.0000E-05	3.0000E-05	7.0000E-05	7.0000E-05
2^{-5}	8.9000E-04	2.4000E-04	4.0000E-05	4.0000E-05	4.0000E-05	2.8000E-04
2^{-6}	9.3000E-04	2.5000E-04	5.0000E-05	1.0000E-05	4.0000E-05	1.0000E-04
2^{-7}	9.5000E-04	2.6000E-04	4.0000E-05	3.0000E-05	2.0000E-05	1.1000E-04
2^{-8}	9.6000E-04	2.6000E-04	5.0000E-05	3.0000E-05	5.0000E-05	1.1000E-04
2^{-9}	9.6000E-04	2.6000E-04	3.0000E-05	4.0000E-05	4.0000E-05	9.0000E-05
2^{-10}	9.6000E-04	2.6000E-04	4.0000E-05	2.0000E-05	3.0000E-05	9.0000E-05
2^{-11}	9.7000E-04	2.6000E-04	4.0000E-05	2.0000E-05	3.0000E-05	2.3000E-04
2^{-12}	9.7000E-04	2.6000E-04	5.0000E-05	2.0000E-05	5.0000E-05	2.3000E-04
2^{-13}	9.7000E-04	2.6000E-04	3.0000E-05	3.0000E-05	2.0000E-05	1.2000E-04
2^{-14}	9.7000E-04	2.6000E-04	4.0000E-05	3.0000E-05	6.0000E-05	3.0000E-04
2^{-15}	9.7000E-04	2.6000E-04	3.0000E-05	5.0000E-05	6.0000E-05	6.0000E-05
2^{-16}	9.7000E-04	2.6000E-04	5.0000E-05	2.0000E-05	5.0000E-05	1.7000E-04
2^{-17}	9.7000E-04	2.5000E-04	4.0000E-05	6.0000E-05	7.0000E-05	2.9000E-04
2^{-18}	9.8000E-04	2.6000E-04	3.0000E-05	2.0000E-05	9.0000E-05	7.0000E-05
2^{-19}	9.7000E-04	2.7000E-04	4.0000E-05	1.0000E-05	1.2000E-04	3.6000E-04
2^{-20}	9.7000E-04	2.6000E-04	3.0000E-05	1.0000E-05	3.0000E-05	1.5000E-04
2^{-21}	9.7000E-04	2.6000E-04	4.0000E-05	2.0000E-05	3.0000E-05	1.1000E-04
2^{-22}	9.7000E-04	2.6000E-04	4.0000E-05	1.0000E-05	2.0000E-05	1.4000E-04
2^{-23}	9.7000E-04	2.6000E-04	4.0000E-05	1.0000E-05	2.0000E-05	5.0000E-05

D ^N by our method	9.7000E-04	2.6000E-04	5.0000E-05	6.0000E-05	1.2000E-04	3.6000E-04
D ^N _{in} (Subburayan & Ramanujam, 2013)	7.0787E-02	3.0352E-02	1.0725E-02	3.7882E-03	1.2551E-03	3.8154E-04

Table 4.9: Maximum absolute error obtained for various values of ϵ for Example 4.3

ϵ	N=16	N=32	N=64	N=128	N=256
0.01	9.4000E-04	2.5000E-04	4.0000E-05	1.0000E-05	2.0000E-05
0.001	9.7000E-04	2.6000E-04	4.0000E-05	3.0000E-05	4.0000E-05
0.0001	9.6000E-04	2.7000E-04	4.0000E-05	1.0000E-05	3.0000E-05

Table 4.10: Solution of Example 4.3 for $\varepsilon = 0.01$

x_i	N=16	N=32	N=64	N=128	N=256	N=512
0.000	1.00000	1.00000	1.00000	1.00000	1.00000	1.00000
0.250	1.01231	1.01241	1.01244	1.01244	1.01244	1.01245
0.500	1.03255	1.03278	1.03284	1.03286	1.03285	1.03287
0.750	1.06582	1.06622	1.06633	1.06634	1.06635	1.06637
1.000	1.12049	1.1211	1.12126	1.12129	1.12129	1.12131
1.250	1.21036	1.21118	1.21139	1.21143	1.21144	1.21145
1.500	1.35809	1.35903	1.35928	1.35932	1.35932	1.35933
1.750	1.60090	1.60170	1.601910	1.60194	1.60195	1.60195
2.000	2.0000	2.0000	2.0000	2.0000	2.0000	2.0000

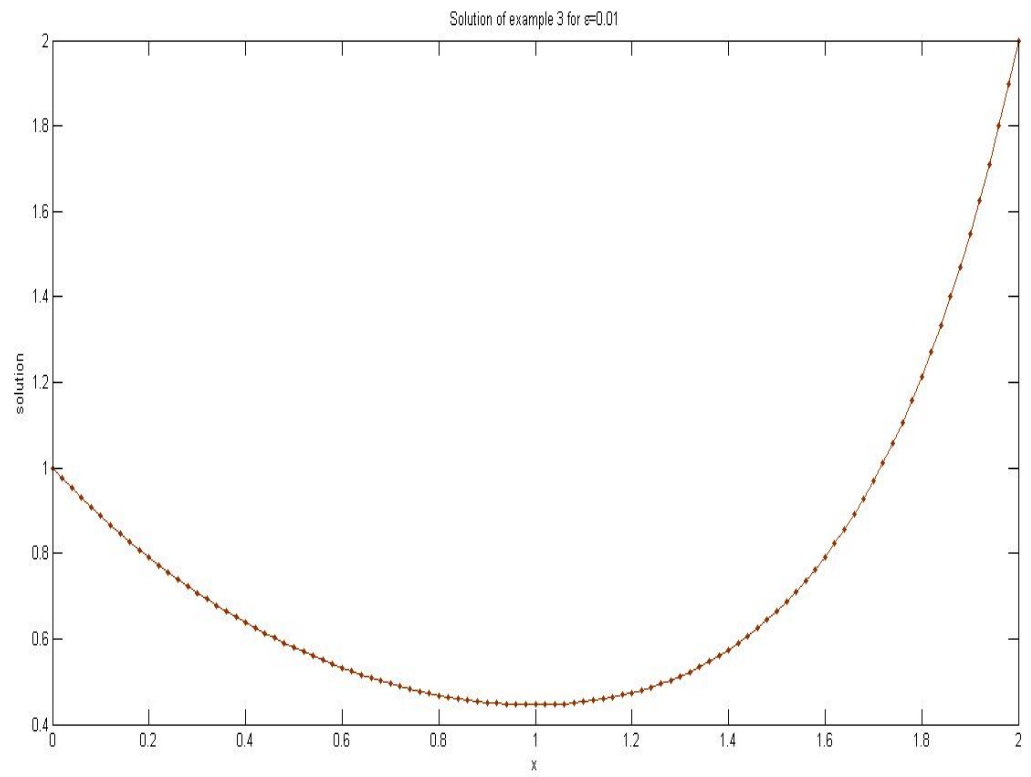


Figure 4.4: Layer behavior of Example 4.3 for $\epsilon = 0.01$

Chapter 5

A comparison of trigonometric B-spline collocation method and exponential B-spline collocation technique

5.1 Introduction

The trigonometric B-spline functions are piecewise continuous functions in the space $\Gamma_m = \text{span} \{1, \cos(x), \sin(x), \dots, \cos(kx), \sin(kx)\}$. These are periodic functions and possess continuous differentiability four times the number of partition points in the domain. (Guido, 1997). The detailed discussion of these functions is already done in chapter 3.

The exponential B-splines are the rectangular functions and obtained by convolution integral operation. The mathematical expression for exponential B-spline functions is obtained by considering the weights as exponential functions. For definition of these functions refer to introduction part of chapter 4.

In recent years, many researchers have worked on exponential B-spline function as well as trigonometric B-spline function for numerical solution of the differential equations. The matrix differential equations of second order are solved by using exponential and trigonometric cubic B-splines by Raslan et al. (Raslan, Hadhoud, & Shaalan, 2018). The maximum absolute error obtained by cubic B-spline, trigonometric cubic B-spline and exponential cubic B-spline are compared for three numerical examples.

5.2 Problem Statement

The following singularly perturbed boundary value is considered for numerical treatment:

$$\begin{cases} -\varepsilon y''(x) + a(x)y'(x) + b(x)y(x-1) = f(x), x \in \Omega^* & (5.1) \\ y(x) = \phi(x), x \in [-1, 0], y(2) = l. & (5.2) \end{cases}$$

$$\text{where } a(x) = \begin{cases} a_1(x), & x \in [0, 1] \\ a_2(x), & x \in (1, 2] \end{cases}$$

$$\text{and } f(x) = \begin{cases} f_1(x), & x \in [0,1] \\ f_2(x), & x \in (1,2] \end{cases}$$

$$a_1(1-) \neq a_2(1+),$$

$$f_1(1-) \neq f_2(1+), a_1(x) \geq \alpha_1 > \alpha > 0 \text{ and } a_2(x) \leq -\alpha_2 < -\alpha < 0, \alpha < \min\{\alpha_1, \alpha_2\} \text{ ag.}$$

And ε is very-very small positive number, $0 < \varepsilon \ll 1$. The functions $a(x)$, $f(x)$ are sufficiently smooth functions and are bounded in region Ω^* . And the function $b(x)$ is a sufficiently smooth function on $\bar{\Omega}$ where $\bar{\Omega} = [0, 2]$, $\Omega = (0, 2)$, $\Omega^* = \Omega^- \cup \Omega^+$, $\Omega^- = (0, 1)$ and $\Omega^+ = (1, 2)$ and ϕ is a smooth function on $[-1, 0]$.

Taylor's series up to second order accuracy is used to handle the delay term.

$$y(x-1) = y(x) - y'(x) + \frac{y''(x)}{2}$$

By using above in equation (5.1), following is obtained:

$$P(x)y''(x) + Q(x)y'(x) + R(x)y(x) = f(x) \quad (5.3)$$

where $P(x) = -\varepsilon + \frac{b(x)}{2}$, $Q(x) = a(x) - b(x)$ and $R(x) = b(x)$

5.3 Existence of Solution

Theorem: The equation (5.1)-(5.2) has solution $y \in C^0(\bar{\Omega}) \cap C^1(\Omega) \cap C^2(\Omega^*)$.

Proof: As discussed by Farrell et al. (Farrell, Hegarty, Miller, O'Riordan, & Shishkin, 2004)

5.4 Selection of mesh

To capture the layer behavior of considered SPDDE the domain is partitioned into the piecewise uniform refined mesh also known as Shishkin mesh.

The interval $[0,2]$ is divided into five subintervals as:

$$[0, \tau_1], [1 - \tau_1, 1], [1, 1 + \tau_2], [1 + \tau_2, 2 - \tau_2], [2 - \tau_2, 2]$$

where $\tau_1 = \min\left(\frac{1}{2}, \frac{2\varepsilon \ln N}{\alpha}\right)$ and $\tau_2 = \min\left(\frac{1}{4}, \frac{2\varepsilon \ln N}{\alpha}\right)$.

The mesh $\{0=x_0 < x_1 < x_2 < \dots < x_N = 2\}$ is defined as:

$$x_0 = 0, x_i = x_0 + ih_1 \text{ for } 1 \leq i \leq \frac{N}{4} \text{ where } h_1 = \frac{4(1-\tau_1)}{N},$$

$$x_i = x_{i-1} + ih_2 \text{ for } \frac{N}{4} \leq i \leq \frac{N}{2} \text{ where } h_2 = \frac{4\tau_1}{N},$$

$$x_i = x_{i-1} + ih_3 \text{ for } \frac{N}{2} \leq i \leq \frac{5N}{8} \text{ where } h_3 = \frac{8\tau_2}{N},$$

$$x_i = x_{i-1} + ih_4, \frac{5N}{8} \leq i \leq \frac{7N}{8} \text{ where } h_4 = \frac{4(1-2\tau_2)}{N},$$

$$x_i = x_{i-1} + ih_3, \frac{7N}{8} \leq i \leq N$$

5.5 Implementation of Collocation Method

The approximate solution of equation is obtained using exponential B-spline basis function. Let the partitioned of the domain be $\{0 \equiv x_0 < x_1 < x_2 < \dots < x_N \equiv 2\}$ where N is total number of partition points and $h = x_{i+1} - x_i$. An approximation to the solution is given as below:

$$y(x) = \sum_{i=-1}^{N+1} \alpha_i EB_i(x) \quad (5.4)$$

where α_i 's are the unknown real coefficients and $EB_i(x)$'s are the exponential B-spline basis functions. The exponential B-splines, $EB_i(x)$ at the partition points can be defined as in chapter 4 (section: 4.3).

Now by using the values of $EB_i(x)$, $EB'_i(x)$ and $EB''_i(x)$ at nodal points from Table 4.1, $y(x)$ and its first two derivatives can be expressed as:

$$y(x_i) = m_1 \alpha_{i-1} + \alpha_i + m_1 \alpha_{i+1},$$

$$y'(x_i) = m_2 \alpha_{i+1} - m_2 \alpha_{i-1},$$

$$y''(x_i) = m_3 \alpha_{i-1} - 2m_3 \alpha_i + m_3 \alpha_{i+1}$$

$$\text{where } m_1 = \frac{s-ph}{2(phc-s)}, m_2 = \frac{p(c-1)}{2(phc-s)}, m_3 = \frac{p^2s}{2(phc-s)}$$

Now, to apply the collocation technique, the collocation points are selected in such a way that they concur with the nodal points. On substituting the values of y_i , y_i' and y_i'' at nodal points in equation (5.4), a system of $N+1$ linear equations in $N+3$ unspecified variables has been obtained as:

$$E_i^l \alpha_{i-1} + E_i \alpha_i + E_i^r \alpha_{i+1} = f_i, \quad 0 \leq i \leq N \quad (5.5)$$

where

$$E_i^l = P(x)m_1 - Q(x)m_2 + R(x)m_3,$$

$$E_i = P(x) - 2R(x)m_3,$$

$$E_i^r = P(x)m_1 + Q(x)m_2 + R(x)m_3$$

The additional variables α_{-1} and α_{n+1} exists when $i = 0$ and $i = n$ will be considered in equation (5.5). To eliminate these variables, using boundary conditions following has been used:

$$\alpha_{-1} = \frac{\phi_0 - \alpha_0 - m_1 \alpha_1}{m_1} \text{ and } \alpha_{n+1} = \frac{\gamma - \alpha_n - m_1 \alpha_{n-1}}{m_1}$$

On substituting these values in equation (5.5) for $i = 0$ and $i = N$, the following is obtained:

$$\alpha_0 \left(\frac{1}{m_1} E_0^l + E_0 \right) + \alpha_1 (E_0^r - E_0^l) = f_0 - \frac{\phi E_0^l}{m_1} \quad (5.6)$$

and

$$\alpha_{n-1} (E_N^l - E_N^r) + \alpha_n \left(E_N - \frac{1}{m_1} E_N^r \right) = f_n - \frac{\gamma E_n^r}{m_1} \quad (5.7)$$

Now we have $N+1$ equations in $N+1$ variables as $A\alpha=B$ where $\alpha = [\alpha_0, \alpha_1, \alpha_2, \dots, \dots, \alpha_N]^T$.

The tridiagonal matrix A is given by

$$\begin{bmatrix} -\frac{1}{m_1}E_0^l + E_0 & E_0^r - E_0^l & \cdots & \cdots & \cdots & \cdots & \cdots & \cdots & 0 \\ E_1^l & E_1 & E_1^r & \cdots & \cdots & \cdots & \cdots & \cdots & 0 \\ \vdots & \vdots & \vdots & \vdots & \vdots & \vdots & \vdots & \vdots & \vdots \\ \vdots & \vdots & \vdots & \vdots & \vdots & \vdots & \vdots & \vdots & \vdots \\ 0 & \cdots & 0 & E_i^l & E_i & E_i^r & 0 & \cdots & \cdots \\ \vdots & \vdots & \vdots & \vdots & \vdots & \vdots & \vdots & \vdots & \vdots \\ \vdots & \vdots & \vdots & \vdots & \vdots & \vdots & \vdots & \vdots & \vdots \\ 0 & \cdots & \cdots & \cdots & \cdots & E_{N-1}^l & E_{N-1} & E_{N-1}^r & \cdots \\ 0 & \cdots & \cdots & \cdots & \cdots & \cdots & E_N^l - E_N^r & E_N - \frac{1}{m_1}E_N^r & \cdots \end{bmatrix}$$

and the right-hand side is a column matrix B, given by

$$\begin{bmatrix} f(x_0) - E_0^l \left(\frac{\phi_0}{m_1} \right) \\ f(x_1) \\ f(x_2) \\ \vdots \\ \vdots \\ \vdots \\ f(x_{n-1}) \\ f(x_n) - \gamma \left(\frac{E_n^r}{m_1} \right) \end{bmatrix}$$

Similar procedure is followed to approximate the solution by using trigonometric cubic B-spline basis functions by considering $y(x) = \sum_{i=-1}^{N+1} \alpha_i T_i(x)$ as approximate solution, where $T_i(x)$'s are the Trigonometric B-spline basis functions.

The value of $y(x)$ and its first two derivatives can be expressed in terms of α_i 's as:

$$y(x_i) = k_1 \alpha_{i-1} + k_2 \alpha_i + k_1 \alpha_{i+1}$$

$$y'(x_i) = k_3 \alpha_{i-1} + k_4 \alpha_{i+1}$$

$$y''(x_i) = k_5\alpha_{i-1} + k_6\alpha_i + k_5\alpha_{i+1}$$

where $k_1 = \sin^2\left(\frac{h}{2}\right) \csc(h) \csc\left(\frac{3h}{2}\right)$,

$$k_2 = \frac{2}{1+2\cos(h)},$$

$$k_3 = -\frac{3}{4} \csc\left(\frac{3h}{2}\right),$$

$$k_4 = \frac{3}{4} \csc\left(\frac{3h}{2}\right),$$

$$k_5 = \frac{3\left((1+3\cos(h))\cos^2\left(\frac{h}{2}\right)\right)}{16\left(2\cos\left(\frac{h}{2}\right)+\cos\left(\frac{3h}{2}\right)\right)}$$

$$\text{and } k_6 = -\frac{3\cot^2\left(\frac{h}{2}\right)}{2+4\cos(h)}$$

Using $y(x_i)$, $y'(x_i)$ and $y''(x_i)$ in (3) we get a system of $N + 1$ linear equations in $N + 3$ unspecified variables as:

$$T_i^l \alpha_{i-1} + T_i \alpha_i + T_i^r \alpha_{i+1} = f_i, \quad 0 \leq i \leq N \quad (5.8)$$

where

$$T_i^l = P(x)k_5 + q(x)k_3 + R(x)k_1$$

$$T_i = P(x)k_6 + R(x)k_2$$

$$T_i^r = P(x)k_5 + Q(x)k_4 + R(x)k_1$$

Here also there exist two additional variables α_{-1} and α_{n+1} whose values are obtained from boundary conditions.

$$\alpha_{-1} = \frac{\emptyset_0 - k_2\alpha_0 - k_1\alpha_1}{k_1} \quad \text{and} \quad \alpha_{n+1} = \frac{\gamma - k_1\alpha_{n-1} - k_2\alpha_n}{k_1}$$

From using above in equation (5.8) $N+1$ equations in $N+1$ variables as $A'\alpha=B'$ is obtained with

$$A' = \begin{bmatrix} T_0 - \frac{k_2}{k_1} T_0^l & T_0^r - T_0^l & \cdots & \cdots & \cdots & \cdots & \cdots & \cdots & 0 \\ T_1^l & T_1 & T_1^r & \cdots & \cdots & \cdots & \cdots & \cdots & 0 \\ \vdots & \vdots & \vdots & \vdots & \vdots & \vdots & \vdots & \vdots & \vdots \\ \vdots & \vdots & \vdots & \vdots & \vdots & \vdots & \vdots & \vdots & \vdots \\ 0 & \cdots & 0 & T_i^l & T_i & T_i^r & 0 & \cdots & \cdots \\ \vdots & \vdots & \vdots & \vdots & \vdots & \vdots & \vdots & \vdots & \vdots \\ \vdots & \vdots & \vdots & \vdots & \vdots & \vdots & \vdots & \vdots & \vdots \\ 0 & \cdots & \cdots & \cdots & \cdots & T_{n-1}^l & T_{n-1} & T_{n-1}^r & \cdots \\ 0 & \cdots & \cdots & \cdots & \cdots & \cdots & T_n^l - T_N^r & T_N - \frac{k_2}{k_1} T_N^r & \cdots \end{bmatrix}$$

$$\text{And } B' = \begin{bmatrix} f(x_0) - T_0^l \left(\frac{\phi_0}{k_1} \right) \\ f(x_1) \\ \vdots \\ \vdots \\ \vdots \\ f(x_{n-1}) \\ f(x_n) - \gamma \left(\frac{T_n^r}{k_1} \right) \end{bmatrix}$$

5.6 Convergence Analysis

This section is preserved for the exploration of the convergence of both the techniques used for approximation of solution. It is presumed that C is a non-specific positive constant independent of δ, ε and N , which may capture different values at different points.

Lemma 5.1

If the functions $a(x), b(x), c(x)$ and $f(x)$ are sufficiently smooth and are independent of ε , then the solution y of (5.1) –(5.2) satisfies

$$|y^{(k)}(x)| \leq C \left(1 + \varepsilon^{-k} e^{-\frac{\beta x}{\varepsilon}}\right), k = 0, 1, 2, \dots \quad (\text{Kumar \& Kadalbajoo, 2012}).$$

Lemma 5.2

Hall error estimation: If $f(x) \in C^2[0,1]$ and $y(x) \in C^4[0,1]$,

Then $\|D^j(y - Y)\| \leq \lambda_j \|y^4\| \bar{h}^{4-j}, j = 0, 1, 2, \dots$ where λ_j are the constants (Hall, 1968).

Lemma 5.3

(Varah, 1975) If A is diagonal dominant by rows and $\alpha = \min_i (|a_{i,i}| - \sum_{i \neq j} |a_{i,j}|)$.

Then $\|A^{-1}\|_\infty < \frac{1}{\alpha}$.

Lemma 5.4

For the refined mesh, $\frac{\bar{h}}{\varepsilon} \leq cN^{-1} \ln N$.

Proof:

As discussed in section 5.4, $[0,2]$ partitioned into four subintervals:

$$[0, \tau_1], [1 - \tau_1, 1], [1, 1 + \tau_2], [1 + \tau_2, 2 - \tau_2], [2 - \tau_2, 2]$$

$$\text{with } \tau_1 = \min\left(\frac{1}{2}, \frac{2\varepsilon \ln N}{\alpha}\right) \text{ and } \tau_2 = \min\left(\frac{1}{4}, \frac{2\varepsilon \ln N}{\alpha}\right)$$

$$\text{If, } 1 \leq i \leq \frac{N}{4}, \bar{h} = \frac{4(1-\tau_1)}{N} \text{ and for } \frac{5N}{8} \leq i \leq \frac{7N}{8}, \bar{h} = \frac{4(1-2\tau_2)}{N}$$

$$\text{For } \frac{N}{4} \leq i \leq \frac{N}{2}, \bar{h} = \frac{4\tau_1}{N}$$

$$\text{For } \frac{N}{2} \leq i \leq \frac{5N}{8} \text{ and } \frac{7N}{8} \leq i \leq N, \bar{h} = \frac{8\tau_2}{N},$$

combining all subintervals, clearly $\frac{\bar{h}}{\varepsilon} \leq cN^{-1} \ln N$.

Lemma 5.5

The trigonometric B-splines T_i 's and exponential B-splines $EB_i(x)$'s, satisfy the inequality $\sum_{i=-1}^{N+1}|EB_i(x)| \leq 10$ and $\sum_{i=-1}^{N+1}|T_i(x)| \leq 10$, $0 \leq x \leq 2$.

Proof: The result can be proved similarly as proved by Kadalbajoo and Aggarwal (Kadalbajoo & Aggarwal, 2005)

Theorem 5.1

Let $S(x)$ be the approximation to the solution $y(x)$ of boundary value problem (5.1)-(5.2). IF $f \in C^2[0,1]$, then the error estimate is given by

$\text{Sup}_\varepsilon \max_i |y(x_i) - S(x_i)| \leq CN^{-2} \ln^3 N$, where $0 \leq i \leq N$ and $0 < \varepsilon \leq 1$ and C is a positive constant as defined above.

Proof:

Consider $Y(x)$ be the unique spline interpolate to the solution $y(x)$ of SPDDE given in (1)-(2) and the estimated error is given by $|y(x) - S(x)|$.

Now by using Hall error estimation as defined in Lemma 5.2 the following estimation has been obtained:

$$\begin{aligned} |Ly(x_i) - LY(x_i)| &= \left| -\varepsilon + \frac{b(x)}{2} \right| |y''(x_i) - Y''(x_i)| + |a(x) - b(x)| |y'(x_i) - Y'(x_i)| \\ &\quad + |b(x)| |y(x_i) - Y(x_i)| \\ &\leq (c_\varepsilon \lambda_3 \bar{h}^2 + (\|b(x)\| + \|b(x)\|) \lambda_1 \bar{h}^3 + \|b(x)\| \lambda_0 \bar{h}^4) \|y^4\| \end{aligned}$$

Using lemma 5.1, results in

$$\begin{aligned} |Ly(x_i) - LY(x_i)| &\leq (c_\varepsilon \lambda_3 \bar{h}^2 + (\|b(x)\| + \|b(x)\|) \lambda_1 \bar{h}^3 + \|b(x)\| \lambda_0 \bar{h}^4) C \left(1 + \right. \\ &\quad \left. \varepsilon^{-4} e^{-\frac{\beta x}{\varepsilon}} \right) \end{aligned} \tag{5.9}$$

By lemma 5.4, $\frac{\bar{h}}{\varepsilon} \leq cN^{-1} \ln N$, following is obtained:

$$|Ly(x_i) - LY(x_i)| \leq CN^{-2} \ln^2 N$$

$$\text{Therefore, } |Ly(x_i) - LY(x_i)| = |f(x_i) - LY(x_i)| \leq CN^{-1} \ln^3 N \quad (5.10)$$

Now consider the boundary value problem as

$$LY(x) = \bar{f}(x_i) \text{ with conditions } Y(x_0) = \phi(0), Y(x_N) = \gamma$$

$A\bar{\alpha} = \bar{B}$ is linear system of equations obtained from above problem, which follows that

$$A(\alpha - \bar{\alpha}) = B - \bar{B} \quad (5.11)$$

$$\text{where } B - \bar{B} = [f(x_0) - \bar{f}(x_0), f(x_1) - \bar{f}(x_1), \dots, f(x_N) - \bar{f}(x_N)]^t$$

$$\text{By using (5.10), } \|B - \bar{B}\| \leq CN^{-2} \ln^2 N \quad (5.12)$$

The matrix A is strictly diagonal dominant for sufficiently small values of h .

Now by exponential scheme:

$$|a_{i,i}| - (|a_{i,i-1}| + |a_{i,i+1}|) = \begin{cases} \left(\frac{m_2}{m_1} - 2m_2 \right) Q(x_0) + \left(-2m_3 - \frac{m_3}{m_1} \right) R(x_0), & \text{from first row} \\ \left(-\frac{m_2}{m_1} + 2m_2 \right) Q(x_N) + R(x_N) \left(-2m_3 - \frac{m_3}{m_1} \right), & \text{from last row} \\ (1 - 2m_1)P(x_i) - 4m_3R(x_i), & \text{otherwise} \end{cases}$$

For trigonometric scheme

$$|a_{i,i}| - (|a_{i,i-1}| + |a_{i,i+1}|) = \begin{cases} \left(k_6 - 2k_5 - \frac{k_2 k_5}{k_1} \right) P(x_0) + \left(-k_3 - k_4 - \frac{k_2 k_3}{k_1} \right) Q(x_0) + (-2k_1)R(x_0), & \text{from first row} \\ \left(k_6 - \frac{k_2}{k_1} k_5 \right) P(x_N) + \left(k_4 - k_3 - \frac{k_2 k_4}{k_1} \right) Q(x_N), & \text{from last row} \\ (k_6 - 2k_5)P(x_i) + (k_2 - 2k_1)R(x_i) - (k_3 + k_4)Q(x_i), & \text{otherwise} \end{cases}$$

Therefore, from 5.13 and lemma 5.3, $\|A^{-1}\| \leq C$ (for both schemes) (5.13)

Now combining (5.11), (5.12), and (5.13), following is obtained.

$$|\alpha - \bar{\alpha}| \leq CN^{-2} \ln^2 N, \quad 0 \leq i \leq N \quad (5.14)$$

Now, by using boundary conditions (5.6) and (5.7), the value of $|\alpha_{-1} - \bar{\alpha}_{-1}|$ and $|\alpha_{N+1} - \bar{\alpha}_{N+1}|$ are estimated,

$$|\alpha_{-1} - \bar{\alpha}_{-1}| \leq CN^{-2} \ln^2 N \text{ and } |\alpha_{N+1} - \bar{\alpha}_{N+1}| \leq CN^{-2} \ln^2 N$$

Therefore, $\max |\alpha_i - \bar{\alpha}_i| \leq CN^{-2} \ln^2 N$, for $-1 \leq i \leq N+1$ (5.15)

Now using lemma 5.5 and (5.15) to estimate

$$|S(x) - Y(x)| = \begin{cases} \sum_{i=-1}^{N+1} (\alpha_i - \bar{\alpha}_i) EB_i(x) & \text{for exponential scheme} \\ \sum_{i=-1}^{N+1} (\alpha_i - \bar{\alpha}_i) T_i(x) & \text{for trigonometric scheme} \end{cases}$$

results in $|S(x) - Y(x)| \leq CN^{-2} \ln^3 N$, which leads to result of theorem with triangle inequality as:

$$\sup(\varepsilon) \max(i) |y(x_i) - S(x_i)| \leq CN^{-2} \ln^2 N, \text{ where } 0 \leq i \leq N \text{ and } 0 < \varepsilon \leq 1.$$

Hence the result is proved.

5.7 Numerical Examples

To validate the proposed scheme two examples are considered for numerical solution. The double mesh principle is used to calculate the maximum absolute error (MAE), $D^N = \max |y_i^N - y_{2i}^{2N}|$ where $1 \leq i \leq N$.

Example 5.1:

$$\begin{aligned}
-\varepsilon y''(x) + 3y'(x) - y(x-1) &= 0, & x \in \Omega^- \\
-\varepsilon y''(x) - 4y'(x) - y(x-1) &= 0, & x \in \Omega^+ \\
y(x) &= 1, & x \in [-1, 0], \quad y(2) = 2.
\end{aligned}$$

Example 5.2:

$$\begin{aligned}
-\varepsilon y''(x) + (3 + x^2)y'(x) - y(x-1) &= 1, & x \in \Omega^- \\
-\varepsilon y''(x) - (4 + x)y'(x) - y(x-1) &= -1, & x \in \Omega^+ \\
y(x) &= 1, & x \in [-1, 0], \quad y(2) = 2.
\end{aligned}$$

5.7.1 Discussion of numerical examples

It is perceptible from the Table 5.2 and 5.6 that with refined mesh for both examples by exponential B-spline collocation technique the maximum absolute error declines as N increases from 16 to 64, and then a fall in absolute error is observed with rise in N . In contrast, maximum absolute error alleviates with magnification in value of N by trigonometric B-spline collocation method. Overall, better numerical solution is obtained by exponential B-spline method for small values of N , whereas trigonometric B-spline collocation method provided superior approximate solution for large values of N . Table 5.3 and 5.7, presents maximum absolute error obtained with uniform mesh for examples and it is found that the maximum absolute error obtained by exponential scheme is less as compared to trigonometric scheme, and error reduces with increment in value of N from 16 to 256 but from $N = 256$ to 1024, error upraised.

In Table 5.1 and 5.5, maximum absolute error by trigonometric scheme with refined mesh are presented for different values of perturbation parameter, also the maximum absolute error obtained is compared by existing method and found less as compared to reported method.

From Table 5.4 and 5.8, the results obtained by trigonometric scheme, shows that maximum absolute error is less for small values of N by uniform mesh, and for large values

of N by refined. Furthermore, with increase in N , Maximum absolute error decreases in same scheme with refined mesh where a fluctuation is perceptible if uniform mesh is used to partition the domain. On flip side, while using exponential scheme little maximum absolute error is obtained by uniform mesh as compared to refined mesh.

Exponential scheme is providing better solution with uniform mesh, but an increase in error is notable if value of N is raised beyond 256. Overall, exponential scheme with uniform mesh approximate improves solution with uniform mesh for $N=16$ to 256, but for $N=512$ and 1024, trigonometric scheme with refined mesh yields better solution as compared to exponential scheme.

From figure 5.2 and 5.5, it is observed that conduct of solution is same by exponential scheme with both mesh and by trigonometric method with uniform mesh. But by trigonometric scheme with refined mesh the vogue of solution is in reverse manner.

5.8 Conclusion

A singularly perturbed delay boundary value problem of second order with discontinuous convection coefficient and source term is considered for numerical treatment by trigonometric B-spline and exponential B-spline on piecewise uniform refined (Shishkin) mesh. Discussion of convergence is carried out by Hall's theorem for both exponential and trigonometric B-spline collocation method and the order of convergence of the method is of almost second order. From numerical results, it is observed that better numerical solution is obtained by exponential B-spline method for small values of N , whereas trigonometric B-spline collocation method provided superior approximate solution for large values of N . The results are also compared by both schemes for uniform as well as refined mesh and it can be concluded that trigonometric scheme with refined mesh yields better solution whereas exponential scheme gives improved solution with uniform mesh. Both basis functions provided the solutions with good accuracy. Hence, the discussed techniques can be applied to other SPDDE for numerical solution.

Table 5.1: Maximum absolute error of Example 5.1 by trigonometric B-spline with refined mesh with $\tau_1=0.3, \tau_2=0.15$

ε	N=16	N=32	N=64	N=128	N=256	N=512	N=1024
2^{-6}	0.115909	0.019628	0.009065	0.004419	0.002195	0.001155	0.000929
2^{-7}	0.116116	0.019476	0.009005	0.004395	0.002186	0.001146	0.000933
2^{-8}	0.116224	0.019395	0.008974	0.004387	0.002173	0.001154	0.000925
2^{-9}	0.116280	0.019354	0.008959	0.004379	0.002170	0.001129	0.000942
2^{-10}	0.116309	0.019333	0.008952	0.004376	0.002172	0.001146	0.000928
2^{-11}	0.116324	0.019324	0.008946	0.004373	0.002174	0.001140	0.000914
2^{-12}	0.116330	0.019317	0.008945	0.004371	0.002169	0.001153	0.000939
2^{-13}	0.116334	0.019315	0.008943	0.004375	0.002167	0.001132	0.000957
2^{-14}	0.116336	0.019314	0.008943	0.004372	0.002172	0.001141	0.000951
2^{-15}	0.116337	0.019313	0.008943	0.004371	0.002174	0.001117	0.000951
2^{-16}	0.116337	0.019313	0.008942	0.004371	0.002179	0.001130	0.000967
2^{-17}	0.116337	0.019313	0.008942	0.004365	0.002179	0.001130	0.000967
2^{-18}	0.116337	0.019313	0.008941	0.004373	0.002167	0.001138	0.000955
2^{-19}	0.116337	0.019312	0.008942	0.004374	0.002169	0.001134	0.000906
2^{-20}	0.116338	0.019313	0.008942	0.004372	0.002172	0.001127	0.000981
2^{-21}	0.116338	0.019313	0.008942	0.004373	0.002176	0.001123	0.000986
2^{-22}	0.116337	0.019313	0.008941	0.004373	0.002172	0.001120	0.000989
2^{-23}	0.116337	0.019313	0.008942	0.004373	0.002174	0.001123	0.001005
2^{-24}	0.116337	0.019313	0.008942	0.004372	0.002171	0.001133	0.000997
2^{-25}	0.116337	0.019313	0.008942	0.004373	0.002172	0.001137	0.000992
2^{-26}	0.116337	0.019313	0.008942	0.004373	0.002172	0.001137	0.000992
2^{-27}	0.116337	0.019313	0.008942	0.004373	0.002172	0.001137	0.000992
D^N	0.116338	0.019628	0.009065	0.004419	0.002195	0.001155	0.001005
D^N in (Subburayan, 2016b)	0.072967	0.047273	0.039152	0.027566	0.018534	0.011663	0.0069885

Table 5.2: Maximum absolute error of Example 5.1 by both schemes with refined mesh

ε	Applied basis functions	N=16	N=32	N=64	N=128	N=256	N=512
2^{-5}	Exponential	0.02984	0.00547	0.00477	0.01469	0.04700	0.10459
	Trigonometric	0.115909	0.019628	0.009065	0.004419	0.002195	0.001155
2^{-10}	Exponential	0.03222	0.00601	0.00477	0.01464	0.04695	0.10522
	Trigonometric	0.116309	0.019333	0.008952	0.004376	0.002172	0.001146
2^{-15}	Exponential	0.03238	0.00604	0.00477	0.01464	0.04702	0.10509
	Trigonometric	0.116337	0.019313	0.008943	0.004371	0.002174	0.001117
2^{-20}	Exponential	0.03238	0.00605	0.00478	0.01466	0.04706	0.10502
	Trigonometric	0.116338	0.019313	0.008942	0.004372	0.002172	0.001127
2^{-25}	Exponential	0.03239	0.00604	0.00477	0.01464	0.04706	0.10525
	Trigonometric	0.116337	0.019313	0.008942	0.004373	0.002172	0.001137

Table 5.3: Maximum absolute error of Example 5.1 by both schemes with uniform mesh

ε	Applied basis functions	N=16	N=32	N=64	N=128	N=256	N=512	N=1024
2^{-5}	Exponential	0.005550	0.001380	0.000320	6E-05	4E-05	0.001650	0.027770
	Trigonometric	0.098240	0.023230	0.009250	0.004190	0.002190	0.003400	0.019370
2^{-10}	Exponential	0.01314	0.00310	0.00073	0.0002	0.00035	0.00255	0.01277
	Trigonometric	0.09593	0.02373	0.00941	0.00396	0.00147	0.00745	0.01985
2^{-15}	Exponential	0.01320	0.00311	0.00074	0.00021	0.00044	0.00228	0.01755
	Trigonometric	0.09577	0.02376	0.00942	0.00398	0.00156	0.0054	0.02251
2^{-20}	Exponential	0.01321	0.00311	0.00074	0.00021	0.00026	0.00287	0.01716
	Trigonometric	0.09577	0.02376	0.00942	0.00393	0.00152	0.00669	0.01843
2^{-25}	Exponential	0.01321	0.00311	0.00073	0.0002	0.00037	0.00272	0.01724
	Trigonometric	0.09577	0.02376	0.00941	0.00396	0.00142	0.00532	0.02245

Table 5.4: Maximum absolute error obtained for Example 5.1 by both schemes and both meshes for $\varepsilon=2^{-6}$

	Mesh type	N=16	N=32	N=64	N=128	N=256	N=512	N=1024
Trigonometric scheme	Refined	0.115909	0.019628	0.009065	0.004419	0.002195	0.001155	0.000929
	Uniform	0.098240	0.023230	0.009250	0.004190	0.002190	0.003400	0.019370
Exponential Scheme	Refined	0.029840	0.005407	0.004770	0.014690	0.047000	0.104590	Not exist
	Uniform	0.005550	0.001380	0.000320	6E-05	4E-05	0.001650	0.027770

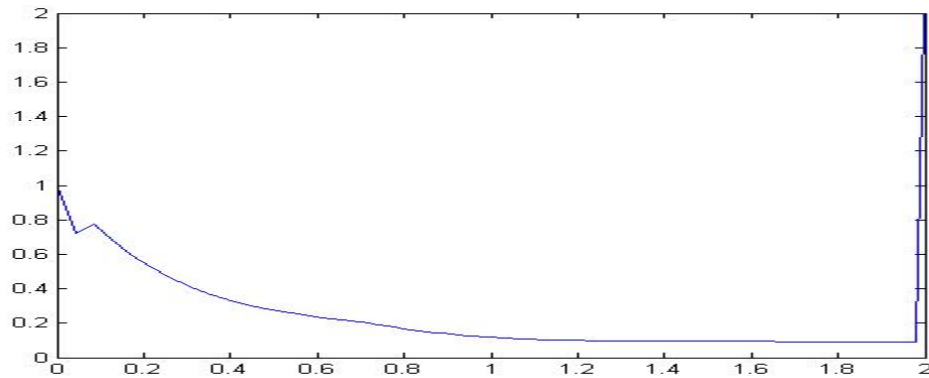


Figure 5.1: Solution of Example 5.1 by trigonometric scheme and refined mesh

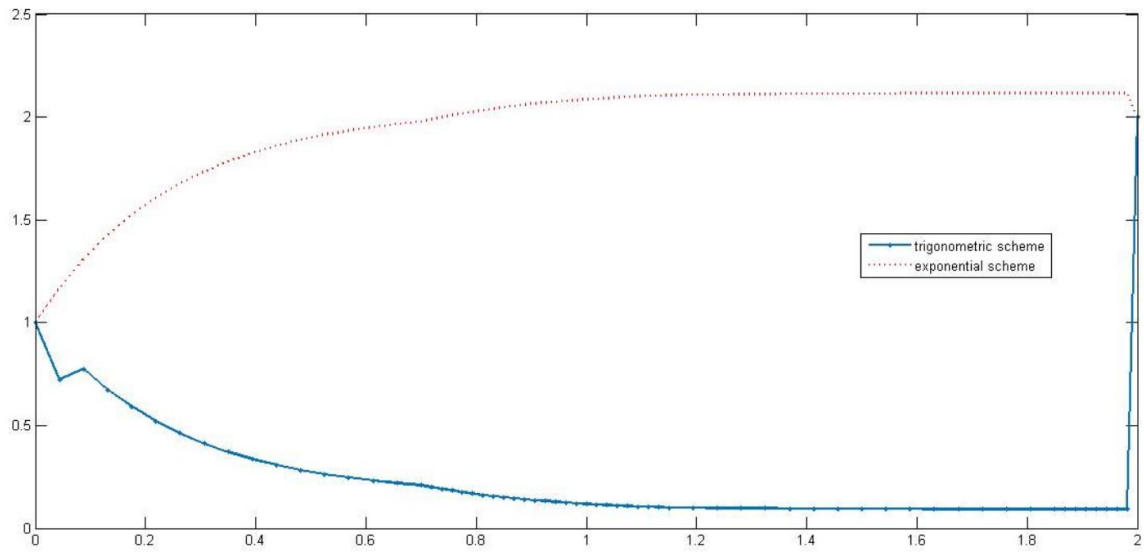


Figure 5.2: Solution of Example 5.1 by both schemes with refined mesh for $N=64$ and $\varepsilon=0.25$

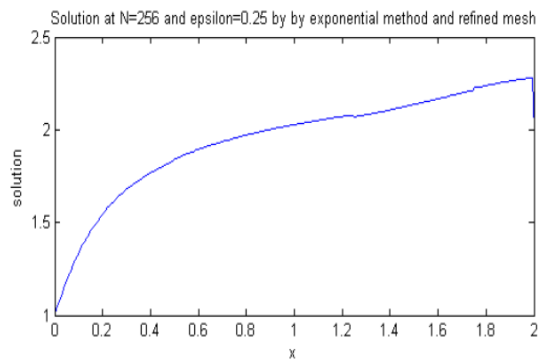
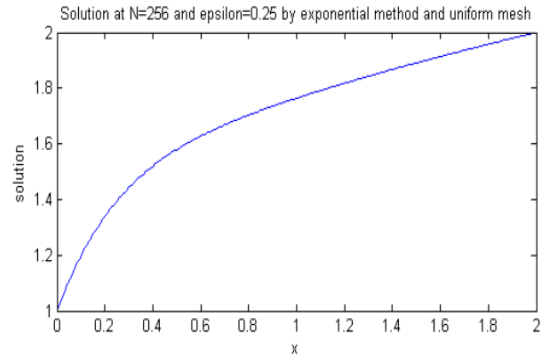
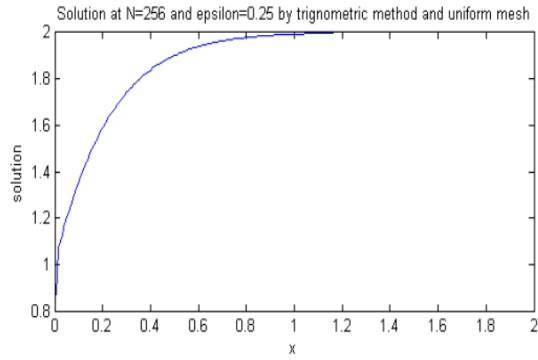


Figure 5.3: Solution of Example 5.1

Table 5.5: Solution of Example 5.2 by trigonometric B-spline by refined mesh with $\tau_1=0.3, \tau_2=0.15$.

ε	N=16	N=32	N=64	N=128	N=256	N=512	N=1024
2^{-6}	0.109726	0.020282	0.008614	0.004059	0.001983	0.000995	0.000580
2^{-7}	0.109806	0.020150	0.008556	0.004034	0.001973	0.000995	0.000538
2^{-8}	0.109850	0.020080	0.008527	0.004020	0.001971	0.000981	0.000530
2^{-9}	0.109871	0.020044	0.008512	0.004015	0.001970	0.000980	0.000596
2^{-10}	0.109883	0.020026	0.008503	0.004013	0.001962	0.000974	0.000572
2^{-11}	0.109889	0.020018	0.008500	0.004009	0.001960	0.000986	0.000555
2^{-12}	0.109892	0.020013	0.008498	0.004010	0.001962	0.000988	0.000540
2^{-13}	0.109894	0.020011	0.008497	0.004011	0.001954	0.000989	0.000557
2^{-14}	0.109894	0.020009	0.008497	0.004012	0.001956	0.000980	0.000561
2^{-15}	0.109894	0.020009	0.008496	0.004011	0.001960	0.000981	0.000558
2^{-20}	0.109895	0.020009	0.008495	0.004011	0.001961	0.000979	0.000578
2^{-25}	0.109895	0.020008	0.008497	0.004008	0.001962	0.000985	0.000580
2^{-27}	0.109895	0.020008	0.008497	0.004008	0.001962	0.000985	0.000580
D^N	0.109895	0.020150	0.008614	0.004059	0.001983	0.000995	0.000596
D^N in (Subburayan, 2016b)	0.047088	0.028800	0.024542	0.016827	0.01337	0.0071177	0.0042869

Table 5.6: Maximum absolute error of Example 5.2 by both schemes with refined mesh

ε	Applied basis functions	N=16	N=32	N=64	N=128	N=256	N=512
2^{-6}	Exponential	0.02168	0.00564	0.00666	0.01476	0.05009	0.10956
	Trigonometric	0.109726	0.020282	0.008614	0.004059	0.001983	0.000995
2^{-10}	Exponential	0.0231	0.00599	0.00667	0.01476	0.05009	0.10954
	Trigonometric	0.109883	0.020026	0.008503	0.004013	0.001962	0.000974
2^{-15}	Exponential	0.02319	0.00603	0.00666	0.01477	0.05007	0.10957
	Trigonometric	0.109894	0.020009	0.008496	0.004011	0.001960	0.000981
2^{-20}	Exponential	0.0232	0.00602	0.00667	0.01477	0.05007	0.10957
	Trigonometric	0.109895	0.020009	0.008495	0.004011	0.001961	0.000979
2^{-25}	Exponential	0.02319	0.00603	0.00666	0.01477	0.05007	0.10957
	Trigonometric	0.109895	0.020008	0.008497	0.004008	0.001962	0.000985

Table 5.7: Maximum absolute error of Example 5.2 by both schemes with uniform mesh

ϵ	Applied basis functions	N=16	N=32	N=64	N=128	N=256	N=512	N=1024
2^{-5}	Exponential	0.00538	0.00129	0.0003	8E-05	6E-05	0.00074	0.00149
	Trigonometric	0.09525	0.02383	0.00919	0.00403	0.00199	0.00134	0.00435
2^{-10}	Exponential	0.00579	0.00138	0.00033	8E-05	6E-05	0.00037	0.00333
	Trigonometric	0.09294	0.02433	0.00932	0.00408	0.00161	0.0026	0.01013
2^{-15}	Exponential	0.00582	0.00139	0.00032	7E-05	0.00013	0.00034	0.00238
	Trigonometric	0.09278	0.02436	0.00933	0.00408	0.00157	0.00268	0.01031
2^{-20}	Exponential	0.00582	0.00139	0.00033	8E-05	0.00014	0.00029	0.00229
	Trigonometric	0.09278	0.02437	0.00933	0.00409	0.0016	0.00276	0.01028
2^{-25}	Exponential	0.00582	0.00138	0.00034	8E-05	0.00011	0.00029	0.00241
	Trigonometric	0.09278	0.02437	0.00932	0.00408	0.00166	0.00257	0.01031

Table 5.8: Maximum absolute error obtained for Example 5.2 by both schemes and both meshes MAE for $\varepsilon=2^{-6}$

	Mesh type	N=16	N=32	N=64	N=128	N=256	N=512	N=1024
Trigonometric scheme	Refined	0.109726	0.020282	0.008614	0.004059	0.001983	0.000995	0.000580
	Uniform	0.09525	0.02383	0.00919	0.00403	0.00199	0.00134	0.00435
Exponential Scheme	Refined	0.02168	0.00564	0.00666	0.01476	0.05009	0.10956	Not exist
	Uniform	0.00538	0.00129	0.0003	8E-05	6E-05	0.00074	0.00149

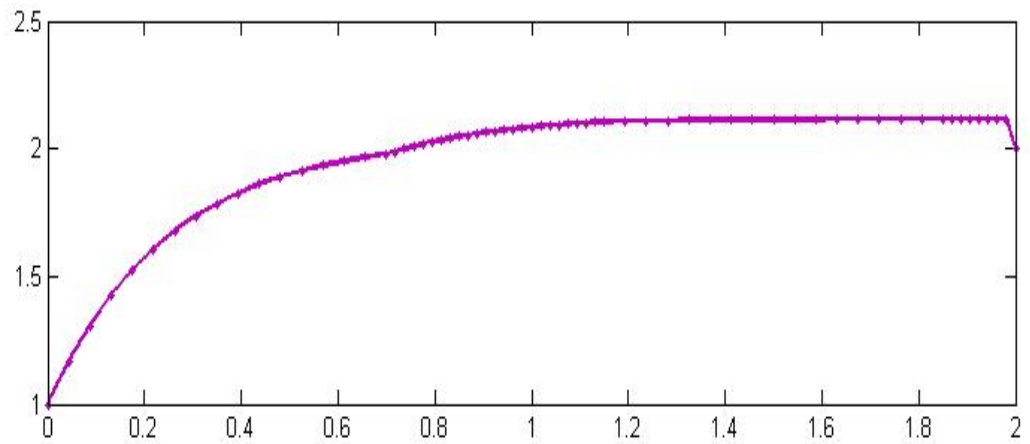


Figure 5.4: Solution of Example 5.2 by exponential scheme for $N=64$ and $\varepsilon=0.25$

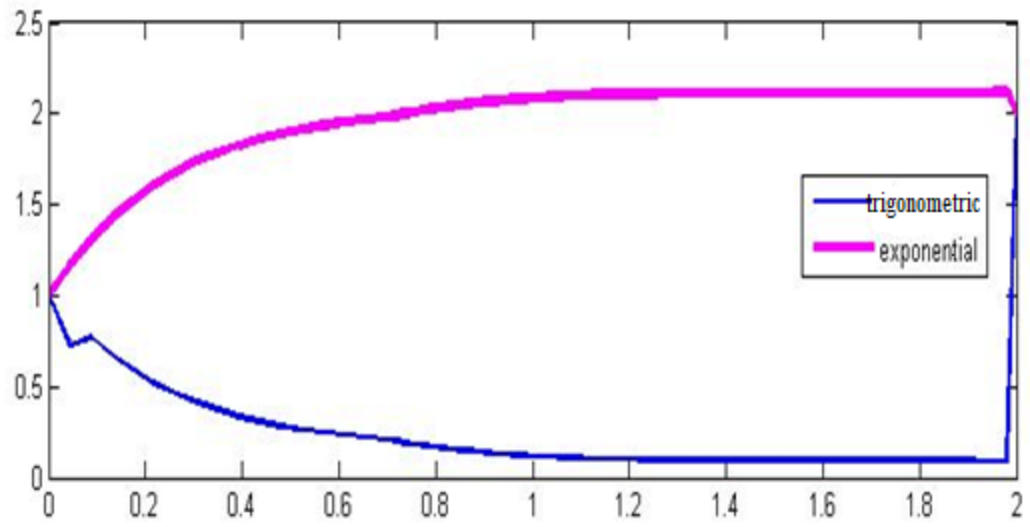


Figure 5.5: Solution of Example 5.2 by both schemes with refined mesh for $N = 64$ and $\varepsilon = 0.25$

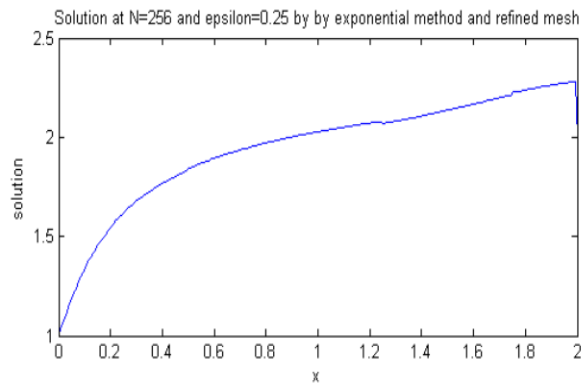
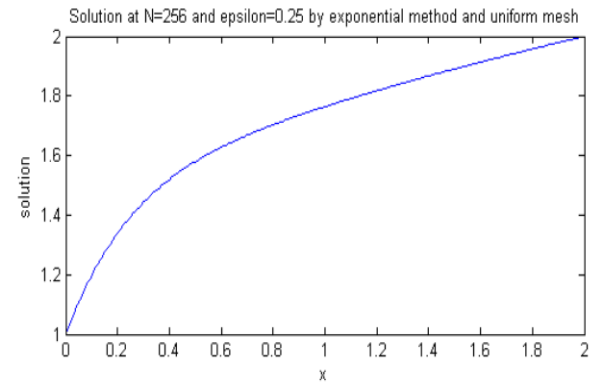
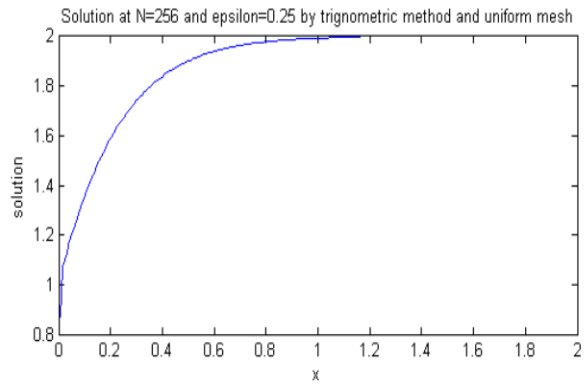


Figure 5.6: Solution of Example 5.2

Chapter 6

Conclusion and Future Directions

6.1 Conclusion

This thesis aims to explore the numerical solution of singularly perturbed delay differential equations. The ramifications of many mathematical models in real life are the singularly perturbed differential equations. These equations are prominent to study due to the broad applications of these equations in the development of science and technology. On the flip side, the challenges to simulate the equation is because of the abrupt change in the solution at the boundary layer, which results when the small parameter $\varepsilon \rightarrow 0$. This small parameter: perturbation parameter appears due to lack of continuity which may be the result of small parameters in the system, if suppressed diminish the order of the differential equation. The other important parameter associated with singularly perturbed delay differential equations is delay (retarded or shift) parameter. This delay comes into picture for any system which involves feedback control mean examination of a process in order to make changes to improve the system, for an instance; in a cricket match, the batsman continuously monitors the ball offered by the fielder and then by using that information he decide to hit the ball in a particular direction with some specific force by controlling his body position. So, the time delay effects the functioning of the system and then the output of the system. Analysis of this small parameter delay help to better understanding of the physical system and to do the best utilization of the resources. As an example, it was observed by the researchers that output of the solar pane is improved if the delay is considered in the modeling of the heating systems as compared to the utility of the solar energy through solar panel without considering the retarded term in the model.

6.2 Highlights of work

In this work, singularly perturbed delay differential equations are numerically treated by various numerical techniques. Various spline basis with collocation method have been used to find the approximate solution of these equations. The concept of fitting of polynomials is selected to solve these equations because of the major advantage of that they are easy to handle and the compact support property of splines for low computational complications. The collocation method is considered as an effortless method in numerical solution as it only involves fitting polynomial at selected points in the domain of the problem.

The SPDDE considered for numerical treatment in the chapters is the result of the mathematical model of various applications in science and technology such as biosciences, control theory, neurobiology, bifurcation and related to problems in the field of sciences.

The main highlights of the chapters are as follows:

Chapter two includes a modified cubic B-spline collocation method used for numerical solution of two SPDDEs of second order. Modified cubic spline has been used because modification in cubic spline provides a diagonal dominant matrix system which is easy to solve. One of the equations considered in this chapter arises in neurobiology which describes the study of nerve cells and the other equation is a general second order SPDDE, that results in four different SPDDEs for different values of the parameters. The singularly perturbed difference equation from Stein model and is described in this work. In this chapter, the domain has been partitioned by uniform as well as Shishkin mesh. The convergence analysis of the scheme has been discussed, and maximum absolute error has been calculated by using double mesh principle. It is clear from the numerical results that maximum absolute error is less if Shishkin mesh is generated for partition of the domain as compared to uniform mesh. The variation in numerical solution has been examined with alteration in the perturbation and delay parameter.

In chapter three, Trigonometric B-spline collocation technique has been adapted for numerical analysis of SPDDE. The reason to select this technique is that trigonometric B-

spline functions are highly periodic and are continuously differentiable 4 times the number of knot points in the partition of the domain. A second order SPDDE has been treated by cubic trigonometric B-spline method and a third SPDDE by quintic trigonometric B-spline scheme. The implementation of the scheme was simple, and the results obtained by this scheme have been found better as compared to the existing method. For both equations, convergence analysis has been carried out separately by using the concept of truncation error and Hall's theorem. Graphs have been plotted to capture the layer behavior of the solution of considered SPDDE and to show the pointwise maximum absolute error in the domain.

Chapter four is devoted to exponential B-splines based scheme for calculating the numerical solution of SPDDE. The exponential B-spline functions have been procured by multifold convolution of rectangular functions. A SPDDE of second order with large delay has been considered for numerical treatment by exponential B-splines collocation technique. In this work, the procedure to find truncation error has been explained well and the method used is second order convergent. The results obtained by the existing method have been found better as compared to the reported scheme. The conduct of solution has been discussed in detail with respect to the number of partition points and perturbation parameter.

Chapter five deals with a comparison of two spline-based schemes. The two schemes are: trigonometric B-spline collocation and exponential B-spline collocation are compared in order to investigate the conduct of solution provided by both schemes. In this work, to partition the domain, refined mesh has been selected. The convergence analysis of both schemes has been carried out through Hall's theorem and both schemes found to be of second order convergent. It was found from the numerical results that exponential B-spline collocation method accord better solution for small values of N whereas trigonometric B-spline collocation scheme provides best solution for large values of N .

6.3 Overall Numerical Work done

The following table briefly describes about the singularly perturbed delay differential equations considered for the numerical solution in present work:

Table 6.1: Summary of the numerical treatments performed on SPDDEs

S.No.	SPDDE	Mesh selected	Method	Conclusion	Order of convergence
1	$\varepsilon^2 y''(x) + a(x)y(x - \delta) + b(x)y(x) = f(x), 0 < x < 1$ subject to conditions: $y(x) = \phi(x)$ on $-\delta \leq x \leq 0$, and $y(1) = \gamma$	Shishkin mesh	Collocation method was used to solve SPDDE using modified B-spline basis functions.	The presented scheme was simple to use and readily adapted for implementation through computer.	Not presented
2	$\varepsilon y''(x) + a(x)y'(x - \delta_1) + b(x)y(x - \delta_2) + c(x)y(x) = f(x), 0 < x < l$ subject to the conditions: $y(x) = \phi(x)$ on $-\delta \leq x < 0$, where $\delta = \max(\delta_1, \delta_2)$ and $y(l) = \gamma$,	Uniform and Shishkin mesh	Modified B-spline collocation method.	The proposed method was significant for the solution of second order singularly perturbed differential equations with small shift and for a general SPDDE.	Two
3	$Ly \equiv \varepsilon y''(x) + a(x)y(x - \delta) + b(x)y(x) = f(x), 0 < x < 1$ subject to constraint: $y(x) = \phi(x), x \in [-\delta, 0]$ and $y(1) = \gamma$	Uniform mesh	Trigonometric cubic B-spline collocation method.	Results obtained are better than the results obtained by the reported method.	Two
4	$-\varepsilon y'''(x) + a(x)y''(x) + b(x)y'(x) + c(x)y(x) + d(x)y'(x - 1) = f(x),$ $x \in \Omega^*$, where $\Omega^* = \Omega^+ \cup \Omega^-$, $\Omega^- = (0,1)$, $\Omega^+ = (1,2)$ subject to the conditions: $y(x) = \phi(x), x \in [-1,0]$ and $y(2) = \gamma$	Uniform mesh	Quintic trigonometric B-spline collocation method	The presented scheme is efficient to simulate a class of third order SPBVP with large delay with discontinuous convection-diffusion coefficient and source term.	One

5	$-\varepsilon y''(x) + a(x)y(x) + b(x)y(x-1) = f(x),$ $x \in \Omega^- \cup \Omega^+, \text{ where } \Omega^- = (0,1), \Omega^+ = (1,2)$ <p>subject to the conditions: $y(x) = \phi(x), x \in [-1,0], y(2) = \gamma$</p>	Uniform mesh	Exponential B-spline collocation scheme	The discussed method of exponential B-spline is capable of obtaining results of required accuracy as compared to existing methods.	Two
6	$\begin{cases} -\varepsilon y''(x) + a(x)y'(x) + b(x)y(x-1) = f(x), x \in \Omega^* \\ y(x) = \phi(x), x \in [-1,0], y(2) = l. \end{cases}$ <p>where $a(x) = \begin{cases} a_1(x), & x \in [0,1] \\ a_2(x), & x \in (1,2] \end{cases}$ and $f(x) = \begin{cases} f_1(x), & x \in [0,1] \\ f_2(x), & x \in (1,2] \end{cases}$ $\Omega^* = \Omega^+ \cup \Omega^-, \Omega^- = (0,1), \Omega^+ = (1,2)$</p>	Uniform and Shishkin mesh	Both mentioned basis functions can provide the solutions with good accuracy	Comparison of Trigonometric and exponential B-spline collocation schemes	Two

6.4 Conclusions from our work

1. The implementation of the scheme (collocation method) is straightforward for computer implementation.
2. The concept of obtaining piecewise continuous polynomials in splines basis provides better solutions as compared to reported methods.
3. The applied techniques are investigated in detail and order of convergence is establishes in each method by using the concept of truncation error and Hall theorem. Procedure to calculate truncation error and to estimate error for the selected mesh strategy is well explained in this work.
4. The conduct of numerical solution is examined and shown through graphs with variation of perturbation parameter and delay parameter.
5. The solution of SPDDE exhibits layer and oscillation behavior depending on the sign of the coefficient of derivative term in the SPDDE.

6.5 Suggestions for Future Work

For future work, following are the suggestions for consideration:

1. Other numerical methods

Collocation method considering spline as basis function has been used; further work can be extended by using some other numerical method such as Galerkin

method or by any other numerical method to find more refine solutions of singularly perturbed delay differential equations.

2. Numerical treatment of singularly perturbed equation of higher order

In this work, only SPDDE of second and third order has been considered, all the discussed methods can be extended to SPDDE of higher order or for the system of simultaneous SPDE.

3. Higher order B-spline

Cubic and quantic B-spline basis function for generation of polynomials has been used here, this work can be extended by considering septic or higher order B-spline.

4. Focus on the obtained solution with selected mesh

So far only maximum absolute error is calculated to validate any numerical scheme but in some works values of few parameters are missing. In present work, the values of the approximated solution have been shown, which can be investigated in detail depending on the chosen mesh for partition of the domain.

5. Other errors

In lieu of concentrating on the maximum absolute error, the conduct of the solution obtained can be analyzed in all respected depending on the values of the retarded and perturbation parameter with the selected mesh strategy.

6. Other mesh strategies

Uniform mesh as well as piecewise uniform mesh has been chosen for this work: Shishkin mesh for the partition of the domain, some other mesh strategies can be chosen to study the numerical solution of SPDE.

7. Improvement in exponential B-spline collocation

In present work, exponential B-spline collocation method has been used to solve a second order singularly perturbed delay differential equation and it was observed that the solution improves as the number of partition points increase but after a certain step, the solution ceases to improve, rather maximum absolute error increases. So, further improvement in the solution can be obtained by amendments

in the method or by doing comprehensive study this odd behavior of the solution can be measured.

8. Practical aspects of the effect of change parameters in the concerned application

The values of the retarded and perturbation parameter with the selected mesh strategy can be well studied with the concerned mathematical model instead of doing general discussion.

References

- Abbas, M., Majid, A. A., Ismail, A. I. M., & Rashid, A. (2014a). The application of cubic trigonometric B-spline to the numerical solution of the hyperbolic problems. *Applied Mathematics and Computation*, 239, 74-88.
- Abbas, M., Majid, A. A., Ismail, A. I. M., & Rashid, A. (2014b). Numerical method using cubic trigonometric B-spline technique for nonclassical diffusion problems. *Abstract and Applied Analysis*, 2014.
- Abd El-Salam, F. (2013). A parametric spline method for second-order singularly perturbed boundary-value problem. *IOSR Journal of Mathematics*, 9(3), 1-5.
- Aggarwal, V. K., & Sharma, K. (2008). An optimized B-spline method for solving singularly perturbed differential difference equations with delay as well as advance. *Neural, Parallel & Scientific Computations*, 16(3), 371.
- Akram, G. (2011). Quartic spline solution of a third order singularly perturbed boundary value problem. *ANZIAM Journal*, 53, E44-E58.
- Akram, G., & Naheed, A. (2013). Solution of Fourth Order Singularly Perturbed Boundary Value Problem Using Septic Spline. *Middle-East Journal of Scientific Research*, 15(2), 302-311.
- Alshomrani, A., Pandit, S., Alzahrani, A., Alghamdi, M., & Jiwari, R. (2017). A numerical algorithm based on modified cubic trigonometric B-spline functions for computational modelling of hyperbolic-type wave equations. *Engineering Computations*, 34(4), 1257-1276.
- Andargie, A., & Reddy, Y. N. (2012). An asymptotic-fitted method for solving singularly perturbed delay differential equations. *Applied Mathematics*, 3(8).
- Arora, G., & Joshi, V. (2016). Comparison of Numerical Solution of 1D Hyperbolic Telegraph Equation using B-Spline and Trigonometric B-Spline by Differential Quadrature Method. *Indian Journal of Science and Technology*, 9(45).
- Arora, G., & Joshi, V. (2018). A computational approach using modified trigonometric cubic B-spline for numerical solution of Burgers' equation in one and two dimensions. *Alexandria Engineering Journal*, 57(2), 1087-1098.
- Arora, G., & Singh, B. K. (2013). Numerical solution of Burgers' equation with modified cubic B-spline differential quadrature method. *Applied Mathematics and Computation*, 224, 166-177.
- Arshed, S. (2017). Quintic B-spline method for time-fractional superdiffusion fourth-order differential equation. *Mathematical Sciences*, 11, 17-26.
- Asahi, T., Ichige, K., & Ishii, R. (2002). Fast Computation of Exponential B-splines. Proceedings of the IEEE.
- Aziz, T., & Khan, A. (2002). A spline method for second-order singularly perturbed boundary-value problems. *Journal of Computational and Applied Mathematics*, 147(2), 445-452.
- Baumert, H., Braun, P., Glos, E., Müller, W.-D., & Stoyan, G. (1980). Modelling and computation of water quality problems in river networks. In *Optimization Techniques* (pp. 482-491): Springer.
- Bear, J., & Verruijt, A. (1987). *Modeling of groundwater flow and pollution*: D.Reidel Publishing Company.
- Botella, O. (2002). On a collocation B-spline method for the solution of the Navier–Stokes equations. *Computers & Fluids*, 31(4-7), 397-420.

- Cengizci, S. (2017). An asymptotic-numerical hybrid method for solving singularly perturbed linear delay differential equations. *International Journal of Differential Equations*, 2017.
- Chakravarthy, P. P., Kumar, D., Rao, R. N., & Ghate, D. (2015). A fitted numerical scheme for second order singularly perturbed delay differential equations via cubic spline in compression. *Advances in Difference Equations*.
- Cimen, E. (2017). A prior estimation of singularly perturbed boundary value problem with delay in convention term. *Journal of mathematical analysis*, 8(1), 202-211.
- Cui, S., & Xu, S. (2007). Analysis of mathematical models for the growth of tumors with time delays in cell proliferation. *Journal of Mathematical Analysis and Applications*, 336(1), 523-541.
- Dag, I., & Ersoy, O. (2016). The exponential cubic B-spline algorithm for Fisher equation. *Chaos, Solitons & Fractals*, 86, 101-106.
- Dag, I., Hepson, O. E., & Kacmaz, O. (2014). The Trigonometric Cubic B-spline Algorithm for Burgers' Equation. *International Journal of Nonlinear Science*.
- Doğan, N., Ertürk, V. S., & Akin, Ö. (2012). Numerical Treatment of Singularly Perturbed Two-Point Boundary Value Problems by Using Differential Transformation Method. *Discrete Dynamics in Nature and Society*, 2012.
- Él'sgol'c, L. É. (1964). *Qualitative methods in mathematical analysis* (Vol. 12): American Mathematical Society.
- Ersoy, O., & Dag, I. (2015a). The exponential cubic B-spline algorithm for Korteweg-de Vries equation. *Advances in Numerical Analysis*, 2015.
- Ersoy, O., & Dag, I. (2015b). The extended B-spline collocation method for numerical solutions of Fisher equation. *AIP Conference Proceedings*, 1648(1), 370011. AIP Publishing LLC.
- Ersoy, O., & Dag, I. (2016). The Exponential Cubic B -Spline Collocation Method for the Kuramoto-Sivashinsky Equation. *International Conference on Recent Advances in Pure and Applied Mathematics*, 30(3), 853-861.
- Ersoy, O., Dag, I., & Adar, N. (2016). The Exponential Cubic B-spline Algorithm for Burgers's Equation. *arXiv:1604.04418*.
- Ersoy, O., Korkmaz, A., & Dag, I. (2016). Exponential B-Splines for Numerical Solutions to Some Boussinesq Systems for Water Waves. *Mediterranean Journal of Mathematics*, 13, 4975–4994.
- Ewing, R. E. (1983). *The mathematics of reservoir simulations*: Society for Industrial and Applied Mathematics.
- Fahmy, M., & Fahmy, G. (2012). Image compression using exponential b-spline functions. *Radio Science (NSRC), National Conference*.
- Farrell, P., Hegarty, A., Miller, J. J. H., O'Riordan, E., & Shishkin, G. I. (2004). Global maximum norm parameter-uniform numerical method for a singularly perturbed convection-diffusion problem with discontinuous convection coefficient. *Mathematical and Computer Modelling*, 40(11-12).
- File, G., Gadisa, G., Aga, T., & Reddy, Y. N. (2017). Numerical Solution of Singularly Perturbed Delay Reaction-Diffusion Equations with Layer or Oscillatory Behaviour. *American Journal of Numerical Analysis*, 5(1), 1-10.
- File, G., & Reddy, Y. N. (2013). Computational Method for Solving Singularly Perturbed Delay Differential Equations with Negative Shift. *International Journal of Applied Science and Engineering*, 11(1), 101-113.

- File, G., & Reddy, Y. N. (2014). Terminal boundary-value technique for solving singularly perturbed delay differential equations. *Journal of Taibah University for Science*, 8(3), 289-300.
- Fitzpatrick, R. (2006). An example calculation. Retrieved from <http://farside.ph.utexas.edu/teaching/329/lectures/node37.html>
- Gorgulu, M. Z., Dag, I., & Irk, D. (2016). Wave Propagation by Way of Exponential B-Spline Galerkin Method. *Journal of Physics: Conference Series*, 766 (1), p. 012031.
- Gorgulu, M. Z., Dag, I., & Irk, D. (2017). Simulations of solitary waves of RLW equation by exponential B-spline Galerkin method. *Chinese Physics B*, 26(8), 080202.
- Govindarajan, N., Visser, C. C. d., & Krishnakumar, K. (2014). A sparse collocation method for solving time-dependent HJB equations using multivariate B-splines. *Automatica*, 50(9), 2234-2244.
- Guido, W. (1997). Identities for trigonometric B-splines with an application to curve design. BIT Numerical Mathematics volume, 37, 189–201.
- Gupta, B., & Kukreja, V. K. (2012). Numerical approach for solving diffusion problems using cubic B-spline collocation method. *Applied Mathematics and Computation*, 219(4), 2087-2099.
- Gupta, R., Lee, B. G., & Lee, J. J. (2007). A new image interpolation technique using exponential B-spline.
- Gupta, Y., Srivastava, P. K., & Kumar, M. (2011). Application of B-spline to numerical solution of a system of singularly perturbed problems. *Mathematica Aeterna*, 1, 405 – 415.
- Hahn, S. Y., Bigeon, J., & Sabonnadiere, P. J. C. (1987). An 'upwind' finite element method for electromagnetic field problems in moving media. *International Journal for Numerical Methods in Engineering*, 24(11), 2071-2086.
- Hall, C. A. (1968). On error bounds for spline interpolation. *Journal of approximation theory*. *Journal of Approximation Theory*, 1(2), 209-218.
- Hepson, O. E., Korkmaz, A., & Dag, I. (2017). Exponential B-spline Collocation Solutions to the Gardner Equation. *International Journal of Computer Mathematics*, 97(4), 837-850.
- Hussain, M. Z., Abbas, S., & Irshad, M. (2017). Quadratic trigonometric B-spline for image interpolation using GA. *PLOS ONE*, 12(6), e0179721.
- Irk, D., & Dag, İ. (2011). Quintic B-spline collocation method for the generalized nonlinear Schrödinger equation. *Journal of the Franklin Institute*, 348(2), 378-392.
- Irk, D., & Keskin, P. (2016). Cubic Trigonometric B-spline Galerkin Methods for the Regularized Long Wave Equation. *Journal of Physics: Conference Series*, 766(1), 012032.
- Jerison, D. (2007). Convergence of Numerical Methods. Retrieved from <http://web.mit.edu/16.90/BackUp/www/pdfs/Chapter2.pdf>
- Jha, N. (2012). Computational Method for Nonlinear Singularly Perturbed Singular Boundary Value Problems using Nonpolynomial Spline. *Journal of Information and Computing Science*, 7(2), 091-096.
- Juhász, I., & Hoffmann, M. (2002). Knot modification of B-spline curves. *I. Magyar Számítógépes Grafika és Geometria Konferencia, Budapest*, 38-44.
- Kadalbajoo, M., & Arora, P. (2009). B-spline collocation method for the singular-perturbation problem using artificial viscosity. *Computers & Mathematics with Applications*, 57(4), 650-663.
- Kadalbajoo, M., & Aggarwal, V. (2005). Fitted mesh B-spline collocation method for solving self-adjoint singularly perturbed boundary value problems. *Applied Mathematics and*

- Computation, 161(3). Retrieved from
https://www.sciencedirect.com/science/article/pii/S0096300304000475?casa_token=gxSFOV6IYUEAAAAA:KLJVivfK6jciE9MOKIfkmwcZknRoUdc1CHdRos80eMZ0Vm_tHPaf7RJyB70zCfAybYRI8eYHtB8#!
- Kadalbajoo, M., & Gupta, V. (2009). Numerical solution of singularly perturbed convection–diffusion problem using parameter uniform B-spline collocation method. *Journal of Mathematical Analysis and Applications*, 355(1), 439-452.
- Kadalbajoo, M., & Kumar, D. (2008). Fitted mesh B-spline collocation method for singularly perturbed differential–difference equations with small delay. *Applied Mathematics and Computation*, 204(1), 90-98.
- Kanth, R. A., & Murali, M. K. (2018). A numerical technique for solving nonlinear singularly perturbed delay differential equations. *Mathematical Modelling and Analysis*, 23(1), 64-78.
- Kaufmann, P., Kaufmann, P. L., Pamboukian, S. V. D., & Moraes, R. V. d. (2012). Signal transceiver transit times and propagation delay corrections for ranging and georeferencing applications. *Mathematical Problems in Engineering* 2012.
- Kellogg, B., & Tsan, A. (1978). Analysis of some difference approximations for a singular perturbation problem without turning points. *Mathematics of Computation*, 32, 1025-1039.
- Kicsiny, R. (2014). New delay differential equation models for heating systems with pipes. *International Journal of Heat and Mass Transfer*, 79, 807-815.
- Kicsiny, R., & Farkas, I. (2012). Improved differential control for solar heating systems. *Solar Energy*, 86(11), 3489-3498.
- Koch, P. E., Lyche, T., Neamtu, M., & Schumaker, L. (1995). Control curves and knot insertion for trigonometric splines. *Advances in Computational Mathematics*, 3, 405-424.
- Kumar, D. (2013). A computational technique for solving Boundary value problem with two small parameters. *Electronic Journal of Differential Equations*, 2013(30), 1–10.
- Kumar, D., & Kadalbajoo, M. (2012). Numerical Treatment of Singularly Perturbed Delay Differential Equations Using B-Spline Collocation Method on Shishkin Mesh. *Journal of Numerical Analysis, Industrial and Applied Mathematics*, 7(3-4), 73-90.
- Lakestani, M., & Dehghan, M. (2012). Numerical solutions of the generalized Kuramoto–Sivashinsky equation using B-spline functions. *Applied Mathematical Modelling*, 36(2), 605-617.
- Lang, F.-G., & Xu, X.-P. (2012). Quintic B-spline collocation method for second order mixed boundary value problem. *Computer Physics Communications*, 183(4), 913-921.
- Lange, C. G., & Miura, R. M. (1982). Singular perturbation analysis of boundary value problems for differential-difference equations. *SIAM Journal on Applied Mathematics*, 42(3), 502-531.
- Lange, C. G., & Miura, R. M. (1994). Singular perturbation analysis of boundary-value problems for differential-difference equations. *SIAM Journal on Applied Mathematics*, 54(1), 273-283.
- Li, X. (2012). Numerical solution of fractional differential equations using cubic B-spline wavelet collocation method. *Communications in Nonlinear Science and Numerical Simulation*, 17(10), 3934-3946.

- Longtin, A., & Milton, J. G. (1988). Complex oscillations in the human pupil light reflex with “mixed” and delayed feedback. *Mathematical Biosciences*, 90(1–2), 183-199.
- Lyche, T., & Winther, R. (1979). A stable recurrence relation for trigonometric B-splines. *Journal of Approximation Theory*, 25(3), 266-279.
- Mallet-Paret, J., & Nussbaum, R. D. (1989). A differential-delay equation arising in optics and physiology. *SIAM Journal on Mathematical Analysis*, 20(2), 249–292.
- Mishra, H. K., & Saini, S. (2013). Numerical Solution of Singularly Perturbed Two-Point Boundary Value Problem via Liouville-Green Transform. *American Journal of Computational Mathematics*, 3(1).
- Mishra, U. (2016). Shape Control of the Cubic Trigonometric B-Spline Polynomial Curve with A Shape Parameter. *International Journal of Sciences and Applied Research*, 3(8).
- Misro, M. Y., Ramli, A., & Ali, J. (2017). Quintic trigonometric Bézier curve with two shape parameters. *Sains Malaysiana*, 46(5), 825-831.
- Mittal, R. C., & Arora, G. (2010). Quintic B-spline collocation method for numerical solution of the Kuramoto–Sivashinsky equation. *Communications in Nonlinear Science and Numerical Simulation*, 15(10), 2798-2808.
- Mittal, R. C., & Bhatia, R. (2013). Numerical solution of second order one dimensional hyperbolic telegraph equation by cubic B-spline collocation method. *Applied Mathematics and Computation*, 220, 496-506.
- Mittal, R. C., & Bhatia, R. (2014). Numerical solution of nonlinear sine-Gordon equation by modified cubic B-spline collocation method. *International Journal of Partial Differential Equations*, 2014.
- Mittal, R. C., & Jain, R. K. (2012a). Cubic B-splines collocation method for solving nonlinear parabolic partial differential equations with Neumann boundary conditions. *Communications in Nonlinear Science and Numerical Simulation*, 17(12), 4616-4625.
- Mittal, R. C., & Jain, R. K. (2012b). Numerical solutions of nonlinear Burgers’ equation with modified cubic B-splines collocation method. *Applied Mathematics and Computation*, 218(15), 7839-7855.
- Mittal, R. C., & Jain, R. K. (2013). Numerical solutions of nonlinear Fisher's reaction–diffusion equation with modified cubic B-spline collocation method. *Mathematical Sciences*, 7 (1), 1-10.
- Mohammadi, R. (2013). Exponential B-spline solution of convection-diffusion equations. *Applied Mathematics*, 4(6).
- Mohammadi, R. (2014). Sextic B-spline collocation method for solving Euler–Bernoulli Beam Models. *Applied Mathematics and Computation*, 241, 151–166.
- Morinishi, Y., Tamano, S., & Nakabayashi, K. (2003). A DNS algorithm using B-spline collocation method for compressible turbulent channel flow. *Computers & Fluids*, 32(5), 751-776.
- Nelson, P. W., & Perelson, A. S. (2002). Mathematical analysis of delay differential equation models of HIV-1 infection. *Mathematical Biosciences*, 179(1), 73-94.
- Nicaise, S., & Xenophontos, C. (2013). Robust approximation of singularly perturbed delay differential equations by the hp finite element method. *Computational Methods in Applied Mathematics*, 13(1), 21-37.
- Pawelek, K. A., Liu, S., Pahlevani, F., & Rong, L. (2012). A model of HIV-1 infection with two time delays: Mathematical analysis and comparison with patient data. *Mathematical Biosciences*, 235(1), 98-109.

- Pedas, A., & Tamme, E. (2014). Numerical solution of nonlinear fractional differential equations by spline collocation methods. *Journal of Computational and Applied Mathematics*, 255(1), 216-230.
- Prandtl, L. (1905). Über Flüssigkeitsbewegung bei kleiner Reibung, Verhandlungen. *Internat. Math. Kongresses*, 3, 484-491.
- Pudykiewicz, J. (1989). Simulation of the Chernobyl dispersion with a 3-D hemispheric tracer model. *Tellus B*, 41(8).
- Rao, S. C. S., & Kumar, M. (2007). Optimal B-spline collocation method for self-adjoint singularly perturbed boundary value problems. *Applied Mathematics and Computation*, 188(1), 749-761.
- Raslan, K., Hadhoud, A., & Shaalan, M. A. (2018). The exponential and trigonometric cubic B-spline methods for second order matrix differential equations. *Journal of Abstract and Computational Mathematics*, 3(1).
- Rihan, F. A. (2013). Delay Differential Equations in Biosciences: Parameter estimation and sensitivity analysis. *Proceedings of the 2013 International Conference on Applied Mathematics and Computational Methods (Venice, Italy September 2013)*, 50-58.
- Sahu, P. K., & Ray, S. S. (2014). Numerical solutions for the system of Fredholm integral equations of second kind by a new approach involving semiorthogonal B-spline wavelet collocation method. *Applied Mathematics and Computation*, 234(15), 368-379.
- Saka, B. (2012). A quintic B-spline finite-element method for solving the nonlinear Schrödinger equation. *Physics of Wave Phenomena*, 20, 107-117.
- Saka, B., Dag, İ., & Irk, D. (2008). Quintic B-spline collocation method for numerical solution of the RLW equation. *The ANZIAM Journal*, 49(3), 389-410.
- Schmitt, K. (1969). On solutions of nonlinear differential equations with deviating arguments. *SIAM Journal on Applied Mathematics*, 17(6), 1171-1176.
- Schoenberg, I. J. (1946). Contributions to the problem of approximation of equidistant data by analytic functions. Part B. On the problem of osculatory interpolation. A second class of analytic approximation formulae. *Quarterly of Applied Mathematics*, 4(2), 112-141.
- Schoenberg, I. J. (1964). On Trigonometric Spline Interpolation. *Journal of Mathematics and Mechanics*, 13(5), 795-825.
- Sekar, E., & Tamilselvan, A. (2018). Singularly perturbed delay differential equations of convection-diffusion type with integral boundary condition. *Journal of Applied Mathematics and Computing*, 59 (1), 701-722.
- Siddiqi, S. S., & Arshed, S. (2013). Quintic B-Spline for the Numerical Solution of Fourth-Order Parabolic Partial Differential Equations. *World Applied Sciences Journal*, 23(12), 115-122.
- Siddiqi, S. S., & Arshed, S. (2014). Quintic B-spline for the numerical solution of the good Boussinesq equation. *Journal of the Egyptian Mathematical Society*, 22(2), 209-213.
- Stein, R. B. (1967). Some models of neuronal variability. *Biophysical Journal*, 7(1), 37-68.
- Subburayan, V. (2016a). An hybrid initial value method for singularly perturbed delay differential equations with interior layers and weak boundary layer. *Ain Shams Engineering Journal*, 9(4), 727-733.
- Subburayan, V. (2016b). A parameter uniform numerical method for singularly perturbed delay problems with discontinuous convection coefficient. *Arab Journal of Mathematical Sciences*, 22(2), 191-206.

- Subburayan, V., & Mahendran, R. (2018). An ε -uniform numerical method for third order singularly perturbed delay differential equations with discontinuous convection coefficient and source term. *Applied Mathematics and Computation*, 331, 404-415.
- Subburayan, V., & Ramanujam, N. (2013). An initial value technique for singularly perturbed reaction-diffusion problems with a negative shift. *Novi Sad J. Math*, 43(2), 67-80.
- Swamy, D. K., Phaneendra, K., Babu, A. B., & Reddy, Y. N. (2015). Computational method for singularly perturbed delay differential equations with twin layers or oscillatory behaviour. *Ain Shams Engineering Journal*, 6(1), 391-398.
- Swamy, D. K., Phaneendra, K., & Reddy, Y. N. (2016). Solution of Singularly Perturbed Differential-Difference Equations with Mixed Shifts Using Galerkin Method with Exponential Fitting. *Chinese Journal of Mathematics*, 2016.
- Tamsir, M., Dhiman, N., & Srivastava, V. K. (2018). Cubic trigonometric B-spline differential quadrature method for numerical treatment of Fisher's reaction-diffusion equations. *Alexandria Engineering Journal*, 57(3), 2019-2026.
- Townsend, A. (2015). On the Spline. Retrieved from <http://www.alatown.com/spline/>
- Varah, J. M. (1975). A lower bound for the smallest singular value of a matrix. *Linear Algebra and its Applications*, 11(1), 3-5.
- Yaseen, M., & Abbas, M. (2018). The application of cubic trigonometric B-spline to the numerical solution of time-fractional telegraph equation. *arXiv:1808.01158*.
- Yaseen, M., Abbas, M., Ismail, A. I., & Nazir, T. (2017). A cubic trigonometric B-spline collocation approach for the fractional sub-diffusion equations. *Applied Mathematics and Computation*, 293, 311-319.
- Yüzbaşı, Ş., & Sezer, M. (2013). Exponential collocation method for solutions of singularly perturbed delay differential equations. *Abstract and Applied Analysis*, 2013. Hindawi.
- Zakaria, N. F., Hassan, N. A., Hamid, N. N. A., Majid, A. A., & Ismail, A. I. M. (2017). Solving Boussinesq equation using quintic B-spline and quintic trigonometric B-spline interpolation methods. *AIP Conference Proceedings*, 1830 (1), p. 020041. AIP Publishing LLC..
- Zhang, Y., Jie, Y., & Meng, X. (2016). The modelling and control of a singular biological economic system in a polluted environment. *Discrete Dynamics in Nature and Society*, 2016.
- Zin, S. M., Majid, A. A., Ismail, A. I. M., & Abbas, M. (2014). Cubic trigonometric B-spline approach to numerical solution of wave equation. *International Journal of Mathematical, Computational, Physical and Quantum Engineering*, 8(10), 1212-1216.

Research publications/Conferences/Workshops attended

Research publications:

1. Geeta Arora and Mandeep Kaur, “Numerical simulation of singularly perturbed differential equation with small shift”. In *AIP Conference Proceedings* (Vol. 1860, No. 1, p. 020047). AIP Publishing. (2017, July)
2. Mandeep Kaur and Geeta Arora, “Solution of Second Order Singular Perturbed Delay Differential Equation Using Trigonometric B-Spline”. *International Journal of Mathematical, Engineering and Management Sciences* Vol. 4, No. 2, 349–360, 2019 ISSN: 2455-7749.
3. Mandeep Kaur and Geeta Arora, “A review on singular perturbed delay differential equations”. ISSN: O: 2319-6475, ISSN, 6(3): 2341-2346, 2017.
4. Mandeep Kaur and Geeta Arora, “Quintic B-spline technique for numerical treatment of third order singular perturbed delay differential equation”, *International Journal of Mathematical, Engineering and Management Sciences* Vol. 4, No. 6, 1471-1482, 2019.
5. Mandeep Kaur and Geeta Arora, “Numerical simulation of singular perturbed differential equation with large delay using exponential B-spline collocation method”, communicated.
6. Geeta Arora and Mandeep Kaur Vaid, “Comparison of exponential and trigonometric B-spline collocation technique for simulation of singular perturbed delay differential equation”, communicated.
7. Geeta Arora and Mandeep Kaur Vaid, “A Numerical Approach for Simulation of Generalized Perturbed Delay Differential Equation Using Shishkin Mesh”, communicated.

Conferences:

1. Paper presented on “Numerical simulation of singularly perturbed differential equation with small shift”, at RAFAS at LPU. (25-26 November 2016).
2. Paper presented on “A numerical approach for simulation of generalized perturbed delay differential equation using Shishkin mesh”, at Recent advances in theoretical and computational partial differential equations with applications, Punjab University Chandigarh. (05-09 December, 2016).

Workshop:

Participated in workshop “Computational techniques for differential equations with MATLAB (CTDE-2015)”, 02-06 July 2015 at Indian institute of technology Roorkee, India.